Tackling immune escape: identifying novel targets and pathways involved in the regulation of CD155 in melanoma

Fenna Floortje Feenstra

ORCID ID:

0000-0003-3692-8858

from Purmerend, Netherlands

Submitted in total fulfilment of the requirements of the joint degree of

Doctor of Philosophy (PhD)

Of

The Medical Faculty

The Rheinische Friedrich-Wilhelms-Universität Bonn

And

The Department of Microbiology and Immunology

The University of Melbourne

Bonn/Melbourne, 2026

Performed and approved by the Medical Faculty of the Rheinische Friedrich-Wilhelms-Universität Bonn and the University of Melbourne.

1. Supervisor: Prof. Dr. Tobias Bald

2. Supervisor: Prof. Dr. Marco Herold

Date of submission: November 2025

Date of oral examination: June 2026

Institute of Experimental Oncology, University Hospital Bonn

Director: Prof. Dr. Michael Hölzel

Table of content

Abbreviations

Special characters

%	Percent
#	Number
°C	Degree Celsius
µg	Microgram
µL	Microlitre
µM	Micromolar
α	alpha
ß	beta
δ	delta
γ	gamma

A

AKT	AKT Serine/Threonine Kinase
AP-1/2	Activator protein 1/2
APC	Antigen presenting cells
ATP	Adenosine tri-phosphate

B

BlastR	Blasticidin resistance cassette
BSA	Bovine Serum Albumin
BRAF	B-raf proto-oncogene

C

cAMP	Cyclic adenosine monophosphate
CD155	Cluster of Differentiation 155, Polio Virus Receptor (PVR) or Necl-5
CNA	Copy-number alterations
CDK	Cyclin-dependent kinase
CDKN	Cyclin-dependent kinase inhibitor
cDNA	Complementary DNA
CO2	Carbon dioxide
CTL	Cytotoxic T lymphocytes
CTLA-4	Cytotoxic T-lymphocyte-associated protein 4
CRISPR	Clustered Regularly Interspaced Short Palindromic Repeats

D

DAPI	4´,6-diamidino-2-phenylindole
DC	Dendritic cell

DEGs	Differentially expressed genes
DLB	Direct lysis buffer
DNA	Deoxyribonucleic acid
dNTPs	Deoxynucleotides
DMSO	Dimethyl sulfoxide
DTIC	DNA-alkylating agent dacarbazine
DYRK1A	Dual Specificity Tyrosine Phosphorylation Regulated Kinase 1A

E

E.coli	Escherichia coli
EMT	Epithelial-to-mesenchymal transition
ER	Endoplasmic reticulum

F

FACS	Fluorescence-activated cell sorting
FCS	Fetal Calf Serum
FDA	US Food and Drug Administration
FDR	False discovery rate
FGF	Fibroblast growth factor

G

g	Gram
gDNA	genomic DNA
GFP	Green fluorescent protein
GSEA	Gene set enrichment analysis

H

H2O	Chemical formula for water
HDR	Homology-directed repair
HRAS	HRAS proto-oncogene
HRP	Horseradish peroxidase

I

ICB	Immune checkpoint blockades
IFN-γ	Interferon gamma
IL	Interleukin
ITIM	Immunoreceptor tyrosine-based inhibitory motif
ITT	Immunoreceptor Tyrosine-based Activation like domain

K

KO	Knock-out

L

LPS	Lipopolysaccharide

M

M	Molar
MAGeCK	Model-based Analysis of Genome-wide CRISPR/Cas9 Knockout
MC1R	Melanocorting-1 receptor
MFI	Mean Fluorescence Intensity
mg	Milligram
MHC	Major histocompatibility complex
min	Minute
MITF	Microphthalmia-associated transcription factor
mL	Millilitre
mM	Millimolar
mRNA	Messenger RNA
MYC	MYC proto-oncogene

N

ng	Nanogram
NGS	Next-Generation Sequencing
NK	Natural killer cell
NRF	Nuclear Respiratory Factor
NRAS	NRAS proto-oncogene
ns	Not significant
NT	Non-treated

P

PAM	Protospacer adjacent motif
PBS	Phosphate-buffered saline
PCA	Principal component analysis
PCR	Polymerase chain reaction
PD-1	Programmed cell death protein 1
PD-L1/2	Programmed cell death-ligand 1 (CD274)/2
PI	Propidium iodide
PI3K	Phosphoinositide 3-kinase
PVR	CD155
PTEN	Phosphatase and tensin homolog

PuroR	Puromycin resistance cassette

Q

qRT-PCR	Quantitative PCR
QVD	Q-VD-OPh, caspase inhibitor

R

RNA	Ribonucleic acid
rpm	Rounds per minute
RT	Room temperature

S

SDS-PAGE	Sodium dodecylsulphate polyacrylamide gel electrophoresis
sec	Second
sgRNA	single-guided RNA
SHP-2	Src homology region 2 domain-containing phosphatase
STRING	Search Tool for the Retrieval of Interacting Genes/Proteins

T

TEM	Trans endothelial migration

TGF-ß	Transforming growth factor beta
TME	Tumor microenvironment
TNF-α	Tumor necrosis factor alpha

U

UV	Ultraviolet

V

V	Volt

W

WT	Wild-type

List of tables

List of figures

Abstract

Melanoma is a highly aggressive form of skin cancer. While targeted therapies show a strong initial response, resistance remains a problem resulting in a five-year progression free survival rate of only 19 %. Immunotherapies provide a better long-term response but only in a small subset of patients. Therefore, there is an urgent need to better understand resistance mechanisms to optimize existing therapies or develop novel therapies.

CD155 is an adhesion molecule of the Nectin-like family with an intrinsic role in promoting tumor growth and extrinsic immunomodulatory functions as a ligand for the inhibitory immune checkpoints TIGIT and CD96, as well as the activating receptor CD226. CD155 is overexpressed across many different cancer types, and patients with overexpression have poor clinical outcome. Furthermore, CD155 is low expressed on healthy tissue making it an interesting target for immunotherapies. Our lab has recently shown that CD155-expressing tumor cells downregulated CD226 on tumor infiltrating CD8+ T cells, which rendered tumor-infiltrating T cells dysfunctional and contributed to resistance to cancer immunotherapies. Little is known about the intrinsic mechanisms regulating CD155 expression in cancer.

We have characterized CD155 in a panel of human melanoma cell lines harbouring different oncogenic driver mutations, and performed a genome-wide CRISPR knock-out screen to identify novel pathways and potentially druggable molecules involved in the intrinsic regulation of CD155. *DYRK1A* was identified and validated as an intrinsic regulator of CD155 surface expression. In addition, *DYRK1A* and the PI3K/AKT pathway were shown as interesting pharmacological therapeutic targets as our data showed that inhibition of the PI3K/AKT pathway reduced CD155 surface expression levels in a *BRAF*-mutant human melanoma cell line. Thus, our data provide the rational to further explore the use of DYRK1A or PI3K/AKT inhibitors alone or in combination with immune checkpoint blockade for the treatment of cancer overexpressing CD155. More validation of these

findings might enable us to reduce or completely abolish CD155 expression in cancer cells in order to improve the efficacy of cancer immunotherapies.

Declaration

The work that is presented in this thesis was conducted at the University of Bonn in the laboratory of Prof. Dr. Tobias Bald and at the University of Melbourne in the laboratory of A/Prof. Dr. Marco Herold. This work was supported by the Deutsche Forschungsgemeinschaft (DFG, German Research Council) within GRK 2168, the Medical Faculty of the Rheinische Friedrich-Wilhelms-Universität Bonn and by the Deutsche Forschungsgemeinschaft under Germany's Excellence Strategy (EXC2151-390873048). Fenna Floortje Feenstra was supported by the Deutsche Forschungsgemeinschaft, the Medical Faculty of the Rheinische Friedrich-Wilhelms-Universität Bonn and the Melbourne International Research Scholarship.

This is to certify that,

1. the thesis only comprises my original work towards the PhD except where indicated
2. due acknowledgement has been made in the text to all other material used
3. the thesis is less than 100,000 words in length, exclusive of tables, maps, bibliographies and appendices.

Melbourne, 15th November 2025 Fenna Floortje Feenstra

Preface

Contribution

My contribution to the experiments within each chapter was as follows:

- Chapter 3: Characterisation of CD155 in human cancers 95 %
- Chapter 4: Identification of molecular signaling pathways regulating CD155 surface expression in human melanoma 90 %
- Chapter 5: Validation using pharmacological and genetic approaches to test their relevance in regulating CD155 surface expression in human melanoma 100 %

I acknowledge the important contributions of others to the experiments presented in:

- Chapter 3 Characterisation of CD155 in human cancers: Jule Schmedding and Laurin Schunke for testing CD155 expression on some melanoma and lung cancer cell lines. Dillon Corvino and Daksh Pamar for helping with RNA sequencing analysis.
- Chapter 4 identification of molecular signaling pathways regulating CD155 surface expression in human melanoma: Marius Jentzsch and Caroline Fandrey for providing quality-controlled genome-wide CRISPR screen lentivirus and Prof. Dr. rer. nat. Jonathan Schmid-Burgk for helping optimizing the screen workflow.

In preparing this work, I used ChatGPT to improve the readability and language of the manuscript. After using this tool, I reviewed and edited the relevant passages and take full responsibility for the content of the published dissertation.

Acknowledgements

This work of the past four years would not have been possible without the help, support and mentorship of many people with who I have had the pleasure and privilege to work with in both Bonn and Melbourne.

Firstly, I would like to express my sincere gratitude to my two PhD supervisors Prof. Dr. Tobias Bald and Prof. Dr. Marco Herold for giving me the opportunity to conduct the research for my PhD thesis in their labs. Thank you for the continuous support and motivation from near and far. Besides my supervisors, I would like to thank Prof. Dr. Thomas Gebhardt and Dr. Philippa Saunders for being part of my Melbourne and Bonn PhD committee.

A special thanks goes to Dr. Maike Effern, who has supported me from the start of my PhD. Teaching me important knowledge needed for CRISPR/Cas9 and beyond, without you this work would not have been possible.

I would also like to thank Dr. Marius Jentzsch and Dr. Caroline Fandrey for helping me with the genome-wide CRISPR knock-out screen and producing the virus, and Prof. Dr. rer. nat. Jonathan Schmid-Burgk for brainstorming together how we could optimize the screens specifically for my PhD project aims. This has been really helpful. I would like to thank the Flow Cytometry Core Facility at the University of Bonn for performing all the FACS sorting, including way too many 7 hours sorting days at the same time on two FACS sorting machines. Peter Wurst and David Kühne thank you for your patience and help with the sorting.

Thank you to the different lab groups at Institute of Experimental Oncology in Bonn and Blood Cancer in Melbourne, thank you for sharing your experience and knowledge, as well as discussing my project or having lunch/coffee together. Furthermore, I would like to thank the coordinators of the Bonn & Melbourne Research and Graduate School Immunosciences, IRTG2168. I cannot put into words how grateful I am to join such an inspiring worldwide program. Living abroad and seeing so much of the world has been an incredible experience. It

requires a lot of organization and none of it would have been possible without Lucie, Marie and Sandra.

Special thanks go to Helena, Freya, Saskia, Teresa, Gonzalo, Michael, Mascha, Alea and Sol for their consistent support and for sharing all my scientific successes (and celebrating them), as well as setbacks and challenges. I am equally grateful to my close friends Dieder, Lisanne, Julia, Maddie, Relinde, Matty, and Leandra, whose encouragement, positivity and friendship beyond the laboratory made this journey possible. The endless voice memos and calls, even though I was on the other side of the world we always knew what was going on. In addition, I want to thank my flatmates from Prinz-Albert Straße 8 in Bonn, Germany, who were amazing support during the first 3 years of my PhD in Bonn, Julia, Andi, Moritz, Leon and Tobias. I also never forget my time on 16th Henderson Street in Melbourne, Australia, where I lived for the last 1,5 years of my PhD. There, Maddie, Michael and Chris became like a second family, making me feel at home, heard and seen on the other side of the world. It truly felt like finding a new family.

Another thank you goes to Charge CrossFit in Melbourne, I would never have thought CrossFit could so much fun, and I am amazed at how much progress I made in just 1 year (including four strict pull ups and lifting heavier than your own bodyweight). Charge has an incredible, amazing, and supportive community, and the coaching is truly exceptional. Thank you charge babes Sol, Cintia, Louise, Jane, Zoe, Farah, Miranda, and Lisa for sharing all the trainings, challenges, and fun times. Special thanks to Your Shot Australia, the DJ competition that I joined in June 2025, where I explored my DJ persona as “Fennergy”. Along this intense journey, I met cool and talented artists who have become my new best friends: Betty, Liv, Sascha, Jesse, and Dion. I am beyond proud to have performed in several venues/clubs in Melbourne including Prince Band room, Tatiana, Circus, 24 Moons, Federation square, Fifty-five bar, Lona, and Evies disco dinner. This creative side job gave me balance, creativity, energy, and joy throughout my PhD.

Last but definitely not least, I want to thank my parents. I cannot put into words how grateful I am for your endless support, optimism, and patience while I lived in Germany and Australia. Although sometimes it might have been hard to understand what I was actually doing in the laboratory, you were always there to listen, no matter on which side of the world I was. You are both incredibly strong and serve as an example for me. To my sister, Sanne: I wish I could tell you that I finally became a doctor. You never understood what I was doing but you never stopped asking: “Fenna, when you will be doctor?”. You have made me realize how life can end way too soon and how important it is to truly enjoy every moment while you still can.

My forever motto is and always has been: “I have never done it before, so I think I can do it” – Pippi Longstocking. It reminds me to embrace challenges, take risks, and approach life with curiosity and courage, something I can highly recommend to everyone.

Introduction

1.1 Cancer

Cancer is a leading cause of death worldwide, with an estimated 19,3 million new cases and nearly 10 million cancer deaths in 2020 (Ferlay et al., 2021). It arises from the transformation of normal to abnormal cells that proliferate in an uncontrolled manner thereby invading and damaging normal tissues. This transformation is often driven by genetic mutations, which can be caused by extrinsic factors such as ultraviolet (UV) exposure or carcinogens like nicotine (Marco Rastrelli et al., 2014; Wu et al., 2018). Under normal conditions, cellular DNA repair mechanisms correct these mutations, however, these repair mechanisms can fail as they become less effective with age or can be disrupted by endogenous factors including hormones and inflammation (Marco Rastrelli et al., 2014; Wu et al., 2018). In addition to genetic mutations, epigenetic dysregulation and changes in the tumor microenvironment (TME) can contribute to tumor initiation and progression (Hanahan, 2022; Hanahan and Weinberg, 2011).

For better understanding of this complex disease, different hallmarks of cancer were defined (Hanahan and Weinberg, 2011). In 2000, Hanahan and Weinberg defined six Hallmarks of cancer: ‘sustaining proliferative signaling, evading suppression, activating invasion and metastasis, enabling replicative immortality, inducing angiogenesis and resisting cell death’. Eleven years later they revisited their concept by adding two additional aspects to the hallmarks of cancer: ‘deregulating cellular energetics and avoiding immune destruction’. Furthermore, they added two enabling characteristics which are not describing the complexity of cancer like the other eight hallmarks but they focus more on the acquisition of cancer: ‘genome instability and mutation, and tumor promoting-inflammation’ (Hanahan and Weinberg, 2011). In 2022, Hanahan and Weinberg published another review in which they explained that cancer can be caused by genetic as well as non-genetic changes, making the origin of cancer even more complex (Hanahan, 2022). First of all, the phenotypic plasticity of cells is important. Cancer

cells are able to disrupt differentiation at different stages in their favour, and resistance can be acquired (Hanahan, 2022). A second hallmark that is not related to either the genome or mutations is epigenetic remodelling. Epigenetic remodelling is caused by changes in DNA methylation and chromatin remodelling, or by factors in the TME such as stress or hypoxia (Hanahan, 2022). In 2018, James Allison and Tasuku Honjo received the Noble Prize for their research on a protein that functions as a brake on our immune system, which could be released by targeting this with monoclonal antibodies, a treatment which is called immunotherapy (Freeman et al., 2000; Krummel and Allison, 1995; van Elsas et al., 1999). The revised hallmarks of cancer and the Noble prize in 2018 highlight the importance of our immune system in cancer.

1.2 Role of the immune system in cancer

1.2.1 Immune surveillance

The role of the immune system in cancer control was pioneered by W. Coley in 1891. W. Coley injected bacteria in untreatable tumors of patients with the aim to reduce their tumor burden, which is regarded as the first instance of immunotherapy (McCarthy, 2006). Later in the 1950s, Burnet and Thomas proposed that cancer cells harbor novel antigenic markers, enabling the immune system to recognize and destroy malignant cancer cells. As such, continuous immune surveillance is a fundamental mechanism by which the immune system protects our body against the development of cancer (Burnet, 1957). The idea of cancer immune surveillance has been confirmed in large clinical cohorts of immune suppressed patients for instance due to a human immunodeficiency virus (HIV) infection as well as an organ transplantation. It is well established that pharmacological or infection-mediated immunosuppression significantly increases the risk of cancer development compared with control cohorts (Huo et al., 2020; Park et al., 2022).

1.2.2 Immunoediting

Despite the ‘immune surveillance theory’ cancer is still a global cause of death indicating that the immune system can fail to prevent cancer. To elucidate this incapability of the immune system the concept of cancer immunoediting was developed by Dunn et al. in 2002. Cancer immunoediting consists of three phases: 1) elimination, 2) equilibrium, and 3) escape (Dunn et al., 2002; Smyth et al., 2006).

The first phase, elimination (1), reflects the classic ‘immune surveillance theory’, which proposes that the immune system is able to recognize and destroy cancer cells (Burnet, 1957). When successful, this process prevents tumor development. However, imperfect elimination leads to the second phase, equilibrium (2), in which residual cancer cells are contained but not eliminated by the immune system. During this stage, tumor and immune cells co-exist in a dynamic balance, allowing immune resistant clones to dominate (Dunn et al., 2002). Over time, cancer cells can acquire additional genetic and epigenetic alterations that reduce their immunogenicity, allowing them to avoid elimination by immune cells and continue to proliferate. Simultaneously, cancer cells can remodel the TME to disrupt the co-existing balance and inhibit anti-tumoral immune cells subsets such as dendritic cells (DCs), T cells, and natural killer (NK) cells via inhibitory cytokines, chemokines or receptors-ligand interactions (Chen and Mellman, 2013; Dunn et al., 2002). Once immune control is lost, cancer cells enter the escape phase (3), characterized by uncontrolled proliferation despite the presence of immune cells (Dunn et al., 2002; O’Donnell et al., 2019). Understanding and exploiting these immune escape mechanisms can potentially re-invigorate the immune system, thereby shifting the balance back towards elimination of cancer cells. Over the last decades, immune escape mechanisms have become major therapeutic targets (Martínez-Jiménez and Chowell, 2025).

Therapies targeting the immune escape phase of cancer cells are known as immune checkpoint blocking agents (ICBs). ICBs inhibit immune checkpoints (Fig. 1), which are inhibitory receptors or ligands expressed on immune and

cancer cells (Qin et al., 2019). Under normal conditions, immune checkpoints play a crucial role in preserving homeostasis and restraining excessive inflammation and tissue damage. However, cancer cells exploit these pathways to evade immune surveillance (Huang and Zappasodi, 2022). Blocking immune checkpoint molecules, such as the Noble prize-winning inhibitory cytotoxic T lymphocyte associated antigen 4 (CTLA-4, Fig. 1) and programmed cell death protein 1 (PD-1; Fig. 1), prevents inhibitory signaling and restores T cell–mediated anti-tumor activity (Cameron et al., 2011; Freeman et al., 2000; Krummel and Allison, 1995; van Elsas et al., 1999). Based on these discoveries, therapeutic antibodies targeting PD-1 were developed, and anti-PD-1 antibodies received U.S. Food and Drug Administration (FDA) approval in 2014 for the treatment of advanced melanoma. Their clinical application has since been expanded to several additional cancer types, including non–small cell lung cancer (NSCLC) and renal cell carcinoma (Wolchok et al., 2017). Clinical studies have demonstrated that ICB therapy can induce durable responses in a subset of patients, with response rates ranging from 20 to 40 % in melanoma and lung cancer**,** with a minority achieving long-term remission (Hargadon et al., 2018). The approvals of anti-CTLA-4 and anti-PD-1 antibodies marked a major breakthrough in immunotherapy**,** highlighting the therapeutic potential of reversing immune escape mechanisms in cancer. However, not all patients respond, and severe immune-related adverse events, including colitis, dermatitis, and endocrinopathies can lead to the discontinuation of the therapies (Hargadon et al., 2018), highlighting the need for better and safer therapies.

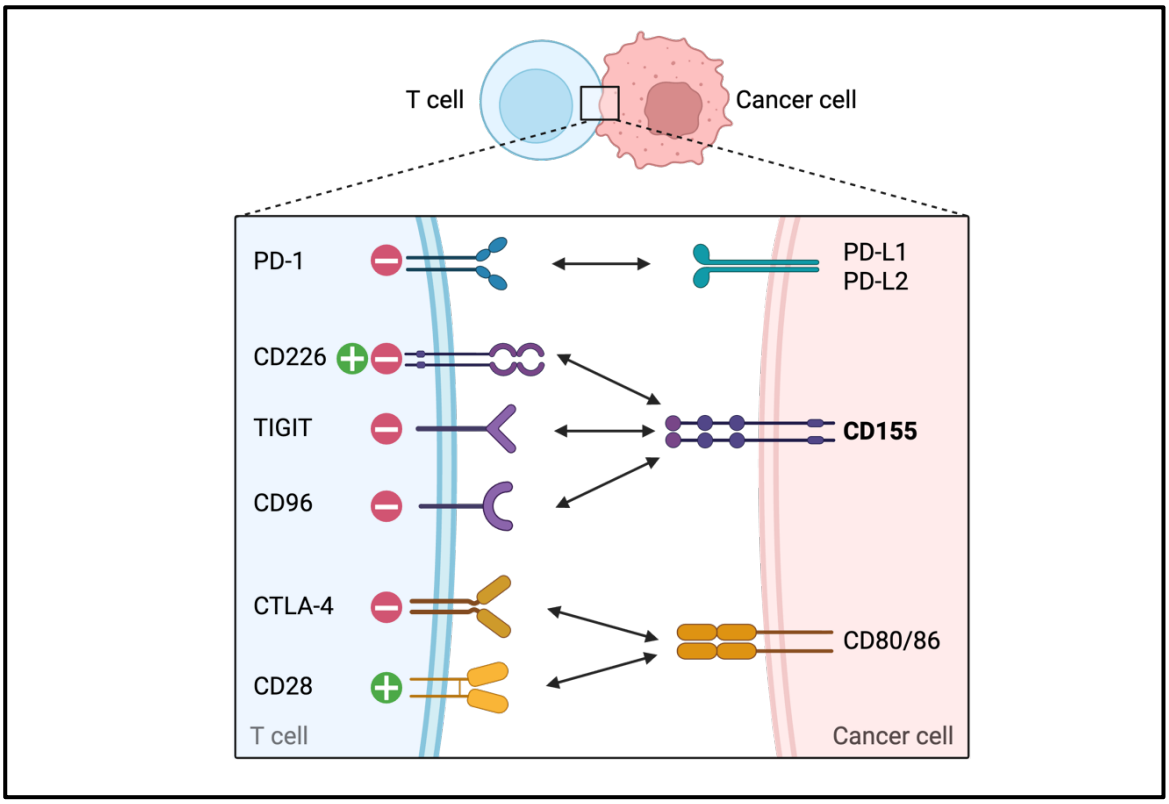

Figure 1: Immune checkpoints with respective ligands. *Plus (+) for stimulating, and minus (-) for inhibitory effect of receptor-ligand interaction in the T cell. Figure created with Biorender.*

1.2.3 Cancer-immunity cycle

While cancer immunoediting focuses on the immune escape of cancer cells, Mellman and colleagues developed the concept of the Cancer-Immunity Cycle to better describe the anti-cancer immune response (Chen and Mellman, 2013). The cancer-immunity cycle describes how our immune system is able to kill cancer cells. This process starts with the release of neoantigens by cancer cells, subsequently professional antigen presenting cells (APCs) are able to take up these neoantigens and present them on the Major Histocompatibility complex (MHC) class I or II (Chen and Mellman, 2013). The presentation of antigens is followed by priming and activation of T cells, which occurs in the tumor-draining lymph nodes. Finally, activated antigen specific T cells, known as cytotoxic T lymphocytes (CTLs), enter the blood stream in order to infiltrate into the TME.

Once the CTLs have entered the TME, they are able to recognize and destroy cancer cells in an antigen-dependent manner (Chen and Mellman, 2013). Cancer cells undergo apoptosis which consequently releases additional antigens. These antigens are taken up by APCs and presented on MHC class I and II to further activate CD8 and CD4 T cells, reinitiating the Cancer-Immunity Cycle. The Cancer-Immunity Cycle can be disturbed, allowing cancer cells to enter the equilibrium phase again, as previously described, and eventually escape immune surveillance.

A recent update on the Cancer-Immunity Cycle showed the importance of T-cell infiltration into the TME, highlighting not only the variability of T-cell infiltration between patients but also the dynamic within individual patients. To classify patients better, Mellman and colleagues described three different 'immunotypes': 'immune-inflamed, immune-excluded and immune-desert' (Mellman et al., 2023). The immune-inflamed subtype, also described as a hot TME, is characterized by high infiltration of immune cells and high expression of activation markers such as interferon gamma (IFN-γ). Patients with an immune-inflamed TME often show a better overall survival and better response to immune checkpoint blockades (Aliazis et al., 2025; Fridman et al., 2023; Mellman et al., 2023). On the other hand, the immune-excluded TME is known as a cold TME, it is characterized by low immune cell infiltration into the tumor and an immunosuppressive TME expressing transforming growth factor beta (TGF-ß) or interleukin 10 (IL-10). CD8+ T cells are present at the tumor margin but appear to be retained at this boundary, failing to infiltrate into the tumor core. Therefore, patients with an immune-excluded TME have a poor prognosis and poor response to immune checkpoint blockades. The third immunotype, known as immune-desert, shares features with the immune-excluded including low immune cell infiltration as well as an immunosuppressive TME. However, in immune-desert tumors both the tumor margin and the tumor core exhibit very low or absent immune cells with a lack of activation, which is associated with an even poorer prognosis for this subtype (Mellman et al., 2023). In melanoma, the concept of immune-desert versus immune-excluded tumors is relevant. Although immune-desert tumors

harbor some neoantigens and are potentially recognizable by the immune system, their lack of T-cell infiltration limits an immediate anti-tumor response. However, once immune cells infiltrate the immune-desert TME, these patients may respond more favourably to immune checkpoint blockade therapies compared to those with immune-excluded melanomas, where activated T cells are present at the margin but physically unable to enter the TME (Mellman et al., 2023).

1.3 Melanoma

1.3.1 Melanocytes are the origin of melanoma

Malignant melanoma is known to be an aggressive type of skin cancer. It arises from dysregulated proliferation of melanocytes, which are the pigment-producing cells of the skin. Melanocytes originate from the neural crest during embryonic development. They act as effectors through their ability to migrate across different layers of the skin (Marco Rastrelli et al., 2014). Although melanocytes are not classical APCs, they can produce various cytokines to help eliminate micro-organisms and viruses (Koike and Yamasaki, 2020). In addition, melanocytes are able to produce melanin which is important to protect cells of the skin against DNA damage caused by UV irradiation (Koike and Yamasaki, 2020; Marco Rastrelli et al., 2014; Shain and Bastian, 2016). The skin is the external barrier of the human body and melanocytes have a critical role including protection against UV and regulation of the temperature. These processes are both regulated by melanin (Lin and Fisher, 2007). In addition to the skin, melanocytes are present in adipose tissue, the inner ear, heart and nervous system. In these non-cutaneous sites, melanocytes contribute to protection against reactive oxygen species (ROS), ion and calcium buffering, and maintaining homeostasis, extending their functions beyond the classical role in skin pigmentation (Coutant et al., 2024; Santeufemia et al., 2023). Most primary melanoma cases arise in the skin, whereas melanocytes in non-cutaneous sites can rarely give rise to primary tumors but generally act as metastatic sites (Kim et al., 2012; Olszańska et al., 2021; Ozyuncu et al., 2006). The incidence of melanoma has increased every

year, and metastatic melanoma is responsible for 90 % of the skin cancer related deaths (Sun et al., 2025). To improve diagnosis, treatment and patient outcome, it is important to understand the underlying risk factors, enabling patient classification and targeted treatment opportunities.

1.3.2 Genetics and risk factors related to melanoma

1.3.2.1 Hereditary/Familial risk factors

Hereditary forms of melanoma account for 3-15 % of the cases worldwide (Debniak, 2004). The most frequent germline mutations in melanoma occur in cyclin-dependent kinase inhibitor 2A (*CDKN2A*) and cyclin-dependent kinase 4 (*CDK4*), which encode tumor suppressors that regulate the cell cycle. Mutations in these genes disrupt cell cycle checkpoint control and increase the lifetime risk of developing melanoma, particularly for *CDKN2A* where increased risk ranges from 14 % in Europe to as high as 91 % increased risk in Australia (Begg et al., 2005; Hussussian et al., 1994; Kamb et al., 1994; Zuo et al., 1996). Additional rare germline variants, such as *BAP1* and *MITF E318K*, have also been associated with familial melanoma susceptibility (Harbour et al., 2010; Paillerets et al., 2014).

1.3.2.2 Pigmentation genetics and indirect UV susceptibility

Genetic variants that affect pigmentation contribute to melanoma risk by modifying the skin's sensitivity to UV irradiation. Eumelanin and pheomelanin are two types of melanin that can be found in the skin, which are both produced by melanocytes (Nasti and Timares, 2015). Eumelanin is produced after activation of the melanocortin-1 receptor (MC1R), and it is important for the production of brown and black pigment. Eumelanin has an important role in both reducing the accumulation of photoproducts and absorbing UV radiation protecting against DNA damage (Nasti and Timares, 2015; Raimondi et al., 2008). Mutations in *MC1R* reduce eumelanin production and increase pheomelanin, which is common in individuals with freckles, red hair, or light skin. These individuals have

a 42 to 142 % higher risk of developing melanoma, due to increased accumulation of UV-induced DNA damage (Raimondi et al., 2008).

Downstream of MC1R is cyclic adenosine monophosphate (cAMP) which activates microphthalmia-associated transcription factor (MITF). MITF has been shown to regulate melanocyte pigmentation, proliferation, differentiation, survival and DNA repair (Giuliano et al., 2010; Strub et al., 2011). In addition, MITF expression plays a key role in regulating melanoma differentiation and shaping the TME. Melanoma cells with high expression of MITF are classified as more differentiated with an immune-cell poor TME. On the other hand, dedifferentiated melanoma cells express c-Jun, a negative regulator of MITF transcription, thereby promoting the recruitment of pro-inflammatory immune cells into the TME (Riesenberg et al., 2015). Taken together, studies have shown that the expression of MITF is important for melanoma progression as well as the differentiation status of melanoma cells, plasticity and response to therapy (Reinhardt et al., 2017; Riesenberg et al., 2015).

1.3.2.3 Environmental risk factors and somatic mutations

The primary risk factor for malignant melanoma is exposure to UV irradiation, responsible for the majority of cases. There are two different types of UV radiation UVA ranging from 315 to 400 nm and UVB ranging from 280 to 315 nm. UV exposure causes cytosine-to-thymidine mutations (C→T), the hallmark of UV-induced mutagenesis, which is present in up to 60 % of all cutaneous melanomas (Anna et al., 2007; Brash, 2015; Hodis et al., 2012; Setlow and Carrier, 1966). Individuals with inherited susceptibility, such as *MC1R* variants or fair skin, red or blonde hair are particularly sensitive to UV-induced DNA damage. As a result, these individuals are at increased risk of acquiring somatic driver mutations in genes such as B-raf proto-oncogene (*BRAF*)^{V600E} (60 % of cases) or NRAS proto-oncogene (*NRAS*, 15-20 % of cases) (Ellerhorst et al., 2011).

Neurofibromin 1 (*NF1*) mutations also contribute to melanoma by promoting melanocyte accumulation and tumor formation. A subgroup of melanomas, known as the Triple Wild-Type (WT) subtype, lack *BRAF*, *NRAS* and *NF1*

mutations. Instead, this subtype is characterized by more somatic copy-number alterations (CNA) compared to the other previously described molecular subtypes (Cancer Genome Atlas Network, 2015). While *BRAF*, *NRAS*, or *NF1* are commonly mutated in melanoma, HRAS proto-oncogene (*HRAS*) mutations account for only 1 % of subcutaneous melanoma cases (Santeufemia et al., 2023). Overall, melanoma is notable for having the highest frequency of somatic mutations caused by UV irradiation, highlighting the critical role of environmental exposure in tumor development (Lawrence et al., 2013).

1.3.3 Therapy of malignant melanoma

Early diagnosis of melanoma is critical. Stage I and II primary melanoma have a favourable prognosis, with surgical resection resulting in a five-year survival rate of 99 % (Saginala et al., 2021). In contrast, metastatic melanoma (stage IV) has a five-year survival rate of only 29.8 % (Erdei and Torres, 2010; Saginala et al., 2021). Screening and earlier detection of melanoma are important for reducing melanoma incidence and mortality (Bandi et al., 2021).

In past years, there has been a lot of developments in the treatment of metastatic melanoma. The first systemic therapy approved for melanoma was DNA-alkylating agent dacarbazine (DTIC) in 1975, with a response rate of only 10 to 15 % and minimal survival benefit (Eggermont and Kirkwood, 2004). Chemotherapy resistance reduces treatment efficacy and remains a problem in melanoma (Kalal et al., 2017). Later, IL-2 became the first FDA-approved immunotherapy (1998), demonstrating durable responses in a subset of patients with metastatic melanoma (Atkins et al., 1999; Rosenberg, 2014).

The identification of driver mutations enabled targeted therapies, particularly for *BRAF*-mutant melanoma. The targeted therapy BRAF inhibitor (Vemurafenib) selectively binds to the ATP binding domain of mutant *BRAF*, reducing mitogen-activated protein kinase (MAPK) pathway signaling (Bollag et al., 2010). Additional FDA-approved BRAF inhibitors are Dabrafenib and Encorafenib, which showed the best overall response rate when combined (Barbato et al., 2024; Schadendorf et al., 2024). MEK inhibitors are effective in 15-30 % of the NRAS

mutated melanomas, but resistance remains a problem (Landras et al., 2022). There are no approved treatments for *NRAS*- or *HRAS*-mutant melanomas, however, recent studies targeting NRAS mRNA have shown promising results. Feichtenschlager and colleagues showed the utility of targeting NRAS mRNA in melanoma cell lines and mouse models. They observed that blockade of NRAS mRNA reduced the mRNA levels of NRAS, consequently inhibiting the MAPK pathway which induced apoptosis and reduction in cancer growth in both *in vitro* and *in vivo* (Feichtenschlager et al., 2025). Effectively blocking oncogenic driver mutant mRNA represents a novel therapeutic approach for melanoma patients. However, while targeted therapies often show high initial response rates, their long-term efficacy is limited due to the development of resistance (Chapman et al., 2011), highlighting the need for more effective therapies.

Immunotherapies harnesses the patient's immune system to recognize and attack cancer cells. In 2011, the FDA approved an immunotherapy targeting CTLA-4 (Ipilimumab) for melanoma (Bollag et al., 2010; Hodi et al., 2010). Ipilimumab improves long-term survival despite a lower initial response, with a five-year survival rate of 26 % (Hodi et al., 2010; Larkin et al., 2019). Programmed cell death protein 1 (PD-1) is another improved target for immunotherapies with monoclonal antibody targeting PD-1 (Nivolumab), showing a five-year survival rate of 44 % in a cohort of more than 300 melanoma patients. Furthermore, combination of Ipilimumab with Nivolumab increased the survival rate to 52 % (Larkin et al., 2019). Another immune checkpoint target is LAG-3. Relatlimab (anti-LAG-3) in combination with nivolumab (anti-PD-1) was FDA-approved in 2022 for the treatment of unresectable or metastatic melanoma, marking the first LAG-3 inhibitor approval for the treatment of cancer (Chocarro et al., 2022; Tawbi et al., 2022). Tiragolumab (anti-TIGIT) has shown promising results in early-phase clinical trials for different cancer types, including melanoma, but is not yet FDA-approved. For instance, a Phase II trial from Hieken et al. (2025) investigated the combination of anti-PD-L1 with tiragolumab in patients with high-risk stage III melanoma. The study showed promising results and safety in 34 patients with stage III melanoma (Hieken et al., 2025).

Immunotherapy often provides durable long-term responses, highlighting its advantage over target therapy in terms of survival, although the initial response rates are limited.

Despite the great success of cancer immunotherapies and combinations, a significant group of patients show primary resistance (no initial response) or acquired resistance (relapse after initial response) to immunotherapy (Grzywa et al., 2017; Sharma et al., 2017). These limitations highlight the need to identify novel immunotherapy targets that can overcome resistance and improve long-term patient outcome.

1.4 Novel immune checkpoint CD155

1.4.1 Structure and function of CD155

An interesting target for novel immune therapy is Cluster of Differentiation 155 (CD155), which was discovered in in 1961 as the polio virus receptor (PVR) (Bowers et al., 2017; Holland and McLaren, 1961; Mendelsohn et al., 1989). Mendelsohn et al. 1989 were the first to describe that CD155 exists of immunoglobin-like domains indicating that it has more functions beyond poliovirus entry (Mendelsohn et al., 1989). CD155 is also known by several alternative names, including NECL-5 (Nectin-like molecule 5), Herpesvirus entry mediator D (HVED), and Tumor-Associated Glycoprotein E4 (TAGE4) but in this thesis CD155 will be used.

CD155 is a type I transmembrane adhesion molecule composed of three main regions. The extracellular region of CD155 contains immunoglobin-like glycoprotein loops, which consists of three immunoglobin-like domains: V is the variable domain and C1 and C2 are consistent domains (Fig. 2) (Chadéneau et al., 1994, 1996; Koike et al., 1990; Mendelsohn et al., 1989). The V domain is important for binding to poliovirus and its three known ligands: DNAX accessory molecule (DNAM-1, CD226), TIGIT and CD96 (Fuchs et al., 2004; Tahara et al., 2024; Zhang et al., 2008). Furthermore, both consistent domains C1 and C2 are able to bind the poliovirus and important for the extracellular structure of CD155

(Kučan Brlić et al., 2019; Tahara et al., 2024; Zhang et al., 2008). The binding between the immunoglobin-like domains within CD155 is flexible and the domains are highly glycosylated, which are both important for its binding to vitronectin for adhesion or to its ligands for its immune regulatory role (Kučan Brlić et al., 2019; Lange et al., 2001; Tahara et al., 2024; Zhang et al., 2008). The other regions of CD155 are the transmembrane part, which is important to anchor the receptor in the plasma membrane, and the cytoplasmic tail, which includes an immunoreceptor tyrosine-based inhibitory motif (ITIM) (Fig. 2) (Koike et al., 1990).

There are four different isoforms of CD155 described, two transmembrane isoforms (α and δ) and two soluble isoforms (γ and β). Both transmembrane isoforms contain an ITIM domain (Fig. 2), which is absent in the soluble isoforms (Koike et al., 1990). These intracellular ITIM domains in transmembrane isoforms α and δ are phosphorylated upon receptor engagement, recruiting Src homology region 2 domain-containing phosphatase (SHP-2) (Oda et al., 2004; Sullivan et al., 2013). Subsequently, focal adhesion kinase (FAK) is dephosphorylated resulting in inhibition of its kinase function, which promotes cell adhesion and migration as well as inhibitory immune pathways (Kakunaga et al., 2004; Lange et al., 2001; Oda et al., 2004; Ohka et al., 2001; Sullivan et al., 2013). These functions are well known for Nectin-like molecules (Takai et al., 2008, 2003).

Furthermore, glycosylation of CD155 plays an important role in its interaction with binding ligands (Fig. 2). CD155 has five predicted N-glycosylation sites (Zhang et al., 2008). Among its three known ligands (CD226, TIGIT and CD96), glycosylation has been described to play a role in the stability and confirmation of CD155 and therefore modulating binding to CD226 or TIGIT (Fuchs et al., 2004; Tahara et al., 2024; Zhang et al., 2008). However, the potential impact of glycosylated CD155 and its interaction with the third ligand CD96 has not yet been investigated.

The γ and β secreted soluble isoforms of CD155 (sCD155) can compete with the transmembrane CD155 isoforms (Okumura et al., 2020) to potentially interfere

with immune regulation. In addition, several studies described sCD155 as a biomarker for cancer progression in breast, gastric, lung and gynaecological cancers (Iguchi-Manaka et al., 2016; Okumura et al., 2020).

For the purpose of this study, we focused on the transmembrane forms of CD155 expressed on cancer cells.

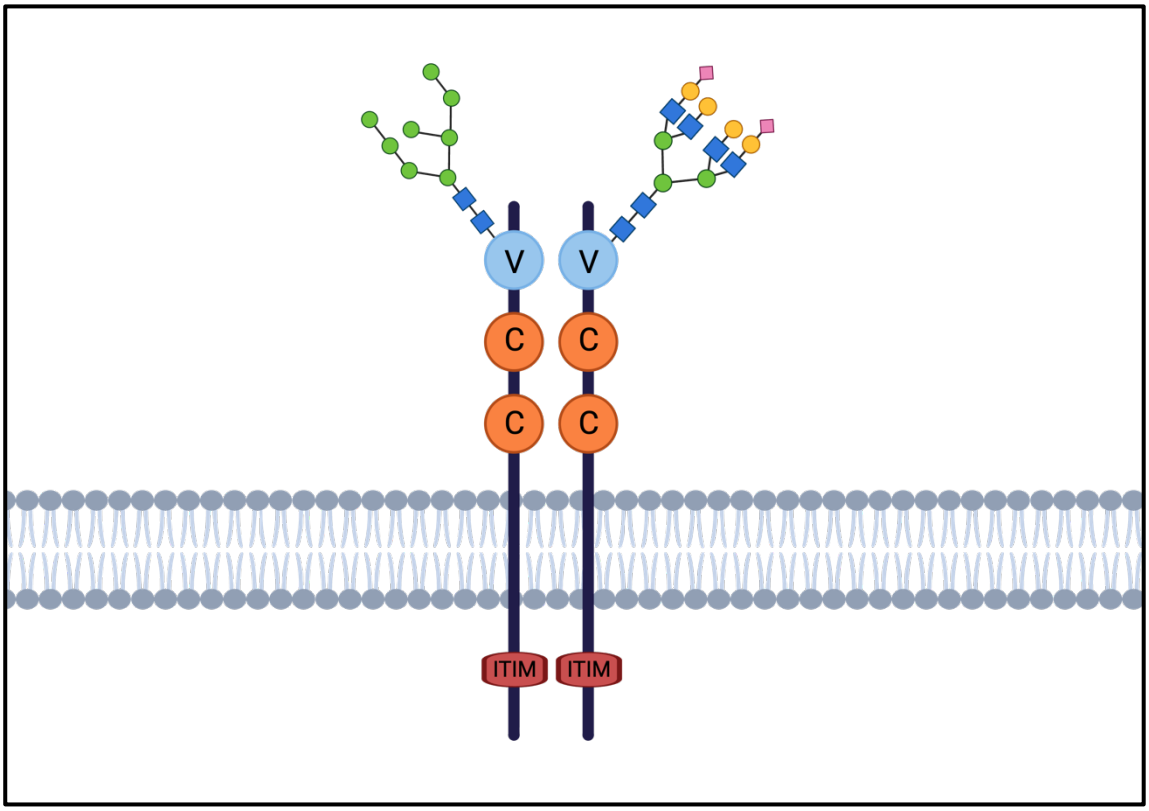

Figure 2: Schematic structure of human CD155. *Showing intracellular ITIM domain (red), and extracellular C-terminal domains (orange) and variable domain (blue) including glycosylation branches.*

1.4.2 CD155 overexpression in cancer

CD155 is expressed at low levels in healthy tissues such as lung, liver, kidney, testes and during phases of development in mesenchymal and ventrally nervous system structures (Molfetta et al., 2020; Solecki et al., 2002). As an adhesion molecule, CD155 is also expressed on endothelial cells at low basal levels, where it induces trans endothelial migration (TEM) (Escalante et al., 2011; Muller, 2009;

Reymond et al., 2004). TEM is important to maintain immune homoeostasis as it can induce an immune response after leukocytes are able to migrate out of the blood stream into the tissue via cell-to-cell junctions (Muller, 2009). In immune cells, CD155 is expressed in low levels on DCs, monocytes and macrophages under healthy conditions in human cells, but upregulated under stress or inflammatory conditions, such as sepsis based on a combination of human *ex vivo* data and *in vivo* experimental models (Fuchs et al., 2004; Fuchs and Colonna, 2006; Yan, 2015; Zhong et al., 2024).

In contrast to the low expression levels in healthy tissues, CD155 is known to be overexpressed in a wide range of cancers, including melanoma, glioblastoma, leukemia, lung, breast, cervical, head and neck, colorectal, liver, pancreatic and gastric cancer (Fig. 3A). Overexpression of CD155 is associated with poor prognosis and increased tumor progression (Abdalla et al., 2025; Bowers et al., 2017; Carlsten et al., 2009; Castriconi et al., 2004; Gromeier et al., 2000; Iguchi-Manaka et al., 2016, 2008; Liu et al., 2025; Masson et al., 2001; Nakai et al., 2010; Ochiai et al., 2004; Pende et al., 2005). Given its upregulation across different cancers and low expression in healthy tissue, CD155 represents a promising target for cancer therapy.

Several mechanisms have been described to contribute to elevated CD155 levels. While gene amplification can lead to an increased gene copy number, this is relatively rare for CD155, indicating that overexpression is driven by additional factors (O'Donnell et al., 2020) (Fig. 3B). Epigenetic regulation, such as DNA methylation or histone modifications, can enhance transcription. In breast cancer, high methylation of CD155 has been associated with elevated CD155 mRNA expression and tumor progression, which has been shown in both Formalin-Fixed Paraffin-Embedded (FFPE) and frozen biopsy samples (Triki et al., 2021). Besides epigenetic regulation, oncogenic signaling pathways have been reported to upregulate CD155 expression including MAPK and PI3K/AKT pathway, as well as extrinsic factors present in the TME, such as hypoxia, inflammatory cytokines (IL-22 and IFN-γ), and the activation of ataxia telangiectasia mutated (ATM) and ATM and Rad3-related (ATF) protein kinases (Fig. 4) (Ardolino et al., 2011;

Escalante et al., 2011; Hirota et al., 2005; Liu et al., 2013; Soriani et al., 2009, 2009; Triki et al., 2021). Additionally, post-translational stabilization of CD155 protein may contribute to its accumulation at the surface of cancer cells (Tahara et al., 2024).

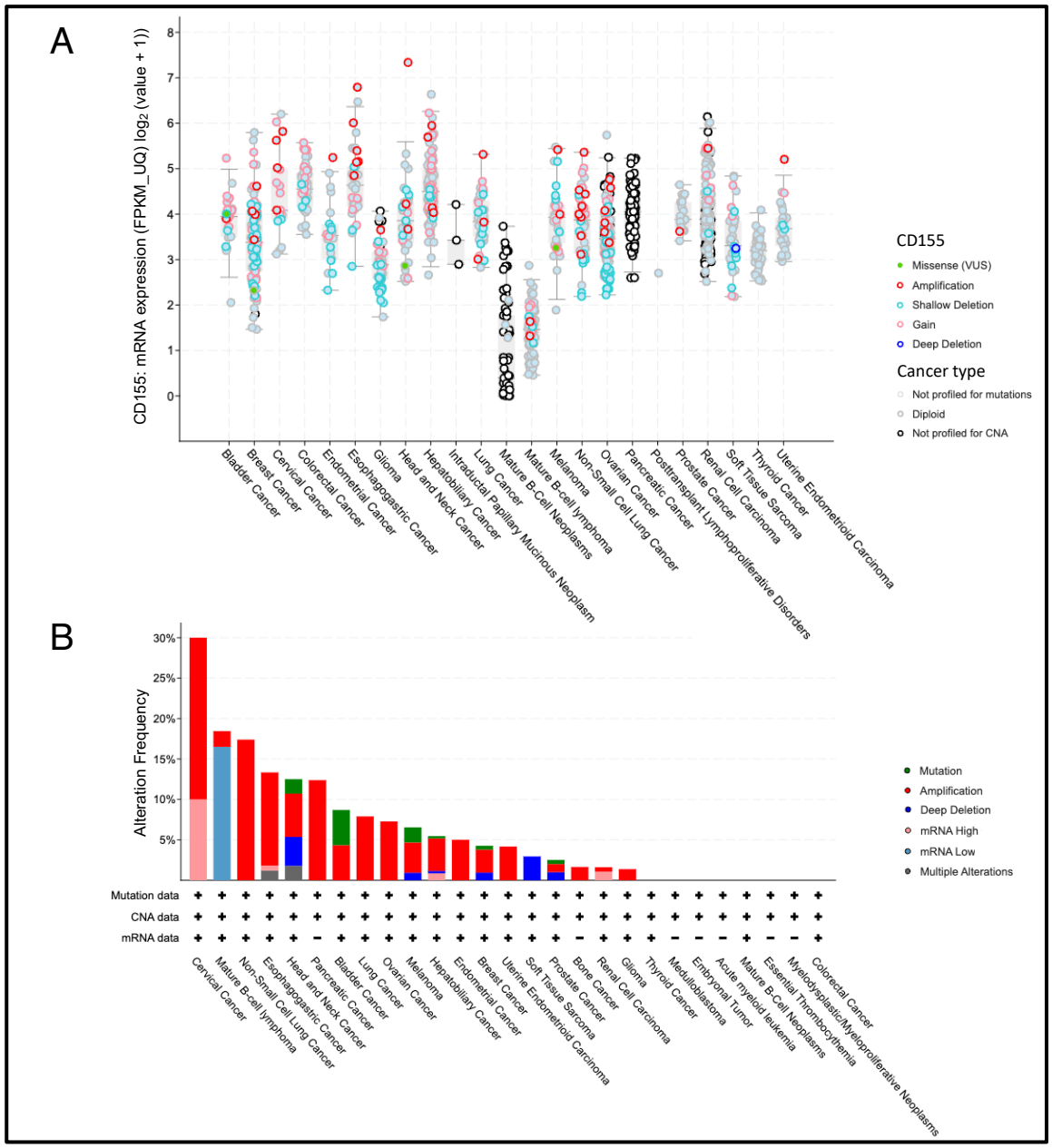

Figure 3: Expression of CD155 and alteration frequency across human cancer types. *A) TCGA data from 2020 showing mRNA expression levels of CD155/PVR across different cancer types. Red = amplification, >1 increase in number of copies of the gene; pink = gain, 1, few additional copies of the gene;*

grey = diploid, 0, normal number of copies of the gene, light blue = shallow deletion, -1; dark blue = deep deletion, -2; black = no profile available for copy number alterations (CNA). B) TCGA data from 2020 showing alteration frequency of CD155 across different cancer types. Green = mutation, red = amplification, blue = deep deletion, pink = mRNA high, light blue = mRNA low, grey = multiple alterations. Different data per cancer + (presence) or – (absence) of mutation data, CNA data, and mRNA data.

1.4.3 Role of CD155 in cancer

The broad, high expression of CD155 across a variety of different cancer types and its low expression in healthy tissues and immune cells, render CD155 a very promising target for novel cancer therapies. Studies have shown that increased CD155 expression is associated with reduced overall survival, advanced tumor stages, higher tumor grade, lymph node (LN) metastasis and other metastasis (Cho et al., 2025; Liu et al., 2019; Tahara et al., 2024; Wang et al., 2022; Zhang et al., 2022). Due to overexpression, CD155 is able to promote tumor cell adhesion, invasion, migration, proliferation, and more interestingly it has an immune modulatory effect (Wang et al., 2022).

CD155 has three different interaction partners including CD96, CD226, and TIGIT (Fig. 4). TIGIT and CD96 are inhibitory immune checkpoints containing an intracellular ITIM, which after binding to CD155 reduce cell proliferation as well as cytokine production resulting in inhibition of the immune response (Chan et al., 2014; Zhang et al., 2016). Given the inhibitory immune function of TIGIT and CD96 upon binding to CD155, these receptors have emerged as promising targets for cancer immunotherapy (Dougall et al., 2017). Inhibition of TIGIT or CD96 may restore immune cell activity and enhance anti-tumor responses by promoting the recognition and elimination of cancer cells. CD155 has different binding affinities to its ligands. The highest binding affinity is between TIGIT and CD155, followed by CD96 (Yu et al., 2009) (Fig. 4). The third ligand with the lowest binding affinity to CD155 is CD226, which has an Immunoreceptor Tyrosine-based Activation like (ITT) domain (Bottino et al., 2003; Chan et al.,

2014; Tahara-Hanaoka et al., 2004). Although CD226 has the lowest binding affinity to CD155, studies have shown that it plays a critical role in promoting immune escape. Braun et al. (2020) showed that upon binding to CD155, CD226 undergoes internalization and proteasomal degradation in CD8+ T cells in mice, leading to immune escape and resistance to immunotherapies in melanoma (Braun et al., 2020). On the contrary, when CD226 is expressed on NK cells or CTLs it is inducing cytotoxic responses (Shibuya et al., 1996).

Furthermore, studies have shown that a knock-down or knock-out of CD155 in either mice or human cancer models can reduce the tumor burden (Abe et al., 2009; Braun et al., 2020; Kawashima et al., 2021; Kono et al., 2008; Mensurado et al., 2024; Sloan et al., 2004; Tane et al., 2013; Xiong et al., 2025; Zheng et al., 2018). Three major effects have been reported across different studies after CD155 knock-out, which are highlighting the importance of the receptor. First, studies have shown that loss of CD155 impairs tumor intrinsic mechanisms, thereby increasing the susceptibility of tumor cells to immune-mediated killing. In addition, CD155 knock-out has been shown to reduce migration, proliferation and metastasis (Braun et al., 2020; Xiong et al., 2025). Second, CD155 knock-out enhances anti-tumor immunity since cells with loss CD155 are unable to engage with inhibitory ligands TIGIT or CD96, as well as activating ligand CD226. The lack of binding to CD226 prevents its internalization, the presence of CD226 allows other ligands to bind and activate CD226, thereby inducing an immune response (Braun et al., 2020; Kawashima et al., 2021; Wang et al., 2022). Studies have shown that high expression of CD155 is linked to resistance to ICBs in several cancers, therefore knock-out of CD155 or blockade of the CD155-axis can make tumors susceptible for ICBs (Johnston et al., 2021; Kawashima et al., 2021). Taken together, these findings demonstrate that CD155 is overexpressed across multiple cancer types, has an immune regulatory role, and that CD155 knock-out enhances anti-tumor immunity. Moreover, targeting CD155 can help to prevent resistance to ICBs. Altogether, these findings highlight the importance of understanding the regulation of CD155 to improve the treatment of cancer.

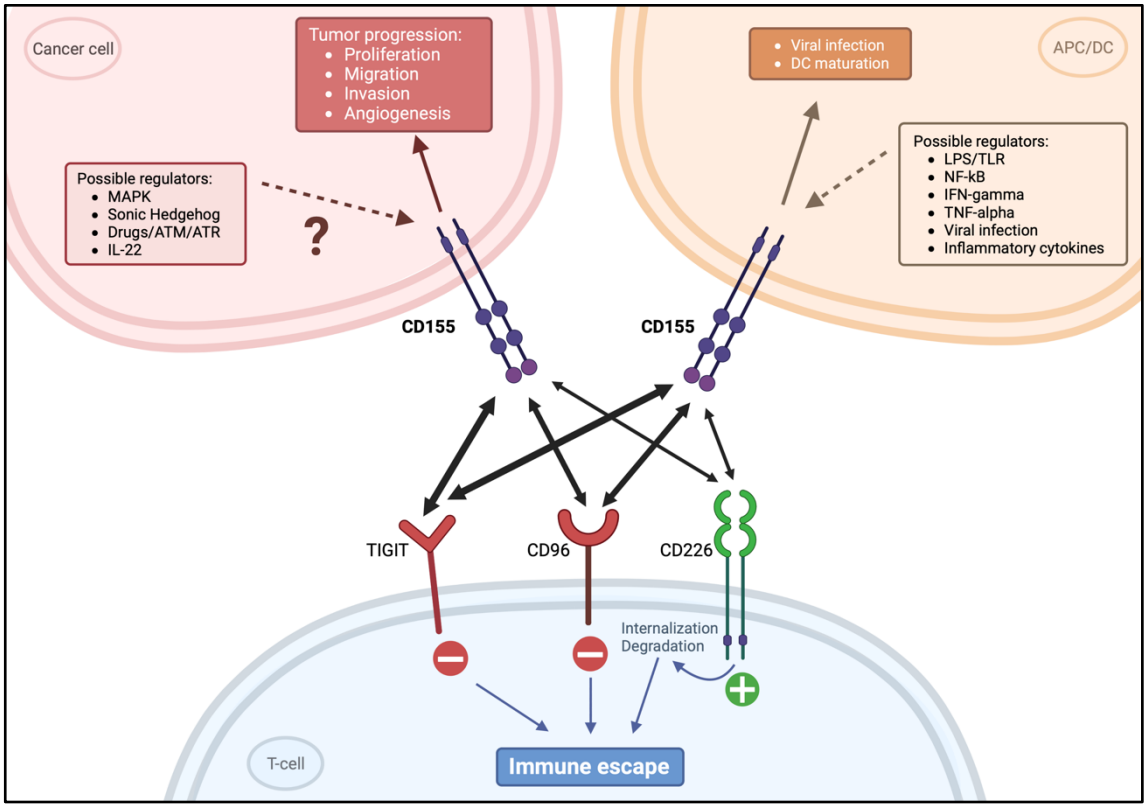

Figure 4: The functions of CD155 and potential regulators of CD155 expression in cancer cells and APCs/DCs. *CD155 has pleiotropic functions contributing to tumor progression and resistance. Its broad expression across a variety of different cancer types, low expression on healthy and immune cells, render CD155 a very promising target for novel cancer therapies. Possible regulators of CD155 are shown based on different in vitro and in vivo studies. However, key pathways regulating the expression of CD155 in cancer remain elusive (depicted as question mark in the cancer cell). The thickness of arrows depicts the binding affinity for CD155 of the following inhibitory ligands TIGIT (highest affinity), CD96 (middle affinity), and activating CD226 (lowest affinity) which are all inducing immune escape. Figure created with Biorender.*

1.4.4 Intrinsic regulation of CD155 in normal and malignant settings

Despite the role of CD155 in immune regulation and its overexpression across multiple tumor types, little is known about the intrinsic regulation of CD155 in cancer. In a healthy setting during embryonic development, the expression of

CD155 has been shown to be induced by the sonic hedgehog pathway (Fig. 4), activating protein 2 (AP-2), NRF, and transcription factor Gli (Solecki et al., 2002). This experiment was *in vitro* based on transcriptional promoter assays in only two human cell lines (Solecki et al., 2002), and no additional studies support this hypothesis. In mice, activating protein 1 (AP-1) and V12Ki-Ras have been shown to upregulate expression of CD155 and activate the MAPK pathway (Fig. 4) (Hirota et al., 2005), which is consistent with the human data as both receptors belong to AP-1/AP-2-family and may have analogous roles in immune regulation. These studies suggests that CD155 regulation may differ between human and mice, but the sonic hedgehog pathway and APs are important in both species.

On APCs, the expression of CD155 has been shown to be induced by toll like receptor ligands (Kamran et al., 2013). CD155 expression in mouse embryonic fibroblast cell lines was upregulated after treatment with fibroblast growth factor (FGF) or transfection with oncogenic Ras, suggesting that activation of the Ras-Raf-MEK-ERK signaling pathway might contribute to the regulation of CD155 expression (Fig. 4) (Hirota et al., 2005), and therefore different oncogenic driver mutations such as *BRAF*, *HRAS*, and *NRAS* could potentially influence CD155 expression. In human vascular endothelial cells, CD155 is present in low levels, but can be upregulated in response to inflammatory cytokines such as IFN-γ (Fig. 4) (Escalante et al., 2011). This suggests extrinsic regulation of CD155 by IFN-γ in human cells.

Several studies have investigated additional factors and treatments that extrinsically modulate CD155 expression on cancer cells (Fig. 4). For instance, Makhloufi et al. (2020) showed that IL-8 produced by patient bone marrow stromal cells, upregulates CD155 expression on human multiple myeloma cells *in vitro*. This upregulation is potentially mediated via the NF-κß pathway (Fig. 4) (Mekhloufi et al., 2020). Similarly, another interleukin, IL-22, has been shown to upregulate CD155 expression on mouse breast and lung cancer cell lines (Fig. 4), which was associated with activation of the STAT3 signalling pathway downstream (Briukhovetska et al., 2023). In prostate cancer cell lines, androgen signaling drives nuclear localization of the androgen receptor, which binds to

CD155 enhancers, leading to increased CD155 transcription, elevated expression levels, and enhanced immune suppression (Wang et al., 2020). Consistently, they showed that CD155 expression was reduced in prostate cancer patient samples treated with androgen ablation, highlighting the role of androgen receptor in regulating CD155 expression (Wang et al., 2020).

In addition to extrinsic factors, intrinsic factors can also regulate CD155 expression. These intrinsic factors include stress and DNA damage, which both have been reported to induce CD155 expression. ROSs and DNA damage responses (DDRs) activate kinase pathways that stabilize and activate of E2F transcription factor 1 (E2F1), demonstrating that E2F1 acts as a transcriptional activator of CD155 in various human cancer cell lines, including cervical and colorectal carcinoma (Soriani et al., 2014, 2009). Another study supporting this mechanism showed that inhibition of E2F1 activity reduced CD155 expression in human breast cancer cell lines (Shrestha et al., 2023). They treated human breast cancer cell lines with small molecules targeting CDK4/6 and analysed CD155 expression. Interestingly CDK4/6 inhibition also reduced surface expression of PD-L1 on breast cancer cells (Shrestha et al., 2023), suggesting that these pathways regulate a broader set of surface receptors rather than specifically CD155.

Consistent with this broader surfaceome regulation, a study in murine ovarian cancer model showed that inhibition of FAK reduces CD155 protein expression as well as PD-L1 and Nectin-2 (Ozmadenci et al., 2022). On the other hand, lactic acid which is a by-product of glycolysis has been shown to induce CD155 and PD-L1 expression in human breast cancer cell lines (Shrestha et al., 2023). Taken together, these treatments with CDK4/6 inhibitors, FAK inhibitors, or lactic acid do not specifically downregulate CD155 expression but instead modulate a broader spectrum of the cancer cell surfaceome.

Post-translational modification of CD155 is another intrinsic mechanism that has been shown to modulate its function. Glycosylation of CD155 is critical for its immune regulatory role, mediating the binding to two of its three different ligands,

TIGIT and CD226 (Fuchs et al., 2004; Tahara et al., 2024; Zhang et al., 2008). Another post-translational modification, SUMOylation, has been reported to play an important role in protein activity (Song et al., 2004). In human multiple myeloma cell lines, the SUMO pathway has been shown to regulate the CD155 expression by modifying CD155, thereby controlling its subcellular location. Inhibition of the SUMO pathway, either pharmacologically or genetically, induced translocation of CD155 to the plasma membrane, resulting in upregulation of surface CD155 expression on human multiple myeloma cell lines (Zitti et al., 2017). These findings are indicating that the SUMOylation of CD155 reduces CD155 surface expression in multiple myeloma. In addition to posttranslational modification of proteins, epigenetic changes can intrinsically regulate CD155 expression. Methylation of CD155 reduces its expression, whereas hypomethylation of CD155 increases its surface expression on breast cancer tissue (Triki et al., 2021). These findings highlight that post-translational modification, including adhesion mediated stabilization and internalization of CD155, as well as epigenetic changes, critically influence CD155 expression and function. Understanding the intrinsic mechanisms regulating CD155 expression is important for improving cancer immunotherapies in melanoma and other cancers.

1.5 Objective of this study

Melanoma is a highly aggressive form of skin cancer. While targeted treatments show a strong initial response, resistance remains a problem resulting in a five-year progression free survival rate of only 19 % (Caroline Robert et al., 2019). In contrast, treating melanoma with immunotherapies shows lower initial response rates but better long-term response (Larkin et al., 2019). Therefore, there is an unmet need for novel immunotherapies to improve patient outcomes. CD155 has emerged as a novel target for immunotherapy due to its immune modulatory role, low expression in healthy tissues, which may protect against potential toxicities, and its overexpression across various cancer types, where it is associated with poor patient outcomes. Therefore, understanding the intrinsic regulation of CD155 holds great potential as a novel immunotherapy target for the treatment of melanoma and other cancers. However, the mechanism underlying the intrinsic regulation of CD155 in cancer remain largely unknown.

The central objective of this study was to identify novel targets and pathways involved in the intrinsic regulation of CD155, with the goal of improving cancer immunotherapies in melanoma and potentially in additional tumor types. In this study, CD155 was characterized across different human cancer cell lines. To investigate the intrinsic regulation of CD155 in an unbiased manner, genome-wide CRISPR knock-out screens and subsequent validation experiments were conducted in human melanoma cell lines to address the following aims:

1. Characterisation of CD155 surface expression in human cancer cell lines (Chapter 3)
2. Identification of molecular signaling pathways regulating CD155 surface expression in human melanoma (Chapter 4)
3. Validation using pharmacological and genetic approaches to test their relevance in regulating CD155 surface expression in human melanoma (Chapter 5)

Materials and methods

2.1 Materials

2.1.1 Antibodies

Table 1: Overview of the antibodies used in this study

This table shows the antibody name, clone, dilution, application and company.

Antibodies	Application	Company
Anti-human CD155 APC Fire 750 (SKII.4 1:50-100)	FACS	Biolegend
Human TruStain FcX™ (Fc Receptor Blocking Solution, 1:200)	FACS	Biolegend
ViaStain AOPI (1:10000, CS2-0106-5ML)	FACS	Revvity
Goat Anti-Mouse IgG Antibody, HRP conjugate (12-349, 1:2000)	WB (secondary ab)	Sigma Aldrich
Goat anti-Rabbit IgG (H+L) Secondary Antibody, HRP (31460,1:2000)	WB (secondary ab)	Thermo Fisher Scientific
Cas9 (S. pyogenes) Rabbit mAb (7A9-3A3, 1:50)	WB (primary ab)	Cell signaling
ß-Actin Mouse mAb (1:2000)	WB (primary ab)	Cell signaling
Akt (pan) Rabbit mAb (C67E7, 1:1000)	WB (primary ab)	Cell signaling
Phospho-Akt (p-AKT) (Ser473) (587F11) Mouse mAb (1:1000)	WB (primary ab)	Cell signaling
Donkey anti-mouse IRDye 680 LT (4051, 1:15000)	WB (secondary ab)	LI-COR Biosciences

Donkey anti-rabbit IRDye 800 CW (1:15000)	WB (secondary ab)	LI-COR Biosciences

2.1.2 Bacteria strains

Table 2: Overview of the bacteria strains used in this study

The table shows the bacteria strains and the origin/source.

Bacteria	Origin/source
Chemically competent Escherichia coli DH10Beta	Originally obtained from the laboratory of Veit Hornung, University Hospital Bonn
ElectroMAX™ Stbl4™ Competent Cells	Thermo Fisher Scientific
One Shot™ Stbl3™ Chemically Competent E. coli	Thermo Fisher Scientific

2.1.3 Cell culture media and supplements

Table 3: Overview of cell culture media and supplements used in this study

The table shows the cell culture media, supplements, concentration, and the company.

Cell culture media and supplements	Company
DMEM	Gibco - Life Technologies
DPBS	Gibco - Life Technologies
EDTA	Carl Roth
Fetal Bovine Serum (FBS/FCS)	Gibco - Life Technologies

HBS 2X	Media preparation Unit - ONJCRI
L-Glutamine	Gibco - Life Technologies
Penicillin – Streptomycin (10000 U/mL)	Gibco - Life Technologies
RPMI 1640 Medium, GlutaMAX™ Supplement	Gibco - Life Technologies
RPMI1640	Gibco - Life Technologies
TrypleE	Gibco - Life Technologies
Trypsin-EDTA (0.05 %)	Gibco - Life Technologies
Complete RPMI cell culture medium	10 % FBS + 1 % pen/strep + RPMI
Complete DMEM cell culture medium	10 % FBS + 1 % pen/strep + DMEM
Freezing medium	10% DMSO + complete RPMI or FBS
Opti-MEM® I, reduced serum medium	Gibco - Life Technologies
ß-Mercaptoethanol (55 mM in DPBS)	Gibco - Life Technologies
TNF-alpha (1000 U/mL)	PeproTech

IFN-gamma (1000 U/mL)	PeproTech
LPS (1 µg/mL)	PeproTech
BEZ235 (5 µM)	SelleckChem
MK2206 (4 µM)	SelleckChem
GSK-690693 (5 µM)	SelleckChem
Q-VD-Oph (20 µM)	SelleckChem
ZSK474 (5 µM)	SelleckChem

2.1.4 Chemicals and reagents

Table 4: Overview of chemicals and reagents used in this study

The table shows buffers, chemicals and the company.

Buffers, chemicals and reagents	**Company**
Agar Agar	Carl Roth
Agarose	Carl Roth
Ampicillin	Carl Roth
Broad Range Markers	Santa Cruz

Calcium chloride (CaCl2)	Carl Roth
Dimethyl sulfoxide	Carl Roth or Sigma-Aldrich
Ethanol	Carl Roth
Gel Loading Dye Purple (6X)	New England BioLabs
GeneRuler 100bp DNA Ladder	Thermo Fisher Scientific
GeneRuler 1kB DNA Ladder	Thermo Fisher Scientific
Glycerol	Carl Roth
H2O Ampuwa	Fresenius
Interferon-gamma (IFN-γ), human	PeproTech
Isopropanol	Carl Roth
Methanol	Carl Roth
Roti Histofix	Carl Roth
SDS (sodium dodecyl sulphate)	Carl Roth

Spectra™ broad range multicolour (26634)	Thermo Fisher Scientific
SYBR™ Safe DNA Gel Stain	Thermo Fisher Scientific
Tris	Carl Roth
Triton X-100	Sigma-Aldrich
Trypan blue solution	Sigma-Aldrich
Tween-20	Carl Roth

2.1.5 Commercially available buffers and reagents

Table 5: Overview of commercially available buffers and reagents used in this study

The table shows commercially available buffers, reagents and the company.

Commercially available buffers and reagents	Company
5X HiScript II QRT SuperMix	Vazyme Biotech Co.
Abemaciclib (1 µM)	Selleckchem
Blasticidin S hydrochloride	Sigma-Aldrich
BSA	Sigma-Aldrich
CalciumChloride	Sigma-Aldrich

Dactolisib (BEZ235) (5 μM)	Medchem Express
DAPI (1:1000)	Thermo Fisher Scientific
dNTPs	Thermo Fisher Scientific
Doxycycline (hydrate)	Cayman
DPBS (Dulbecco's Phosphate Buffered Saline)	Gibco - Life Technologies
GSK-690693 (4 μM)	Medchem Express
H2O Ampuwa	Fresenius
HBS	Media preparation Unit - ONJCRI
LB-medium (Lennox)	Carl Roth
LIVE/DEAD fixable blue staining kit	Thermo Fisher Scientific
Luna Universal qPCR Master Mix M3003E	New England BioLabs
MK-2206 dihydrochloride (MK-2206 (2HCl)) (2 μM)	Medchem Express
Magnesium chloride	Carl Roth

NEBuffer™ r2.1	New England BioLabs
NEBuffer™ r3.1	New England BioLabs
Phosphatase inhibitor cocktail tablets	Roche
Polybrene	Sigma-Aldrich
Proprium iodide (PI) (1:1000)	Sigma-Aldrich
Protease inhibitor cocktail tablets	Roche
Puromycin (dihydrochloride)	Cayman
Q-VD-Oph (QVD) (20 μM)	Medchem Express
RIPA lysis buffer	Merk Millipore
RLT buffer	Qiagen
RW1 buffer	Qiagen
S-broth	Media preparation Unit - ONJCRI
SOC media	Thermo Fisher Scientific

TBST	BioRad
UltraPure™ DNase/RNase-Free Distilled Water	Thermo Fisher Scientific
Zombie Green™ Fixable Viability Kit	BioLegend
ZSTK474 (5 µM)	Medchem Express
Zymo RNA wash buffer	Zymo Research

2.1.6 In house made buffers, chemicals and reagents

Table 6: Overview of in house made buffers, chemicals and reagents used in this study

The table shows commercially available buffers, reagents and the company.

In house made buffers, chemicals and reagents	Recipe
Annealing buffer	100 mM NaCl 50 mM HEPES in H2O, pH 7.4
Blotting buffer (1X)	25 mM TRIS 192 mM Glycine 20 % Methanol in H2O
BSA blocking buffer	50 g/L Albumin Fraction V in TBS-T
Direct lysis buffer (DLB)	10 mM Tris-HCl 1 mM CaCl2 1 mM MgCl2 1 mM EDTA 1% Triton X 100

FACS buffer	DPBS 10 % FCS 0.2 mM EDTA
Laemmli buffer (1X)	120 mM 1 M Tris-HCl pH 6.8 20 % Glycerol 4 % SDS 20 mM β-Mercaptoethanol 0.02% Bromophenol-blue
LB agar	20 g/L LB 15 g/L Agar in H2O
LB medium	20 g/L LB in H2O
Plasmid miniprep buffer N3	4.2 M Guanidine Hydrochloride 0.9 M Potassium acetate in H2O, pH 4.8
Plasmid miniprep buffer P1	50 mM Tris-HCl 10 mM EDTA 100 µg/mL RNAse A in H2O, pH 8.0
Plasmid miniprep buffer P2	200 mM NaOH 1 % SDS in H2O
Plasmid miniprep buffer PE	10 mM Tris-HCl 80 % Ethanol in H2O, pH 7.5
Roti Histofix	Carl Roth
Running buffer (10X)	25 mM TRIS 192 mM Glycine 0.1 % SDS in H2O
TAE buffer (1X)	40 mM Tris pH 8.0 20 mM Acetic acid 1 mM EDTA in H2O
TBS buffer (10X)	30 g/L Tris base 80 g/L NaCl in H2O, pH 7.6 (titration with HCl)

TBS-T buffer	10 % TBS buffer (10x) 0.05 % Tween-20 in H2O
Tris (1 M, pH 6.8)	121.1 g/L Tris base in H2O, pH 6.8 (titration with HCl)

2.1.7 Commercially available kits

Table 7: Overview of commercially available kits used in this study

The table shows commercially available kits and the company.

Commercially available kits	Company
PureLink™ HiPure Plasmid Midiprep Kit	Life Technologies
NucleoSpin® RNA kit	Macherey-Nagel
NucleoSpin® Tissue kit	Macherey-Nagel
MEGAquick-spin™ Plus Total Fragment DNA Purification Kit	iNtRON Biotechnology
RNeasy® Plus Mini Kit	Qiagen
MiSeq® v2 reagent kit	Illumina

2.1.8 Enzymes

Table 8: Overview of enzymes used in this study

The table shows enzymes and the company.

Name	Company
Proteinase K	Qiagen
PureLinkTM RNase A	Invitrogen

Q5® High-Fidelity DNA Polymerase	New England Biolabs
RNAse A	Life Technologies
RNAse A	Thermo Fisher Scientific
T4 DNA Ligase	New England Biolabs
T4 Polynucleotide Kinase	New England Biolabs
Restriction enzymes (BbsI, BsmBI-v2)	New England Biolabs

2.1.9 Experimental models

Table 9: Overview of experimental models used in this study

The table shows the experimental models and the origin/source.

Cell lines	**Origin/source**
Human: HEK293T	ATCC (CRL-3216) Human embryonic kidney cells used for the generation of retroviral particles for transduction.
Human: MaMel15	From Julia Reinhardt, originally from (S. Urugel et al. 2007)
Human: MaMel37a	From Julia Reinhardt, originally from (S. Urugel et al. 2007)
Human: MaMel48a	From Julia Reinhardt, originally from (S. Urugel et al. 2007)
Human: MaMel54a	From Julia Reinhardt, originally from (S. Urugel et al. 2007)

Human: MaMel55	From Prof. Dr. med. Schadendorf, Essen originally from (S. Urugel et al. 2007)
Human: MaMel59b	From Prof. Dr. med. Schadendorf, Essen originally from (S. Urugel et al. 2007)
Human: MaMel60	From Prof. Dr. med. Schadendorf, Essen originally from (S. Urugel et al. 2007)
Human: MaMel65	From Julia Reinhardt, originally from (S. Urugel et al. 2007)
Human: MaMel67a	From Julia Reinhardt, originally from (S. Urugel et al. 2007)
Human: MaMel82	From Prof. Dr. med. Schadendorf, Essen originally from (S. Urugel et al. 2007)
Human: MaMel85	From Julia Reinhardt, originally from (S. Urugel et al. 2007)
Human: MaMel92d	From Prof. Dr. med. Schadendorf, Essen originally from (S. Urugel et al. 2007)
Human: MaMel102	From Julia Reinhardt, originally from (S. Urugel et al. 2007)
Human: MZ7	From Julia Reinhardt, originally from T. Wölfel, Mainz, Germany
Human: SK-MEL-28	From Julia Reinhardt, originally from T. Wölfel, Mainz, Germany
Human: HCC4006	From Johannes Brägelmann, Köln, Germany
Human: NCI-H2023	From Johannes Brägelmann, Köln, Germany

Human: NCI-H2087	From Johannes Brägelmann, Köln, Germany
Human: PC-9	From Johannes Brägelmann, Köln, Germany
Human: BEL-1	From Teresa Sadras, Melbourne, Australia
Human: K562	From Teresa Sadras, Melbourne, Australia
Human: NALM-6	From Teresa Sadras, Melbourne, Australia
Human: Mino	From Teresa Sadras, Melbourne, Australia
Human: MOLM-13	From Teresa Sadras, Melbourne, Australia
Human: SEM	From Teresa Sadras, Melbourne, Australia
Human: SUP-B15	From Teresa Sadras, Melbourne, Australia
Human: NOZ	From Laura Jenkins, Melbourne, Australia
Human: Mz-ChA-1	From Laura Jenkins, Melbourne, Australia
Human: SK-ChA-1	From Laura Jenkins, Melbourne, Australia
Human: SNU-1196	From Laura Jenkins, Melbourne, Australia

Human: TKF-1	From Laura Jenkins, Melbourne, Australia
Human: DIFI	From Laura Jenkins, Melbourne, Australia
Human: HT-29	From Laura Jenkins, Melbourne, Australia
Human: LIM2551	From Laura Jenkins, Melbourne, Australia
Human: LS180	From Laura Jenkins, Melbourne, Australia
Human: SNU283	From Laura Jenkins, Melbourne, Australia
Human: SW837	From Laura Jenkins, Melbourne, Australia
Human: MaMel48a stable Cas9	Generated during this study. Melanoma cell line expressing stable Cas9
Human: MaMel54a stable Cas9	Generated during this study. Melanoma cell line expressing stable Cas9
Human: MaMel65 stable Cas9	Generated during this study. Melanoma cell line expressing stable Cas9
Human: SK-MEL-28 stable Cas9	Generated during this study. Melanoma cell line expressing stable Cas9
Human: MaMel48a inducible Cas9	Generated during this study. Melanoma cell line expressing doxycycline inducible Cas9
Human: MaMel54a inducible Cas9	Generated during this study. Melanoma cell line expressing doxycycline inducible Cas9

Human: MaMel60 inducible Cas9	Generated during this study. Melanoma cell line expressing doxycycline inducible Cas9
Human: MaMel65 inducible Cas9	Generated during this study. Melanoma cell line expressing doxycycline inducible Cas9
Human: MaMel67a inducible Cas9	Generated during this study. Melanoma cell line expressing doxycycline inducible Cas9
Human: MaMel85 inducible Cas9	Generated during this study. Melanoma cell line expressing doxycycline inducible Cas9
Human: SK-MEL-28 inducible Cas9	Generated during this study. Melanoma cell line expressing doxycycline inducible Cas9
Human: MaMel48a BFP Cas9	Generated during this study. Melanoma cell line expressing BFP Cas9
Human: MaMel54a BFP Cas9	Generated during this study. Melanoma cell line expressing BFP Cas9
Human: MaMel60 BFP Cas9	Generated during this study. Melanoma cell line expressing BFP Cas9
Human: MaMel48a mCherry Cas9	Generated during this study. Melanoma cell line expressing mCherry Cas9
Human: MaMel54a mCherry Cas9	Generated during this study. Melanoma cell line expressing mCherry Cas9
Human: MaMel60 mCherry Cas9	Generated during this study. Melanoma cell line expressing mCherry Cas9
Human: MaMel48a GFP Cas9	Generated during this study. Melanoma cell line expressing GFP Cas9
Human: MaMel54a GFP Cas9	Generated during this study. Melanoma cell line expressing GFP Cas9

Human: MaMel60 GFP Cas9	Generated during this study. Melanoma cell line expressing GFP Cas9
Human: MaMel65 CD155 KO4 (px458)	Generated during this study. Melanoma cell line expressing a genetic knock-out of CD155 for RNAseq
Human: MaMel65 CD155 KO6 (px458)	Generated during this study. Melanoma cell line expressing a genetic knock-out of CD155 for RNAseq
Human: MaMel54a stable Cas9 CD155 KO4	Generated during this study. Melanoma cell line expressing stable Cas9 and a genetic knock-out of CD155
Human: MaMel65 stable Cas9 CD155 KO4	Generated during this study. Melanoma cell line expressing stable Cas9 and a genetic knock-out of CD155
Human: SK-MEL-28 stable Cas9 CD155 KO4	Generated during this study. Melanoma cell line expressing stable Cas9 and a genetic knock-out of CD155
Human: MaMel48a inducible Cas9 CD155 KO4	Generated during this study. Melanoma cell line expressing doxycycline inducible Cas9 and a genetic knock-out of CD155
Human: MaMel54a inducible Cas9 CD155 KO4	Generated during this study. Melanoma cell line expressing doxycycline inducible Cas9 and a genetic knock-out of CD155
Human: MaMel60 inducible Cas9 CD155 KO4	Generated during this study. Melanoma cell line expressing doxycycline inducible Cas9 and a genetic knock-out of CD155
Human: MaMel65 inducible Cas9 CD155 KO4	Generated during this study. Melanoma cell line expressing doxycycline inducible Cas9 and a genetic knock-out of CD155
Human: SK-MEL-28 inducible Cas9 CD155 KO4	Generated during this study. Melanoma cell line expressing doxycycline inducible Cas9 and a genetic knock-out of CD155
Human: MaMel48a inducible Cas9 CD155 KO6	Generated during this study. Melanoma cell line expressing doxycycline inducible Cas9 and a genetic knock-out of CD155
Human: MaMel54a inducible Cas9 CD155 KO6	Generated during this study. Melanoma cell line expressing doxycycline inducible Cas9 and a genetic knock-out of CD155

Human: MaMel60 inducible Cas9 CD155 KO6	Generated during this study. Melanoma cell line expressing doxycycline inducible Cas9 and a genetic knock-out of CD155
Human: MaMel54a inducible Cas9 DYRK1A KO1	Generated during this study. Melanoma cell line expressing doxycycline inducible Cas9 and a genetic knock-out of DYRK1A
Human: MaMel60 inducible Cas9 DYRK1A KO1	Generated during this study. Melanoma cell line expressing doxycycline inducible Cas9 and a genetic knock-out of DYRK1A
Human: MaMel54a inducible Cas9 DYRK1A KO5	Generated during this study. Melanoma cell line expressing doxycycline inducible Cas9 and a genetic knock-out of DYRK1A
Human: MaMel60 inducible Cas9 DYRK1A KO5	Generated during this study. Melanoma cell line expressing doxycycline inducible Cas9 and a genetic knock-out of DYRK1A
Human: MaMel54a mCherry Cas9 DYRK1A KO1	Generated during this study. Melanoma cell line expressing mCherry Cas9 and a genetic knock-out of DYRK1A
Human: MaMel60 mCherry Cas9 DYRK1A KO1	Generated during this study. Melanoma cell line expressing mCherry Cas9 and a genetic knock-out of DYRK1A
Human: MaMel54a mCherry Cas9 DYRK1A KO5	Generated during this study. Melanoma cell line expressing mCherry Cas9 and a genetic knock-out of DYRK1A
Human: MaMel60 mCherry Cas9 DYRK1A KO5	Generated during this study. Melanoma cell line expressing mCherry Cas9 and a genetic knock-out of DYRK1A
Human: MaMel54a mCherry Cas9 CD5L KO1	Generated during this study. Melanoma cell line expressing mCherry Cas9 and a genetic knock-out of CD5L
Human: MaMel60 mCherry Cas9 CD5L KO1	Generated during this study. Melanoma cell line expressing mCherry Cas9 and a genetic knock-out of CD5L
Human: MaMel54a mCherry Cas9 CD5L KO2	Generated during this study. Melanoma cell line expressing mCherry Cas9 and a genetic knock-out of CD5L
Human: MaMel60 mCherry Cas9 CD5L KO2	Generated during this study. Melanoma cell line expressing mCherry Cas9 and a genetic knock-out of CD5L

Human: MaMel54a mCherry Cas9 GMFB KO4	Generated during this study. Melanoma cell line expressing mCherry Cas9 and a genetic knock-out of GMFB
Human: MaMel60 mCherry Cas9 GMFB KO4	Generated during this study. Melanoma cell line expressing mCherry Cas9 and a genetic knock-out of GMFB
Human: MaMel54a mCherry Cas9 GMFB KO5	Generated during this study. Melanoma cell line expressing mCherry Cas9 and a genetic knock-out of GMFB
Human: MaMel60 mCherry Cas9 GMFB KO5	Generated during this study. Melanoma cell line expressing mCherry Cas9 and a genetic knock-out of GMFB
Human: MaMel54a mCherry Cas9 PTK6 KO1	Generated during this study. Melanoma cell line expressing mCherry Cas9 and a genetic knock-out of PTK6
Human: MaMel60 mCherry Cas9 PTK6 KO1	Generated during this study. Melanoma cell line expressing mCherry Cas9 and a genetic knock-out of PTK6

2.1.10 General consumables

Table 10: Overview of general consumables used in this study

The table shows the general consumables and the company.

Consumables	**Company**
Blotting paper	VWR
Cell culture plate (6-, 12-, 24-, 48- and 96-well, flat-bottomed)	Sarstedt
Cell culture plate (96-well, U-bottomed)	Greiner Bio-One
Cryo vials (CryoPure, 1.8 mL)	Sarstedt
DNA spin columns	Centic Biotec

Eppendorf® DNA LoBind tubes	Eppendorf
FACS tubes	Sarstedt
Gloves (Peha-soft nitrile white)	Hartmann AG
Nitrocellulose membrane (pore size: 0.2 µm)	GE Healthcare
NuPAGE 4-12% Bis-Tris Gel 1.5 mm x 15 well	Thermo Fisher Scientific
Parafilm® M	Amcor
Pasteur glass pipettes	VWR
PCR adhesive seals	Sarstedt
PCR plate, 96-well, standard	Thermo Fisher Scientific
PCR stripes and lids (8-well)	Axygen
Petri dishes	Sarstedt
Pipette tips, TipOne®	Star Lab
Reaction tubes (1-5, 2.0 mL)	Eppendorf

Reaction tubes (15, 50 mL)	Sarstedt
Syringe pore filters 0.45 µm	VWR
Serological pipettes (5,10 and 25 mL)	Greiner Bio-One, Corning® CoStar Stripettes
Syringe (1 mL, 5 mL, 10 mL, 20 mL)	B. Braun
TC Flaks T-25, T-75, T-175	Sarstedt
Zymo Spin IIIC columns	Zymo Research

2.1.11 General laboratory equipment

Table 11: Overview of general laboratory equipment used in this study

The table shows the general laboratory equipment and the company.

Name	**Company**
T100™ Thermal Cycler	Eppendorf
Centrifuge (5417R, 5810)	Eppendorf
Cytek Aurora™	Cytek Biosciences
NanoDrop™ 2000	Thermo Fisher Scientific
QuantStudio 6 Pro	Thermo Fisher Scientific

BD FACSymphony™ A3 Cell Analyzer	BD Biosciences
FACSAria™III	BD Biosciences
FACSAria™Fusion	BD Biosciences
MiSeq sequencer	Illumina
NGS sequencer	Illumina
Cell counting chambers	Hirschmann
Axio Vert A1 Microscope	Zeiss
CoolCell™ LX Cell Freezing Container	Corning®
Mini Trans-Blot® Cell	Bio-Rad
Mini-PROTEAN® Tetra Cell Systems	Bio-Rad
Odyssey® DLx Imaging system	LI-COR® Biosciences
Odyssey® Sa Imaging system	LI-COR® Biosciences
Pipetboy pipetting aid	Integra Biosciences

PIPETMAN Classic™	Gilson™
Roller mixer SRT9	Stuart®
Scale TE601	Sartorius
SPARK® Multimode Microplate Reader	TECAN
ThermoMixer®	Eppendorf
Mr Frosty™ freezing container	Thermo Fisher Scientific

2.1.12 Oligonucleotides

Table 12: Overview of oligonucleotides used in this study

The table shows the oligonucleotides, sequence and the company.

Oligonucleotides	**Company**
Cas9_2_f ctaagctggaaagcgagttcg	Microsynth
Cas9_2_r cgtttgtctcgatcagaggcc	Microsynth
hCD155_KO4_TS caccGATGTTCGGGTTGCGCGTAG	Microsynth
hCD155_KO4_BS AAACctacgcgcaacccgaacatc	Microsynth
hCD155_KO6_TS CACCgcatgtgtcacagctgactt	Microsynth

hCD155_KO6_BS AAACaagtcagctgtgacacatgc	Microsynth
hCD155_KO10_TS CACCGcgggaacgtgacgaacaggc	Microsynth
hCD155_KO10_BS AAACgcctgttcgtcacgttcccgC	Microsynth
hDYRK1A_KO1_TS caccgTCAGCAACCTCTAACTAACC	Microsynth
hDYRK1A_KO1_BS AAACggttagttagaggttgctgaC	Microsynth
hDYRK1A_KO5_TS caccGTGGTCCCTCGGGTGTATTT	Microsynth
hDYRK1A_KO5_BS AAACaaatacacccgagggaccac	Microsynth
hCD5L_KO1_TS caccgACACCACCTTTGCGGCCCGG	Microsynth
hCD5L_KO1_BS aaacCCGGGCCGCAAAGGTGGTGTc	Microsynth
hCD5L_KO2_TS caccgATCCAATCAGTCAGTTGCAC	Microsynth
hCD5L_KO2_BS aaacGTGCAACTGACTGATTGGATc	Microsynth
hCD5L_KO5_TS caccgAGGACGAGAAGCAACCCTTC	Microsynth
hCD5L_KO5_BS aaacGAAGGGTTGCTTCTCGTCCTc	Microsynth

hGMFB_KO4_TS caccgTGACAAGGATAAACGCCTGG	Microsynth
hGMFB_KO4_BS aaacCCAGGCGTTTATCCTTGTCAc	Microsynth
hGMFB_KO5_TS caccGGAAGGACACCGCCTCGTTC	Microsynth
hGMFB_KO5_BS aaacGAACGAGGCGGTGTCCTTCC	Microsynth
hPTK6_KO1_TS caccgCGCACCCGACAGGACGTAGT	Microsynth
hPTK6_KO1_BS aaacACTACGTCCTGTCGGGTGCGc	Microsynth
Brunello_NT1_TS CACCGTTTTACCTTGTTCACATGGA	Microsynth
Brunello_NT1_BS aaacTCCATGTGAACAAGGTAAAAc	Microsynth
Brunello_NT2_TS CACCGTACTGGAGTTTGCGACTCGG	Microsynth
Brunello_NT2_BS aaacCCGAGTCGCAAACTCCAGTAc	Microsynth
pX330_U6_seq_2 #478 agggcctatttcccatgattc	Microsynth
NGS_CD155-KO4_f ACACTCTTTCCCTACACGACGCTCTTCCGATCTgctattcggagtccaaacggctg	Microsynth
NGS_CD155-KO4_r TGACTGGAGTTCAGACGTGTGCTCTTCCGATCTctccccgctctttgccaacttc	Microsynth

NGS_CD155-KO6_f ACACTCTTTCCCTACACGACGCTCTTCCGATCTgggtctgacaccttctcttcgg	Microsynth
NGS_CD155-KO6_r TGACTGGAGTTCAGACGTGTGCTCTTCCGATCTgaacatcctcagcgaggcattc	Microsynth
GAPDH_f AAGGTGAAGGTCGGAGTCAA	Microsynth
GAPDH_r AATGAAGGGGTCATTGATGG	Microsynth
hCD155_f TGTCCCGTAACGCCATCATC	Microsynth
hCD155_r CATGCTCTGTACTCGAGGGA	Microsynth
hBRAF_V600E/K_f GCTTGCTCTGATAGGAAAATGAG	Microsynth
hBRAF_V600E/K_r GTTGAGACCTTCAATGACTTTCT	Microsynth
hNRAS_G12D_f GAACCAAATGGAAGGTCACAC	Microsynth
hNRAS_G12D_r GGGTAAAGATGATCCGACAAGT	Microsynth
hNRAS_Q61K/L_f2 CCAGATAGGCAGAAATGGGC	Microsynth
hNRAS_ Q61K/L_r3 GCTCTATCTTCCGTGTGG	Microsynth
hHRAS_G13I_f AGGAGACCCTGTAGGAGGA	Microsynth

Human CRISPR Knockout Pooled Library (Brunello)	Addgene
miseq_gRNA_fw_S0 ACACTCTTTCCCTACACGACGCTCTTCCGATCTATCTTGTGGAAAGGACGAAACAC	IDT
miseq_gRNA_fw_S1 ACACTCTTTCCCTACACGACGCTCTTCCGATCTCATCTTGTGGAAAGGACGAAACAC	IDT
miseq_gRNA_fw_S2 ACACTCTTTCCCTACACGACGCTCTTCCGATCTGCATCTTGTGGAAAGGACGAAACAC	IDT
miseq_gRNA_fw_S3 ACACTCTTTCCCTACACGACGCTCTTCCGATCTAGCATCTTGTGGAAAGGACGAAACAC	IDT
miseq_gRNA_fw_S4 ACACTCTTTCCCTACACGACGCTCTTCCGATCTCAACATCTTGTGGAAAGGACGAAACAC	IDT
miseq_gRNA_fw_S6 ACACTCTTTCCCTACACGACGCTCTTCCGATCTTGCACCATCTTGTGGAAAGGACGAAACAC	IDT
miseq_gRNA_fw_S7 ACACTCTTTCCCTACACGACGCTCTTCCGATCTACGCAACATCTTGTGGAAAGGACGAAACAC	IDT
miseq_gRNA_fw_S8 ACACTCTTTCCCTACACGACGCTCTTCCGATCTGAAGACCCATCTTGTGGAAAGGACGAAACAC	IDT
oMJ55_Brunello_rev23 TGA CTG GAG TTC AGA CGT GTG CTC TTC CGA TCT CCG ACT CGG TGC CAC TTT TTC AA	IDT

2.1.13 Software and algorithms

Table 13: Overview of software and algorithms used in this study

The table shows the softwares, algorithms and the company/website.

Software and algorithms	Company/website
Outknocker	www.outknocker.org (Schmid-Burgk et al., 2014)

Prism V9	GraphPad
QuantStudio Design & Analysis 2	Thermo Fisher Scientific
RStudio	RStudio
SnapGene Viewer	GSL Biotech LLC Voom
FlowJo v10	Tree Star, Inc.
STRING	STRING analysis protein-protein interaction
Depmap	Depmap gene expression
Zen Software	Carl Zeiss
GSEA (gene set enrichment analysis	GSEA, Subramanian, Tamayo, et al. (2005, PNAS 102, 15545-15550) and Mootha, Lindgren, et al. (2003, Nat Genet 34, 267-273) http://software.broadinstitute.org/gsea/index.jsp
TCGA	The Cancer Genome Atlas via cBioportal
FACS Diva software	BD Biosciences
CRISPick	Broad institute https://portals.broadinstitute.org/gppx/crispick/public
ChatGPT-5	https://chatgpt.com/

2.1.14 Vectors and plasmids

Table 14: Overview of vectors and plasmids used in this study

The table shows the vectors, plasmids, and the company.

Name	Origin/company
p.MD2.G	Addgene #12259
ps.PAX2	Addgene #12260
pMDLg/pRRE	Addgene #12251
pRSV-Rev	Addgene #12253
pVSV-G	Gift from Eicke Latz
LentiCas9-Blasti	Addgene #52962
LentiGuide-Puro	Addgene #52963
LentiGuide-Puro CD155 KO4	Generated during this study
LentiGuide-Puro CD155 KO6	Generated during this study
LentiGuide-Puro CD155 KO10	Generated during this study
LentiGuide-Puro DYRK1A KO1	Generated during this study
LentiGuide-Puro DYRK1A KO5	Generated during this study

LentiGuide-Puro CD5L KO1	Generated during this study
LentiGuide-Puro CD5L KO2	Generated during this study
LentiGuide-Puro CD5L KO5	Generated during this study
LentiGuide-Puro GMFB KO4	Generated during this study
LentiGuide-Puro GMFB KO5	Generated during this study
LentiGuide-Puro PTK6 KO1	Generated during this study
Edit-R™ Inducible Lentiviral Cas9	Gift from Jonathan Schmid-Burgk, Horizon Discovery
FUCas9BFP	Generated by Marco Herold lab
FUCas9Cherry	Addgene #70182
FUCas9GFP	Addgene #85555
pSPCas9(BB)-2A-GFP (short: px458)	Addgene #48138
px458 CD155 KO4	Generated during this study
px458 CD155 KO6	Generated during this study

2.2 Molecular cloning techniques

2.2.1 Oligonucleotide annealing

Oligonucleotides were designed and top strand and bottom strand were ordered at Microsynth. Oligonucleotides were reconstituted to a final concentration of 100 µM, and 1 µL of the top- and bottom-strand oligonucleotide were annealed in a total volume of 50 µL annealing buffer (100 mM NaCl, 50 mM HEPES in ultrapure water; pH 7.4). Oligonucleotides were annealed in a thermocycler using the following program:

90 °C 4 min

70 °C 10 min

69 °C 1 min (decrease 1 °C / 1 min)

4 °C ∞

2.2.2 Restriction enzyme digest

For molecular cloning, 10 µg of LentiGuide-Puro (Addgene, 52963) was digested with 5 µL of restriction enzyme BsmBI-v2 (NEB, R0739) in NEBuffer™ r3.1 (NEB) in a total volume of 30 µL for 8 hours at 55 °C. Px458 was digested with BbsI (NEB, R0539) in NEBuffer™ r2.1 (NEB). After restriction digest, plasmid was purified with MEGAquick-spin™ Plus Total Fragment DNA Purification Kit (iNtRON Biotechnology).

2.2.3 Ligation

For the ligation, 100 ng of BsmBI-digested LentiGuide-Puro plasmid DNA or BbsI-digested px458 and 1 µL of annealed oligonucleotides were incubated with 1 µL T4 DNA ligase and 1 µL of the corresponding T4 DNA ligase buffer for overnight ligation at 16 °C.

2.2.4 Agarose gel electrophoresis

Restriction digests were size separated using agarose gel electrophoresis. Agarose gels (0.7 – 1.5 %) were prepared using 1X TAE buffer (1 mM EDTA Na2, 40 mM TRIS, 20 mM acetic acid) and SYBR™ Safe DNA gel stain (S33102, Thermo fisher Scientific). Gels were run at 140 V for 45 min and DNA was visualized using UV light.

2.2.5 Transformation

DH10ß: 50 µL of competent Escherichia coli DH10β were thawed on ice and 5 µL of the ligation mixture was added and incubated for 10 min on ice. this mixture was heat-shocked for 45 sec at 42 °C, and incubated on ice for another 2 min. Subsequently, transformed bacteria were streaked on LB agar plates containing 100 mg/mL ampicillin. The agar plates were incubated upside down overnight at 37 °C.

Stbl3: 25 µL of Stbl3 bacteria were thawed on ice and 5 µL ligation mixture was added an incubated for 30 min on ice. Afterwards, this mixture was heat-shocked for 45 sec at 42 °C, and incubated on ice for another 2 min. To recover the bacteria 125 µL of SOC-media was added and incubated for 1 hour at 300 rpm at 37 °C. After recovery, 50-100 µL was streaked on LB agar plates containing 100 mg/mL ampicillin. The agar plates were incubated upside down overnight at 37 °C.

2.2.6 Plasmid DNA preparation from bacterial cultures

For both small-scale (mini preparation) and medium-scale (midi preparation) plasmid preparations, 1.5 mL or 100 mL LB broth containing 100 mg/mL ampicillin were inoculated with a single bacterial colony. Cultures were incubated overnight at 37 °C at 180 rpm.

For small-scale plasmid preparations, bacteria were pelleted at 6,000 x g for 10 min and resuspended in 180 µL resuspension buffer P1 containing RNAse. Following resuspension, 180 µL lysis buffer P2 was added and mixed by inverting

five times. To neutralize, 250 µL of N3 buffer was added and mixed by inverting. The suspension was centrifuged at full speed for 10 min and supernatant was transferred to a spin column for DNA isolation. The column was centrifuged at 10,000 rpm, and the plasmid DNA bound to the column was washed twice with 750 µL PE washing buffer. A dry spin was performed to get rid of residual buffers, and plasmid DNA was eluted in 40 µL ultrapure H2O.

Resuspension buffer P1: 50 mM Tris-HCl (pH 8.0), 10 mM EDTA, 50 µg/mL RNAseA

Lysis buffer P2: 200 mM NaOH, 1 % SDS

Neutralization buffer N3: 4.2 M Guanidine hydrochloride, 0.9 mM potassium acetate; pH 4.8

Wash buffer PE: 10 mM Tris-HCl (pH 7.5), 80 % Ethanol

Medium-scale plasmid preparations were performed using the PureLink® HiPure Plasmid Midiprep Kit according to the manufacturer's instructions. Plasmid was reconstituted in 100-500 µL ultrapure H2O.

DNA concentrations of both plasmid preparation methods were measured using the spectrophotometer NanoDrop 2000.

2.3 Tissue culture

All human melanoma cell lines were cultured in a humidified incubator (5 % CO2, 37 °C) in complete RPMI 1640 GlutaMAX media (Gibco) containing 10 % FBS and 100 U/mL penicillin, 100 µg/mL streptomycin. HEK 293T cells were cultured in complete DMEM10 (Gibco) containing 10 % FBS, 2 mM L-glutamine, 100 U/mL penicillin, 100 µg/mL streptomycin. All cell lines were negative for mycoplasma and tested on a monthly basis by PCR.

The CD155 gene was knocked out using CRISPR/Cas9 technology to generate melanoma CD155 KO cell lines.

2.4 CRISPR/Cas9-techniques used in this study

2.4.1 Generation of Cas9 expressing human melanoma cell lines

In order to generate Cas9-expressing human melanoma cell lines, transduction was performed with either LentiCas9-Blast (Addgene, 52962), FUCas9Cherry (Addgene, 70182), FUCas9 BFP or GFP were generated by Marco Herold laboratory and not commercially available or Edit-R Inducible Lentiviral Cas9 (Horizon). Lentiviral particles were produced via the Calcium Chloride method by transfecting HEK 293T cells with the target plasmid together with lentivirus packaging plasmids psPAX2 (Addgene, 12260) plus envelope plasmid pMD2.G (Addgene, 12259), or another packaging and envelop set consisting of pMDLg (Addgene, 12251), pCMV VSV-G (Addgene, 8454) and pRSV-Rev (Addgene, 12253). The media was refreshed after 24 hours. The following day, the supernatant of the HEK293T cells, containing lentiviral particles, was filtered with 0.45 µM syringe filter and added to the human melanoma cells once or twice together with polybrene (10 µg/mL, Santa-Cruz). Transduced cells were selected 48 hours post-transduction with blasticidin (5 µg/mL, Sigma-Aldrich) for at least 7 days for LentiCas9-Blast or Edit-R Inducible Lentiviral Cas9. FUCas9Cherry transduced cells were FACS-sorted for mCherry-positive expression 48 hours post-transduction and subsequentially expanded.

Table 15: Overview of Cas9 construct used in this study

The table shows different Cas9 constructs, stable or inducible and the promoter.

Cas9 constructs	Cas9 stable/inducible	Promoter
LentiCas9-Blast	Stable	EFS-NS
Edit-R Inducible Lentiviral Cas9	Inducible with doxycycline	Tet-On® 3G
FUCas9BFP	Stable	Ubiquitin
FUCas9Cherry	Stable	Ubiquitin
FUCas9GFP	Stable	Ubiquitin

Cas9 expression was confirmed with qRT-PCR and Western blot. The functionality of Cas9 was accessed via a single CD155 gene knock-out experiment, with knock-out frequency qualified by Next Generation Sequencing (NGS) using the Illumina MiSeq platform. MiSeq PCRs were performed that amplify the region of interest, followed by a second PCR incorporating barcodes to the amplicon.

1st MiSeq PCR

2.5 µL 5 x Phusion buffer HF

0.25 µL dNTPs (10 mM each)

0.625 µL Forward primer and reverse primer for target region (5 µM each)

1 µL Template gDNA

0.125 µL Phusion High-Fidelity DNA Polymerase

8 µL ultrapure H2O

The first MiSeq PCR reaction was incubated in a PCR thermocycler using the following thermocycling conditions:

Initial denaturation	98 °C 30 sec
Denaturation	98 °C 10 sec
Annealing	57 °C 15 sec
Extension	72 °C 30 sec
Repeat for 18 rounds	
Final extension	72 °C 3 min
Hold	12 °C ∞

2nd MiSeq PCR

5 µL 5 x Phusion buffer HF

0.5 µL dNTPs (10 mM each)

2.5 µL Forward primer and reverse barcode primer (5 µM each)

2 µL DNA product from 1st MiSeq PCR

0.25 µL Phusion High-Fidelity DNA Polymerase 1

4.75 µL ultrapure H2O

The second MiSeq PCR reaction was incubated in a PCR thermocycler using the following thermocycling conditions:

Initial denaturation	98 °C 30 sec
Denaturation	98 °C 10 sec
Annealing	57 °C 15 sec
Extension	72 °C 30 sec
Repeat for 18 rounds	
Final extension	72 °C 3 min
Hold	12 °C ∞

The final PCR product was analysed by gel electrophoresis. Samples were pooled and run on the Illumina MiSeq. The results were analysed using the web tool OutKnocker (Schmid-Burgk et al., 2014). OutKnocker is a deep-sequencing and evaluation tool allowing reliable, convenient and cost-effective identification of knockout cell lines. The web tool is able to align an amplicon to a reference sequence, detect mismatches and determine indel size.

2.4.2 Generation of CD155 knock-out human melanoma cell lines

2.4.2.1 Generation of CD155 knock-out in wildtype melanoma cell lines

Small oligo nucleotides (sgRNAs) targeting CD155 were either designed by the Broad Institute CRISPICK tool or taken from the Brunello library (Addgene, 73179). These sgRNAs were cloned into the pSPCas9(BB)-2A-GFP (short: px458, Addgene, 48138) and successful cloning was confirmed with Sanger sequencing.

Melanoma cells were seeded in 48-well plate and transfected upon adherence with 1 µg of px458 plasmid (mock, CD155 KO4 or CD155 KO6; containing sgRNA targeting CD155) in OptiMEM® using FuGENE® HD transfection reagent, according to manufacturer's instructions. Following expansion, transfected cells were FACS-sorted based on GFP positive expression levels or CD155 knock-out efficiency. Sorted populations were further expanded and routinely monitored for CD155 expression to confirm stable knockout.

2.4.2.2 Generation of CD155 knock-out in Cas9-expressing melanoma cell lines

Small oligo nucleotides (sgRNAs) targeting CD155 were either designed by the Broad Institute CRISPICK tool or taken from the Brunello library (Addgene, 73179). These sgRNAs were cloned into the LentiGuide-Puro vector (Addgene, 52963), and successful cloning was confirmed with Sanger sequencing.

The CalciumChloride method was used to co-transfecting HEK293T cells with either the LentiGuide-Puro backbone containing sgRNA targeting CD155 (CD155 sgRNA KO4 or KO6) or mock LentiGuide-Puro backbone (without additional inserts), along with packaging plasmid psPAX2 (Addgene, 12260) and envelope plasmid pMD2.G (Addgene, 12259). The supernatant of the HEK 293T cells containing lentiviral particles was filtered with 0.45 µM syringe filter and used to transduce the Cas9-expressing melanoma cells (stable Cas9, inducible Cas9 or fluorescent Cas9). For inducible Cas9 expressing cells, doxycycline (1000 ng/mL, Cayman, 24390-14-5) was added 24 hours before transduction and an additional

24 hours post-transduction. Transduced cells were selected with puromycin (2 µg/mL, Cayman, 58-58-2) 48 hours after transduction. On day 5, 7 and 9 the surface expression of CD155 was analysed using flow cytometry. In addition, cells from each timepoint were collect to quantify the knock-out frequency using previously described MiSeq approach.

2.4.3 Genome-wide CRISPR knock-out screen

The Cas9 expressing melanoma cell lines MaMel48a, MaMel54a and MaMel60 were transduced with the human genome-wide CRISPR-KO sgRNA pooled library (Brunello, Addgene, 73178) including polybrene (10 µg/mL, Santa-Cruz, SC-134220). Cells were in complete RPMI 1640 GlutaMAX media (Gibco) containing 10 % FBS (Sigma, lot: 0001650764) and 100 U/mL penicillin, 100 µg/mL streptomycin. The quality control of the lentiviral particles containing the human genome-wide CRISPR-KO sgRNA pooled library was performed by the Schmid-Burgk lab. The library transduction was performed in four technical replicates per cell line of each 16 * 10^6 cells to achieve coverage of 500. Cas9 expressing cell lines were stimulated with doxycycline (1000 ng/mL, Cayman, 24390-14-5) 24 hours before transduction and an additional 24 hours after transduction. Transduced cells were selected with puromycin (2 µg/mL, Sigma-Aldrich) 48 hours post-transduction. Cells were cultured for an additional 7 days in puromycin to establish the CD155- phenotype. Prior preparation of the tubes with direct lysis buffer (DLB) with proteinase K, UV treatment was performed to clean the workspace and sterilizing all materials needed prior performing the PCRs (PCR plates, plate film, pipets, racks, tubes).

On day 7, an unsorted transduced population of 10 * 10^6 cells was harvested to serve as a control. Genomic DNA was isolated and frozen. Another 100 * 10^6 library transduced cells as harvested and stained with DAPI or PI and CD155 APC/Fire 750 as described in ‘Methods, FACS’. Cells were sorted into DNA LoBind tubes (Eppendorf, 022431021). After 7 hours ±460,000 to 1,400,000 cells per replicate per cell line CD155 lowest 3-5 % of total were sorted. The CD155-low cells were lysed in direct lysis buffer 1X (DLB, 25,000 cells/50 µL DLB)

including proteinase K (1:100), and gDNA was isolated by cooking 10 minutes at 65 °C followed by 15 minutes at 95 °C. First, 50 µL of lysate/96-well was used for a PCR reaction of 16 cycles with 50 µL NEBNext High Fidelity 2X PCR Mix (NEB, M0541L), and 1 µL Brunello primer mix consisting of eight Brunello forward primers targeting the U6 promoter of LentiGuide-Puro with additional stagger regions to increase sequence complexity was performed and one reverse primer (added 8 times higher concentration to the mix to bind all different eight stagger primers) (Fig. 12). Different replicates were used per fraction due to different cell numbers/lysate volume: 10-12 for the unsorted fraction and 2-4 replicates for the CD155- fraction.

This was followed by a second PCR in duplicates, taking 1 µL of first PCR product with 5 µL NEBNext High Fidelity 2X PCR Mix, and 1 µL of barcoding primers for 16 cycles, ending up with a PCR product which in total has 32 cycles. The PCR product was PCR purified (Qiagen, 175019145) Gel electrophoresis in 1-2 % agarose E-gel EX (Invitrogen, G401002) was performed to quantify the PCR amplicon (249 base pairs). The amplicon of the unsorted fraction and the CD155-sorted fraction was gel purified (Qiagen, 169044800), and PCR purified. After measuring the genomic DNA concentration, samples were sent to MiSeq for quality control. The MiSeq results show the number of reads that are received after loading a certain percentage on the cartridge. This number is used to determine the amount of genomic DNA that will be loaded on the NextSeq 1000/2000 on a P2 reagent cartridge 100 cycles (Illumina, 20044468).

Both the first (volume 100 µL) and second (volume 10 µL) NGS PCR reaction was incubated in a PCR thermocycler using the following thermocycling conditions:

Initial denaturation	98 °C 3 min
Denaturation	98 °C 20 sec
Annealing	65 °C 20 sec
Extension	72 °C 30 sec

Repeat for 15 rounds	
Final extension	72 °C 3 min
Hold	4 °C ∞

2.4.4 Validation of enriched genes by single knock-out

Lentiviral particles were generated using the third-generation packaging system, consisting of the packaging plasmid pMDLg/pRRE, the Rev expression plasmid pRSV-Rev, and the envelope plasmid pMD2.G (encoding VSV-G). to co-transfecting HEK293T, the CalciumChloride method was used cells with either the LentiGuide-Puro backbone containing sgRNA targeting CD155 (CD155 sgRNA KO4 or KO6) or sgRNA targeting DYRK1A (DYRK1A sgRNA KO1 or KO5) or mock LentiGuide-Puro backbone (without additional inserts). The supernatant of the HEK 293T cells containing lentiviral particles was filtered with 0.45 µM syringe filter and used to transduce the Cas9-expressing target cells. For inducible Cas9 expressing cells, doxycycline (1000 ng/mL, Cayman, 24390-14-5) was added 24 hours before transduction and an additional 24 hours post-transduction. Transduced cells were selected with puromycin (2 µg/mL, Cayman, 58-58-2) 48 hours after transduction. On day 5, 7 and 9 the surface expression of CD155 was analysed using flow cytometry. In addition, cells from each timepoint were collect to quantify the knock-out frequency using previously described MiSeq approach.

2.5 qRT-PCR

Cells were lysed in RLT buffer (Qiagen) and total RNA was isolated using Zymo Spin II columns (Zymo Research) with wash buffer RW1 (Qiagen) and Zymo RNA Wash Buffer (Zymo Research). RNA concentrations were determined using a NanoDrop Spectrophotometer. cDNA synthesis was performed using either 500 or 1000 ng of RNA with 5X HiScript II QRT SuperMix (NEB, NB-54-0177). RNA was kept on ice. Quantitative RT-PCR (qRT-PCR) was performed using Luna Universal qPCR MasterMix (NEB, M3003) with 40 amplification cycles, using primer pairs specific for Cas9 or housekeeping gene GAPDH.

2.6 Immunoblotting

Melbourne, similar to publication from Herold lab (Gong et al., 2025):

Total cell lysates were prepared using lysis buffer RIPA and complete protease inhibitor and phosphatase inhibitor. Lysis was performed on ice, afterwards samples were spin down at 13,000 rpm for 10 min at 4 °C. Supernatant was taken into a new tube, and lysates were diluted using 4X SDS buffer together with Laemmli and denatured by boiling at 100 °C for 5 min. Protein concentrations were determined using the Bradford assay (Bio-Rad #5000002). SDS NuPAGE 4-12 % Bis-Tris (Invitrogen) was used to separate proteins (30 µg of each sample). Subsequently, the gel was transferred onto nitrocellulose membrane (Invitrogen #LC2009) using iBlot2 Dry Blotting System (Thermo Fisher Scientific). Membranes were blocked for 1 hour at room temperature in blocking buffer containing 3 % bovine serum albumin (BSA) in Tris-buffered saline (TBS) with 0.5 % Tween-20. Primary antibody stain was performed overnight at 4 °C. Primary antibodies used are Actin (Cell Signaling, 1:2,000), HSP70 (Cell Signaling, 1:10,000), Cas9 (S. pyogenes) (Cell Signaling, 1:50), AKT (Cell Signaling, 1:1,000), p-AKT (Cell Signaling, 1:1,000). The next day, membranes were washed in TBST and incubated with specific secondary antibody for 1 hour at room temperature. Secondary antibodies used were either goat anti-mouse IgG-HRP (Cell Signaling, 1:2,000) or anti-rabbit (Cell Signaling, 1:2,000). Before imaging, membranes were washed in TBST. Imaging was performed on a ChemiDoc system (Bio-Rad) after adding Immobilon Forte (Merck Millipore #WBLUF0500). Ladder used was Spectra™ broad range multicolour (Thermo Fisher Scientific, #26634).

Bonn:

Total cell lysates were prepared by incubating the cells in 1X Laemmli buffer at 95 °C for 5 min. Cell lysates were loaded on 10 % SDS-PAGE gel and proteins were transferred to a nitrocellulose membrane (pore size 0.2 µm) by wet blotting. The membrane was blocked for 1 hour with 5 % (BSA) in TBS with 0.5 % Tween-20. Primary antibody stain was performed overnight at 4 °C. Primary antibodies

used are Actin (Cell Signaling, 1:10,000) and Cas9 (S. pyogenes) (Cell Signaling, 1:50). The next day, membranes were washed in TBST and incubated with specific secondary antibody for 1 hour at room temperature. Secondary antibodies used were either donkey anti-mouse IRDye 680 LT (LI-COR Biosciences, 1:15,000) or donkey anti-rabbit (LI-COR Biosciences, 1:15,000). Before imaging, membranes were washed in TBST. Imaging was performed on the Odyssey Sa Imaging system (LI-COR Biosciences). Ladder used was Broad Range Markers (Santa Cruz).

Laemmli buffer:	4 % SDS, 20 % Glycerol, 120 mM Tris-HCl (pH 6.8), 0.02 % bromophenol blue, 20 mM Dithiothreitol
Running buffer:	25 mM Tris, 192 mM glycine, 0.1 % SDS
Blotting buffer:	25 mM Tris, 192 mM glycine, 20 % methanol
TBS:	50 mM Tris (pH 7.6), 150 mM NaCl

2.7 Flow cytometry

Melanoma cell lines were harvested and washed with PBS. Afterwards, the cells were stained with antibodies in full RPMI (RPMI with 10% FBS and 100 U/mL penicillin, 100 µg/mL streptomycin). Dead cells were stained with either LIVE/DEATH Fixable blue 1:1000 (Thermofisher, L23105) or DAPI (Bioledgend, 422801) or propidium iodide 1:500 (PI) (500X 250 µg/mL). In addition, human Fc receptor blocking 1:200 (Bioledgend, 422301) was used and anti-human CD155 (PVR) APC/Fire 750 clone SKII.4 1:50 (Bioledgend, 337626). Ten to hundred thousand events in the life cell gate were recorded on the Cytek Aurora 4 Laser (16UV-16V-14B-8R, Cytek Biosciences) or BD FACSymphony™ A3 Cell Analyzer (BD Biosciences) and analysed with FlowJo software.

2.8 Sanger sequencing

For genomic DNA (gDNA) extraction, 5 * 10^5 cells were collected and gDNA was extracted with the NucleoSpin® Tissue Kit (Macherey-Nagel). The gDNA was eluted in Ampuva H2O and measured using NanoDrop spectrophotometer. For

PCR amplification 200 ng of gDNA was used in 100 µL PCR reaction which was ran for 30 cycles.

gDNA amplification PCR 100 µL reaction:

20 µL Q5 High-Fidelity DNA polymerase

2 µL dNTPs (10 mM each)

5 µL Forward primer and reverse barcode primer (10 µM each)

x µL gDNA (200 ng)

1 µL Q5 High-Fidelity DNA Polymerase

Top up to 100 µL with x µL ultrapure H2O

PCR reaction was incubated in a PCR thermocycler using the following thermocycling conditions:

Initial denaturation	98 °C 3 min
Denaturation	98 °C 10 sec
Annealing	58 °C 30 sec
Extension	72 °C 20 sec
Repeat for 30 rounds	
Final extension	72 °C 2 min
Hold	4 °C ∞

The PCR product was quantified using NanoDrop spectrophotometer. A minimum of 90 ng DNA was send for Sanger sequencing (Microsynth) together with 3 µL primer (20 µM; forward or reverse) in a final reaction volume of 12 µL adjusted with H2O.

2.9 RNA sequencing

MaMel65 WT, MaMel65 CD155 KO4 and MaMel65 CD155 KO6 were treated with either control media, TNF-α (1000 units/mL), IFN-γ (1000 units/mL) or LPS (1 µg/mL) for 48 hours. Total RNA from these treated cells was extracted as

described previously in 2.5 qRT-PCR. RNA concentrations were measured using NanoDrop spectrophotometer. 3´mRNA-Seq library preparation was performed using the forward QuantSeq 3´mRNA-Seq Library Prep Kit for Illumina according to the manufacturer's protocol, which was performed by the NGS Core Facility at the University Hospital Bonn. Computational analyses were performed using the R-based Bioconductor computing environment. Bioinformatic analyses were performed by Dr. Dillon Corvino (Bonn) and Daksh Amar (Melbourne) with R studio.

2.10 Treatment of melanoma cells with AKT inhibitors

Human melanoma cells were seeded and allowed to adhere for 6 hours before treatment with indicated AKT inhibitors (table 16). After 48 hours, cells were harvested, stained, and subsequently analysed by flow cytometry.

Table 16: Overview of AKT inhibitors used in this study

The table shows AKT inhibitors, controls and concentration used for our cell lines.

AKT inhibitor/control	Concentration
DMSO	0.5 %
BEZ235 (Dactolisib)	5 µM
GSK-690693	4 µM
MK-2206	2 µM
ZSTK474	5 µM
Q-VD-OPh	20 µM

2.11 Data analysis

To analyse the results of the deletion of CD155 and the genome-wide CRISPR knock-out screen an unpublished program (xyPlot v2) from the Schmid-Burgk lab was used, which allowed us to quantify the read counts of sgRNAs in order to determine the enrichment of genome-wide CRISPR knock-out library of sgRNA sequences in the unsorted fraction and the sorted CD155- fraction of transduced cells. Statistical significance of reduction in CD155 surface expression in validation experiments was analysed in GraphPad Prism using one-way ANOVA test. P-values below 0.05 were considered as statistically significant. In addition, R studio with MAGeCK, Biorender, STRING, SpectroFlo, and FlowJo were used.

Results

3. Chapter 3: Characterisation of CD155 surface expression in human cancer cell lines

3.1 Introduction

CD155 has recently emerged as a potential target for cancer therapy. It has an important immune modulating function binding to CD96, TIGIT and CD226 as well as tumor cell intrinsic functions. Our laboratory previously showed that CD155 promotes immune escape by inducing internalization of CD226 expressed on CD8+ T cells (Braun et al., 2020). Importantly, CD155 expression is low in healthy tissues but overexpressed in melanoma and many other cancer types (Abdalla et al., 2025; Adhikari et al., 2023; Chan et al., 2010; Iguchi-Manaka et al., 2016; Liu et al., 2023; Masson et al., 2001; Nakai et al., 2010; Pende et al., 2005), making it a promising target for the development of new immunotherapies. However, the intrinsic regulation of CD155 in cancer cells remains poorly understood.

In this chapter, we first assessed CD155 expression across a panel of human melanoma cell lines and investigate whether its expression corelates with mutations in key oncogenic drivers of the MAPK pathway (*BRAF*, *NRAS*, *HRAS*, and *NF1*) or with phenotypic differentiation status (differentiated or dedifferentiated). To determine whether CD155 overexpression is specific to melanoma or overexpressed across different types of cancer, we extended the analysis to additional cancer cell lines derived from human cancers, which were previously reported to express high levels of CD155 (Abdalla et al., 2025; Adhikari et al., 2023; Chan et al., 2010; Iguchi-Manaka et al., 2016; Liu et al., 2023; Masson et al., 2001; Nakai et al., 2010; Pende et al., 2005).

To further elucidate its functional role, we generated multiple CD155 knock-out melanoma cell lines using distinct Cas9 systems, including both constitutive and inducible variants in the laboratory of Tobias Bald Bonn, as well as fluorescent tagged Cas9 constructs with a strong ubiquitin promoter which were generated

in the laboratory of Marco Herold, Melbourne, during the final year of my PhD. Finally, to investigate how CD155 is intrinsically regulated, bulk RNA sequencing was performed on wild-type and CD155 knock-out human melanoma cell lines under basal conditions and following stimulation with inflammatory cytokines IFN-γ, TNF-α, or toll-like receptor ligand LPS.

Together, this chapter establishes the expression landscape of CD155, oncogenic regulation, and downstream gene expression changes driven by CD155 knock-out in human melanoma cell lines, advancing the role of CD155 as both a biomarker and therapeutic target.

3.2 High CD155 expression across human melanoma is not determined by oncogenic driver mutation or differentiation status

Previous work using immunohistochemistry analysis showed that CD155 was overexpressed across different cancer types (Liu et al., 2025). Here, we assessed the CD155 surface expression in a panel of fifteen well-characterized human melanoma cell lines via flow cytometry (Fig. 5A). All tested human melanoma cell lines showed CD155 overexpression. CD155 surface expression was the highest in MaMel92d, and the lowest in MaMel48a, although this expression was still relatively high (Fig. 5A). The other thirteen cell lines showed intermediate levels between those two. In order to correlate the oncogenic driver mutations (*BRAF*, *HRAS*, and *NRAS*) with the CD155 surface expression results, the mutations were first confirmed and monitored overtime by Sanger sequencing (Fig. 5B). This analysis was performed to ensure that the cell lines retained the reported mutations. Our panel of fifteen human melanoma cell lines all harboured the reported oncogenic driver mutation as described previously (Ugurel et al., 2007). MaMel15, negative for all tested oncogenic driver mutations, showed intermediate expression of CD155 compared to the other cell lines harbouring indicated oncogenic driver mutations (Fig. 5A). The *BRAF*-mutant cell lines (MaMel54a, 55, 59b, 67a, 85, 92d, MZ7 and SKMel28) showed intermediate to high expression of CD155 based on flow cytometry analysis (Fig. 5A). Similar expression levels were observed in the *NRAS*-mutant cell lines (Fig. 5A). In our

panel, only one cell line harboured a *HRAS* mutation, MaMel48a, which showed lower CD155 expression compared to intermediate expressing cell lines (Fig. 5A).

Furthermore, the differentiation status of the different melanoma cell lines, which has been described in previous studies from our institute (Reinhardt et al., 2017; Riesenberg et al., 2015), was compared to the level of CD155 surface expression (Fig. 5B). Differentiated melanoma cell lines MaMel15 and 67a showed similar intermediate CD155 expression. Whereas, the dedifferentiated cell lines (MaMel54a, 59b, 60, 65, 85, 92d, and SKMel28) showed intermediate and high expression levels. The other cell lines (MaMel37a, 48a, 55, 82, 102 and MZ7), which are in between differentiated and dedifferentiated phenotype, expressed CD155 in different intermediate and high levels.

These results showed that CD155 surface expression is independent of mutational status and differentiation status in human melanoma cell lines, suggesting that CD155 is regulated by separate mechanisms. To explore this further in an unbiased approach, we performed a genome-wide CRISPR knock-out screen to investigate the intrinsic regulation of CD155 in melanoma. The screen was performed in three different cell lines harbouring different oncogenic driver mutations to evaluate intrinsic regulation of CD155 independent of those mutations and to minimize the influence of cell line dependent effects. In addition, CD155 surface expression levels are important to consider. We selected three different CD155 surface expression levels (relatively low, intermediate and high) with the aim to identify regulators of CD155 under varying baseline conditions. In terms of the differentiation status, we selected dedifferentiated cell lines as previous studies have shown that patients with dedifferentiation tumors exhibit poorer clinical outcomes, including increased metastasis and therapy resistance (Agaimy et al., 2021; Hölzel and Tüting, 2016; Reinhardt et al., 2017; Riesenberg et al., 2015). However, only one *HRAS*-mutant cell line (MaMel48a) was available, which is intermediate-differentiated. The following three cell lines were selected as candidates for the genome-wide CRISPR knock-out screen: MaMel48a (*HRAS*-mutant, relatively low CD155 expression, intermediate-differentiated), MaMel54a (*BRAF*-mutant, intermediate CD155 expression,

dedifferentiated), and MaMel60 (*NRAS*-mutant, high CD155 expression, dedifferentiated).

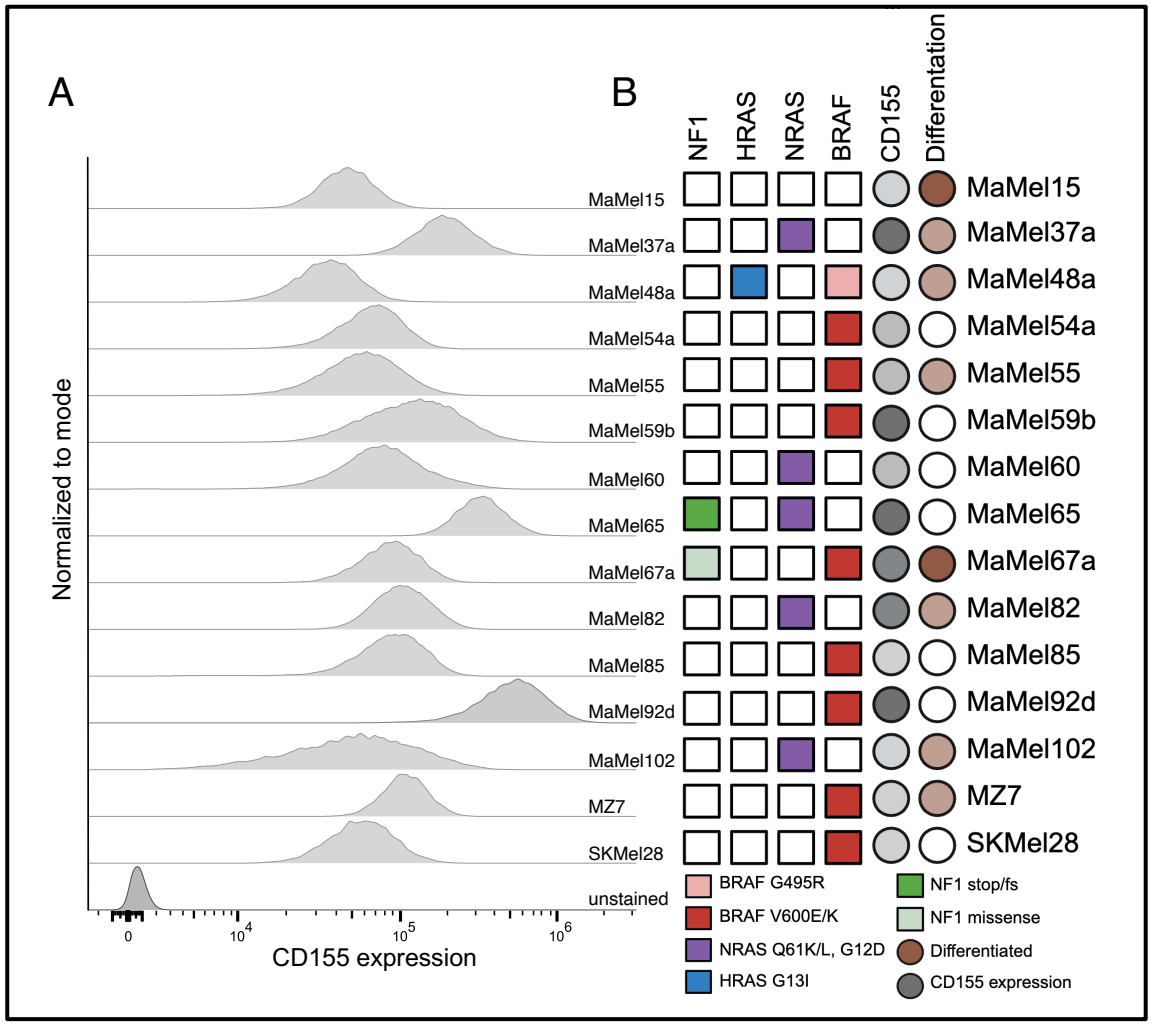

Figure 5: CD155 surface expression, oncogenic driver mutation, and differentiation status in a panel of fifteen human melanoma cell lines. *A) Representative histogram plots showing the baseline surface expression of CD155 based on flow cytometry in different indicated human melanoma cell lines. B) Schematic overview of CD155 expression (grey = high expression, light grey = intermediate expression), differentiation status (brown = differentiated, light brown = intermediate-differentiated, white = dedifferentiated), and oncogenic driver mutations (red = BRAF V600E/K, pink = BRAF G459R, purple = NRAS Q16K/L, G12D, blue = HRAS G13I, green = NF1 stop/fs, light green = NF1 missense). Figure created with Biorender.*

3.3 Expression of CD155 in human blood, colon, gastric and non-small cell lung cancer cell lines

In addition to melanoma, previous studies have shown that CD155 is overexpressed across multiple cancer types (Adhikari et al., 2023; Carlsten et al., 2009; Cho et al., 2025; Iguchi-Manaka et al., 2016; Liu et al., 2025; Masson et al., 2001; Nakai et al., 2010; Ren et al., 2024; Xiong et al., 2025). During this study CD155 surface expression levels have been assessed in various blood, colon, gastric, and lung cancer cell lines (Fig. 6). In blood cancers, consistent with previous studies (Cho et al., 2025; Ren et al., 2024; Xiong et al., 2025), our flow cytometry experiments showed that CD155 surface expression was only present in myeloid-derived leukemias which express intermediate CD155, whereas lymphoid-derived cell line SUP-B15 was slightly positive for CD155, and B-cell-derived cell lines did not express CD155 or extremely low (Fig. 6A). In contrast to leukemia, colon and gastric cancer cell lines all expressed intermediate-levels of CD155 on their surface (Fig. 6A, B, C). Whereas NSCLC cell lines exhibited relatively high surface expression levels of CD155 (Fig. 6D). These results suggest that CD155 is a potential target for future cancer immunotherapies, not only in melanoma but also across other cancer types.

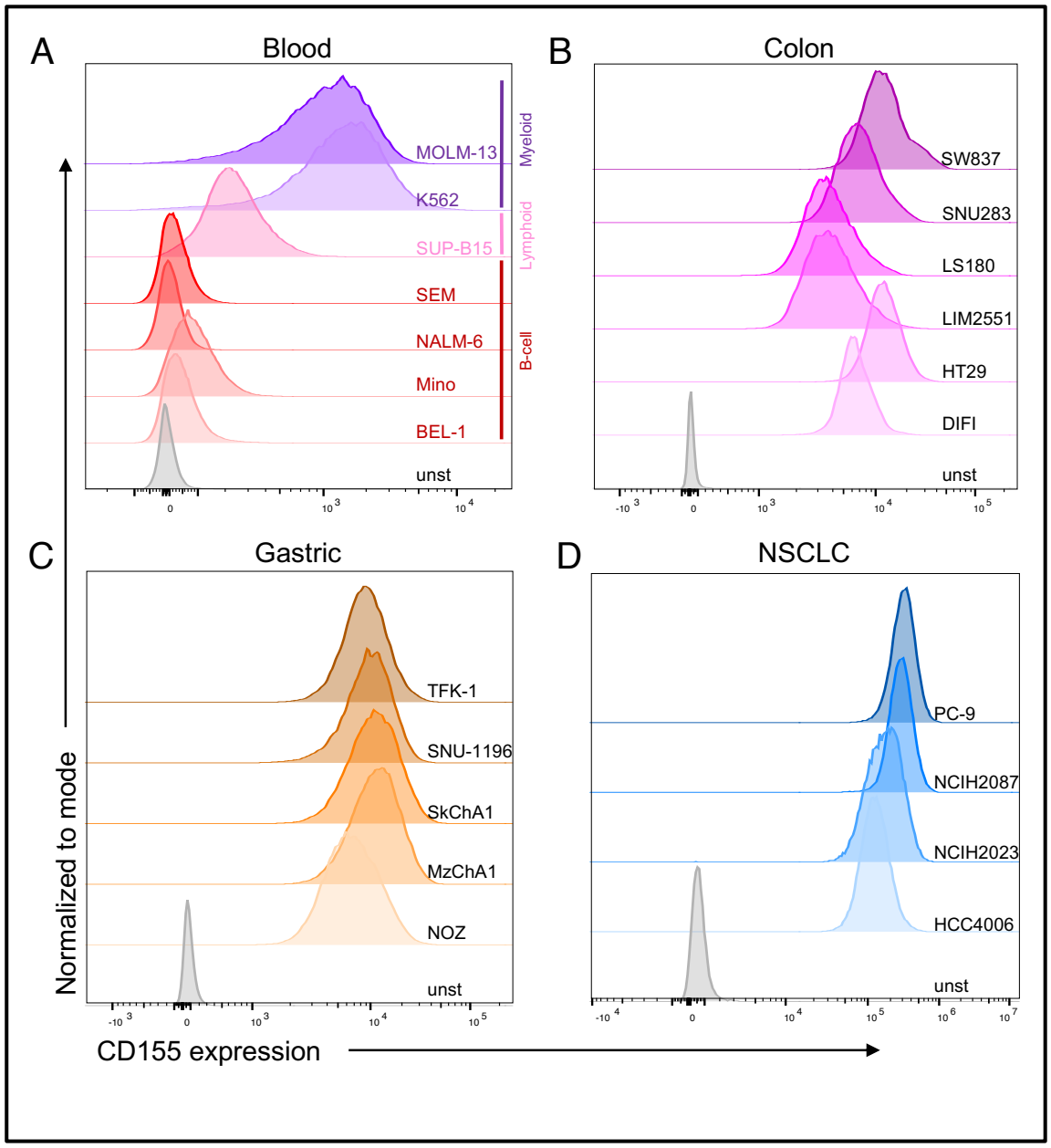

Figure 6: CD155 surface expression in human cancer cell lines. *Representative histogram plots showing the surface expression of CD155 based on flow cytometry in different types of cancer: blood (A) divided into B-cell leukemia (red), lymphoid leukemia (pink) and myeloid leukemia (purple), colon cancer cell lines (B), gastric cancer cell lines (C), and lung cancer cell lines (NSCLC) (D).*

3.4 Generation of Cas9-expressing human melanoma cell lines

To further explore the role of CD155, we generated CD155 knock-out human melanoma cell lines using CRISPR/Cas9 technology. To achieve this, cell lines stably expressing Cas9 were established and different sgRNAs targeting CD155 were designed with CRISPick (Doench et al., 2016; Sanson et al., 2018). During this study three different Cas9 variants were tested. Two of the variants contained a Blasticidin resistance cassette both stable Cas9 variant, with constitutive Cas9 expression, and the inducible Cas9 variant, in which Cas9 expression was induced after stimulation with doxycycline. The third Cas9 variant had a fluorescent marker instead of an antibiotic resistance cassette which allowed for enrichment of the Cas9+ cells via FACS. Moreover, each plasmid had a different promoter. The fluorescent Cas9 variant was driven by a relative strong ubiquitin promoter whereas the stable Cas9 variant had an EFS-NS promoter, and the inducible Cas9 variant had a Tet-On® 3G promoter.

First, we generated human melanoma cell lines stably expressing LentiCas9-Blast (Fig. 7A). To confirm Cas9 expression, mRNA was isolated and qRT-PCR was performed which showed that both cell lines MaMel65 and SKMel28 had robust expression of Cas9 mRNA (Fig. 7B). Additionally, Western blot analysis was performed (data not shown) to quantify Cas9 on protein level. Cas9 was detected in Western blot analysis for both MaMel65 and SKMel28 transduced with LentiCas9-Blast. After the expression of Cas9 was confirmed on both mRNA and protein levels, the functionality of Cas9 was assessed. A CD155 single knock-out transduction experiment was performed and the knock-out frequency of CD155 surface expression was measured. Figure 7C shows that the knock-out frequency of surface CD155 expression on day 7 post-transduction with LentiGuide-Puro CD155 sgRNA KO4, including 5 days of puromycin selection, was only 10 % for SKMel28 and 24 % for MaMel65. Ten different sgRNAs targeting CD155 at different exons were tested, with the aim to eliminate the possibility that the low knock-out efficiency was caused by the region of CD155 that was targeted with the sgRNA. However, similar knock-out frequencies were observed with all tested sgRNAs. Each sgRNA targeted different parts of the

CD155 gene (data not shown). Consequently, we concluded that stable Cas9 was not the best system for our purpose.

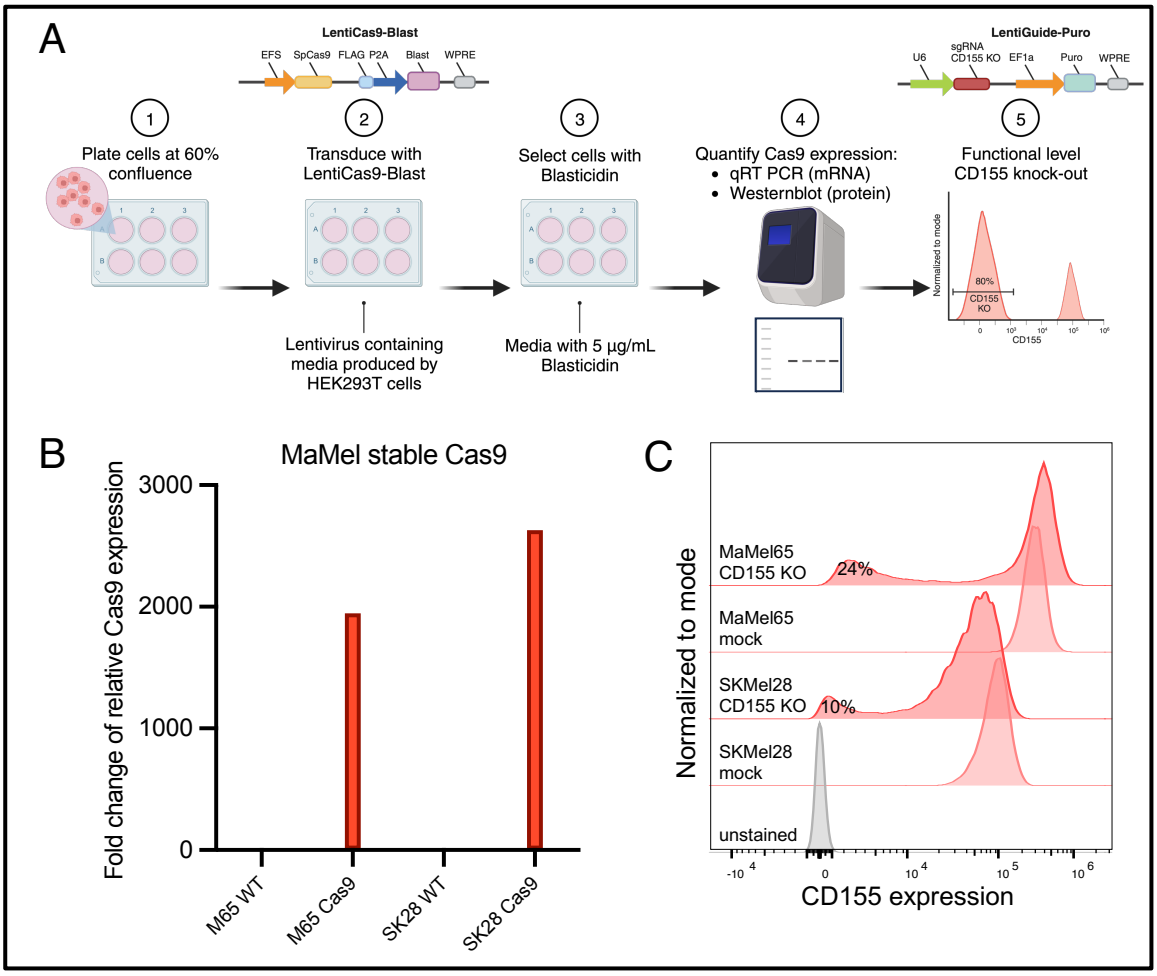

Figure 7: Characterisation of stable Cas9 expressing human melanoma cell lines. *A) Schematic overview of the generation and Characterisation of stable Cas9 expressing cell lines. Figure created with Biorender. B) Quantification of Cas9 mRNA expression in MaMel65 (M65) and SKMel28 (SK28) transduced with LentiCas9-Blast, mRNA Cas9 expression is relative to GAPDH. C) Flow cytometric assessment of CD155 surface expression upon CRISPR-mediated deletion of CD155 in M65 and SK28 cell lines expressing Cas9 stable. Mock-transduced constructed were transduced with empty LentiGuide-Puro vector and used as a control. The percentages represent the knock-out frequency of surface CD155 expression on day 7 after transduction. Dead cells and debris were excluded based on forward/side scatter and viability dye.*

In order to improve the knock-out efficiency, we tested an alternative Cas9 system utilizing doxycycline-inducible Cas9 (iCas9). Similar to the stable Cas9 expressing cell lines, quantification of iCas9 was performed on both mRNA and protein level, however, samples were stimulated with doxycycline to induce Cas9 expression for 48 hours before analysis (Fig. 8B and 8D). Different incubation times of doxycycline treatment were tested to determine the optimal stimulation length. Figure 8D shows the Western blot analysis of three iCas9 transduced cell lines we selected for the genome-wide CRISPR knock-out screen (Chapter 4). In all three cell lines, 48 hours of doxycycline treatment was sufficient to induce iCas9 expression on protein level (Fig. 8D). The qRT-PCR data showed that four out of six generated iCas9 human melanoma cell lines expressed iCas9 at similar mRNA levels (Fig. 8B). Notably, MaMel48a exhibited much lower iCas9 expression, while MaMel85 showed almost no Cas9 expression (see Fig. 8B). In MaMel54a iCas9 unstimulated with doxycycline was still low expression of iCas9 visible, which might indicate a minor leakage in the system. Although iCas9 mRNA levels were low in MaMel48a iCas9, protein analysis indicated that iCas9 was present at similar levels as measured in MaMel54a iCas9 and MaMel60 iCas9 (Fig. 8D).

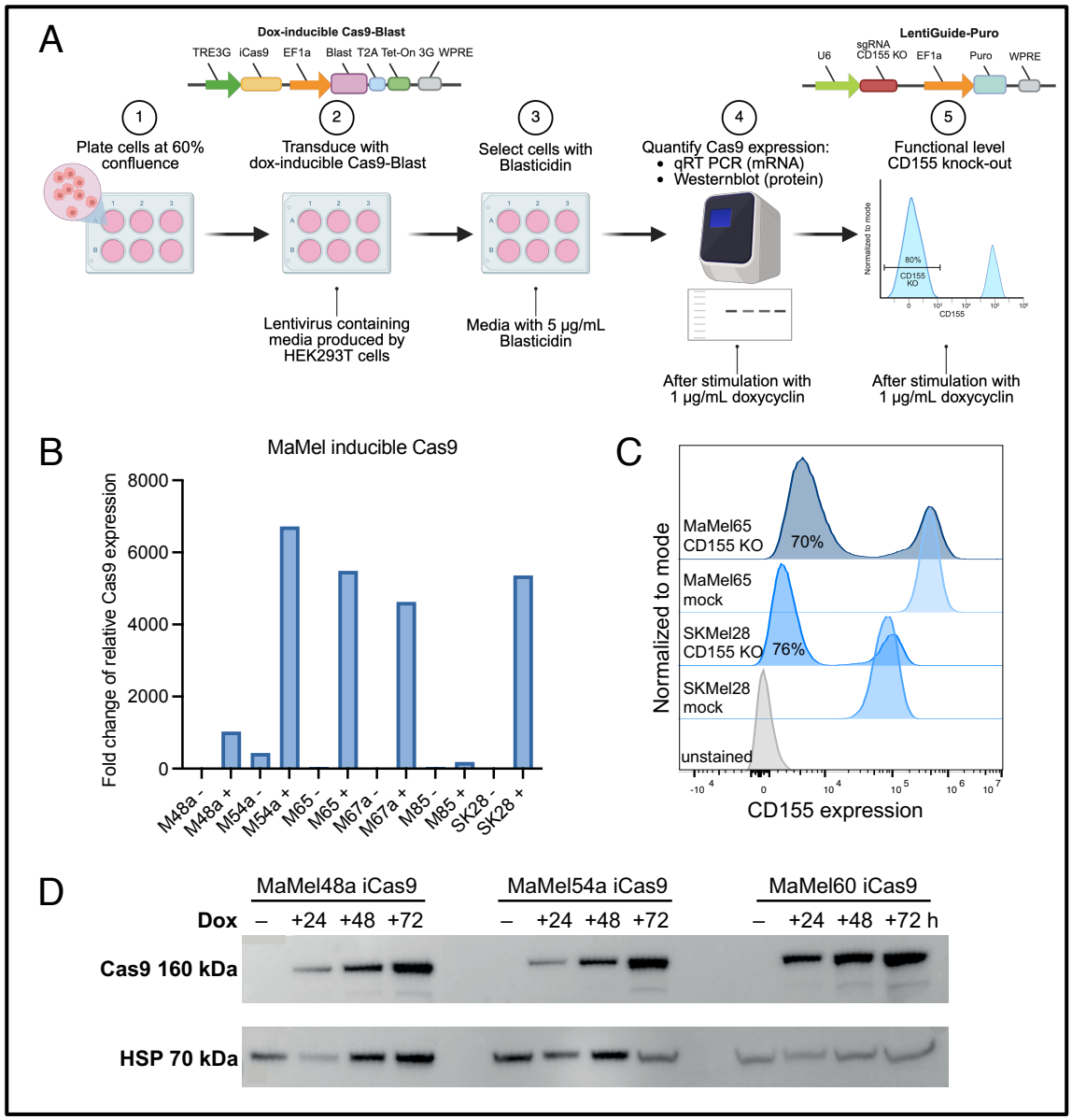

Figure 8: Characterisation of inducible Cas9 expressing human melanoma cell lines. *A) Schematic overview of the generation and Characterisation of inducible Cas9 expressing cell lines. Figure created with Biorender. B) Quantification of Cas9 mRNA expression after induction with doxycycline for 48 hours (+) in M48a, M54a, M65, M67a, M85 and SK28 transduced with iCas9 construct, mRNA Cas9 expression is relative to GAPDH. + = doxycycline stimulation for 48 hours; - = unstimulated. C) Flow cytometric assessment of CD155 surface expression upon CRISPR-mediated deletion of CD155 in M65 and SK28 iCas9 cell lines transduced with LentiGuide-Puro CD155 KO4. Mock-transduced constructed were transduced with empty LentiGuide-Puro vector and*

used as a control. The percentages represent the knock-out frequency of surface CD155 expression on day 7 after transduction. Dead cells and debris were excluded based on forward/side scatter and viability dye. D) Western blot analysis of human melanoma cell lines transduced with inducible Cas9 construct. Cas9 was induced by doxycycline treatment (1 µg/mL) for 24, 48 or 72 hours. Actin was used as a loading control. + = with doxycycline treatment (1 µg/mL), and - = without doxycycline treatment.

To assess the effectiveness of the doxycycline-inducible Cas9 system, again single knock-out transduction experiments targeting CD155 were performed in MaMel54a, MaMel65, MaMel67a and SKMel28 cell lines expressing iCas9. Seven days post-transduction with LentiGuide-Puro CD155 KO4, including 48 hours of doxycycline stimulation, the knock-out frequency of CD155 was measured by flow cytometry. Figure 8C shows the knock-out frequency in MaMel65 iCas9 and SKMel28 iCas9 was between 70 and 76 % respectively (Fig. 8C), similar results were observed in the other iCas9 melanoma cell lines (data not shown). The higher knock-out frequency of CD155 indicated that the inducible Cas9 system is much more effective in deleting CD155 compared to the stable Cas9 system. In addition, cell proliferation and CD155 expression were analysed (data not shown), and no differences were observed compared to either mock transduced or wildtype cells. Confirming that the random integration from inducible Cas9 in the genome of the iCas9 cell lines was not interfering with general cellular processes. Therefore, we decided to proceed with the inducible Cas9 system for the genome-wide CRISPR knock-out screens presented in Chapter 4.

In the final year of my PhD in Melbourne, after performing the genome-wide CRISPR screens in Bonn, my supervisor Marco Herold provided us with three different fluorescent Cas9 variants (BFP, GFP, and mCherry). We wanted to assess if the ubiquitin promoter driven Cas9 expression would make a difference in the knock-out frequency of CD155. In order to generate fluorescent Cas9 expressing cell lines, cells were transduced with FUCas9cherry (or BFP or GFP) (Fig. 9A), and subsequently sorted on live mCherry+ cells (or BFP+ or GFP+)

(Fig. 9B). After expansion of the mCherry+, BFP+ or GFP+ Cas9 expressing MaMel54a cell lines, the functional test of fluorescent Cas9 system was performed as previously described with a CD155 single knock-out transduction experiment. The functional test was performed in MaMel54a expressing all three different fluorescent Cas9 variants. The knock-out frequency of CD155 surface expression in all three fluorescent Cas9 variants ranged between 95 and 98 % (Fig. 9C). These results indicated that the fluorescent Cas9 system (independent of fluorescent colour) was the most effective in deleting CD155 compared to the stable and inducible Cas9 system in human melanoma cell lines. We proceeded with fluorescent Cas9 variant, instead of the previously used inducible Cas9 variant, for our validation experiments in Chapter 5.

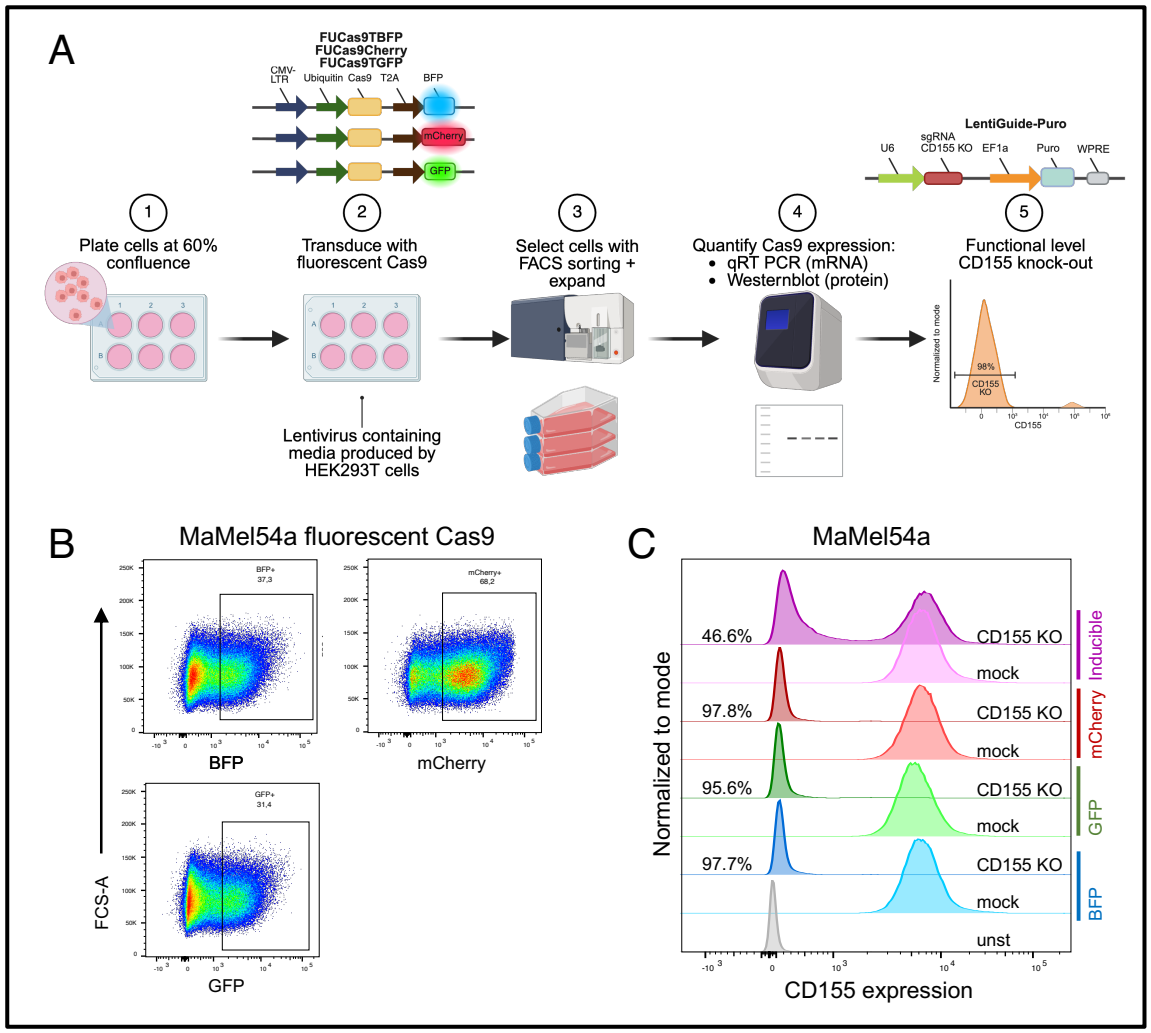

Figure 9: Characterisation of fluorescent Cas9 expressing human melanoma cell lines. *A) Schematic overview of the generation and Characterisation of fluorescent Cas9 expressing cell lines. Figure created with Biorender. B) Representative flow cytometry plots showing the sorting strategy for live M54a cells expressing BFP Cas9 (37 % positive), mCherry Cas9 (68 % positive) or GFP Cas9 (31 % positive). Dead cells and debris were excluded based on forward/side scatter and viability dye. C) Flow cytometric assessment of CD155 surface expression upon CRISPR-mediated deletion of CD155 in M54a cell lines expressing either inducible Cas9 (purple) or fluorescent Cas9 (BFP in blue, mCherry in red or GFP in green). Mock-transduced constructed were transduced with empty LentiGuide-Puro vector and used as a control. The percentages represent the knock-out frequency of surface CD155 expression on day 7 after transduction.*

3.4 RNA sequencing analysis of wildtype and CD155 knock-out human melanoma cells

To better understand CD155, bulk RNA sequencing was performed on MaMel65 wildtype cell line and two MaMel65 CD155 knock-out cell lines (KO4 and KO6). Due to time constrains and technical challenges in generating CD155 knock-outs via transduction in the beginning of this project, we used transfection as an alternative approach to generate CD155 knock-out cell lines for bulk RNA sequencing (Fig. 10A). Moreover, we were able to validate the designed CD155-targeting sgRNAs during the transfection experiment to confirm their functionality and used this experiment to trouble shoot the challenges encountered during our transduction experiments. The CD155 knock-out in MaMel65 for RNA sequencing was generated via transfection with px458 CD155 sgRNA KO4 or sgRNA KO6 followed by sorting of GFP-positive cells, expansion of sorted cells, and Sanger sequencing to verify the knock-out on the genomic level (Fig. 10A). Wildtype and CD155 knock-out cells were treated with different inflammatory cytokines IFN-γ, TNF-α or LPS, and untreated cells were used as controls in triplicates (Fig. 10A). We used IFN-γ as previous studies have shown that it could upregulate CD155 expression in human vascular endothelial cells (Escalante et al., 2011). After 48 hours of treatment, RNA was isolated and sequenced.

RNA sequencing showed that CD155 RNA expression is significantly lower in the CD155 knock-out cells compared to the wildtype MaMel65 cells in untreated condition (Fig. 10B), confirming the CD155 knock-out on RNA level. To investigate the effect of the inflammatory stimuli on CD155 expression, we compared wildtype and knock-out cells treated and untreated. In wildtype MaMel65 cells, TNF-α treatment reduced the CD155 RNA levels significantly (Fig. 10B). Similar effects were observed in CD155 knock-out cell lines (Fig. 10B). In addition, TNF-α treated cells, both MaMel65 wildtype and CD155 knock-out, clustered together in the Principal Component Analysis (PCA) (Fig. 10C), suggesting that TNF-α treatment might destabilize CD155 RNA or inhibit CD155 transcription. One out of three MaMel65 CD155 knock-out untreated sample (sgRNA KO4, called M4C2) was detected as an outlier on the PCA plot which

was likely caused by the low library size after mapping, meaning that there was a limited number of reads successfully aligned to the reference transcriptome. This can potentially lead to increased technical variability in gene expression estimations and distort the sample's expression profile, which making the outlier appear biologically distinct from the other samples. Treatment with IFN-γ or LPS did not show significant effects on CD155 RNA levels for MaMel65 wildtype and CD155 knock-out cells (Fig. 10B-C). Figure 10D shows the number of significantly ($p<0.05$) differentially expressed genes (DEGs) after removing non-protein coding genes and gene counts below 10. The highest number of DEGs was observed when comparing MaMel65 wildtype or CD155 knock-out cells with TNF-α treated cells. Figure 10D shows volcano plot comparing MaMel65 wildtype untreated cells with CD155 knock-out untreated cells. Significantly downregulated genes in the MaMel65 CD155 knock-out cells were *HLA-DRB1*, *HLA-DRA*, *HLA-DPB1*, *HLA-DPA1*, *HLA-DQB1*, and *HLA-DMB*, which are related to immune signaling and antigen presentation (Fig. 10D-E). Another significantly downregulated gene in MaMel65 CD155 knock-out cells was *NALF1*, which is a component of sodium leak channel. In contrast, the upregulated genes in CD155 knock-out cells (*DSP*, *DSG2*, *PTN*, *SYT1*, *IL33*, and *DLX3*) were associated with cell adhesion, growth and stress responses (Fig. 10D-E). These results suggest that a genetic CD155 knock-out induces metabolic adaptation and compensatory activation of growth and adhesion pathways, likely due to reduced signaling resulting from the absence of CD155 surface expression. Furthermore, other enriched biological pathways that were upregulated in untreated MaMel65 CD155 knock-out cells were epithelial development, inflammatory response and exocytosis/synaptic signalling (Fig. 10E). Downregulated pathways in untreated MaMel65 CD155 knock-out cells were T cell activation, regulation of immune effector process, and cytokine-mediated signaling pathway (Fig. 10E).

Figure 10F shows the DEGs after treatment with TNF-α in MaMel65 wildtype cells (left) and MaMel65 CD155 knock-out cells (right). Significantly upregulated genes in MaMel65 wildtype treated with TNF-α were *IL-32, TNFRSF9, CTSS, GPR68,*

IL-4I1, C3, and *CCL5* (Fig. 10F). Significantly upregulated genes in MaMel65 CD155 knock-out cells were as well *IL-32, TNFRSF9, GPR68, C3,* and *CCL5*, and in addition *ICAM1* and *IL-34* (Fig. 10F). These genes are related to immune and inflammation pathways, which is expected after treatment with inflammatory stimulus TNF-α. The similar upregulated genes following TNF-α treatment in MaMel65 wildtype cells and CD155 knock-out cells suggests that these genes are associated with TNF-α induced pathways, rather than playing a regulatory role in CD155 expression.

Taken together, these RNA expression changes indicate that the loss of CD155 in *BRAF*-mutant MaMel65 activates transcriptional networks that compensate for reduced immune and signaling activity while enhancing pathways involved in cell adhesion and growth.

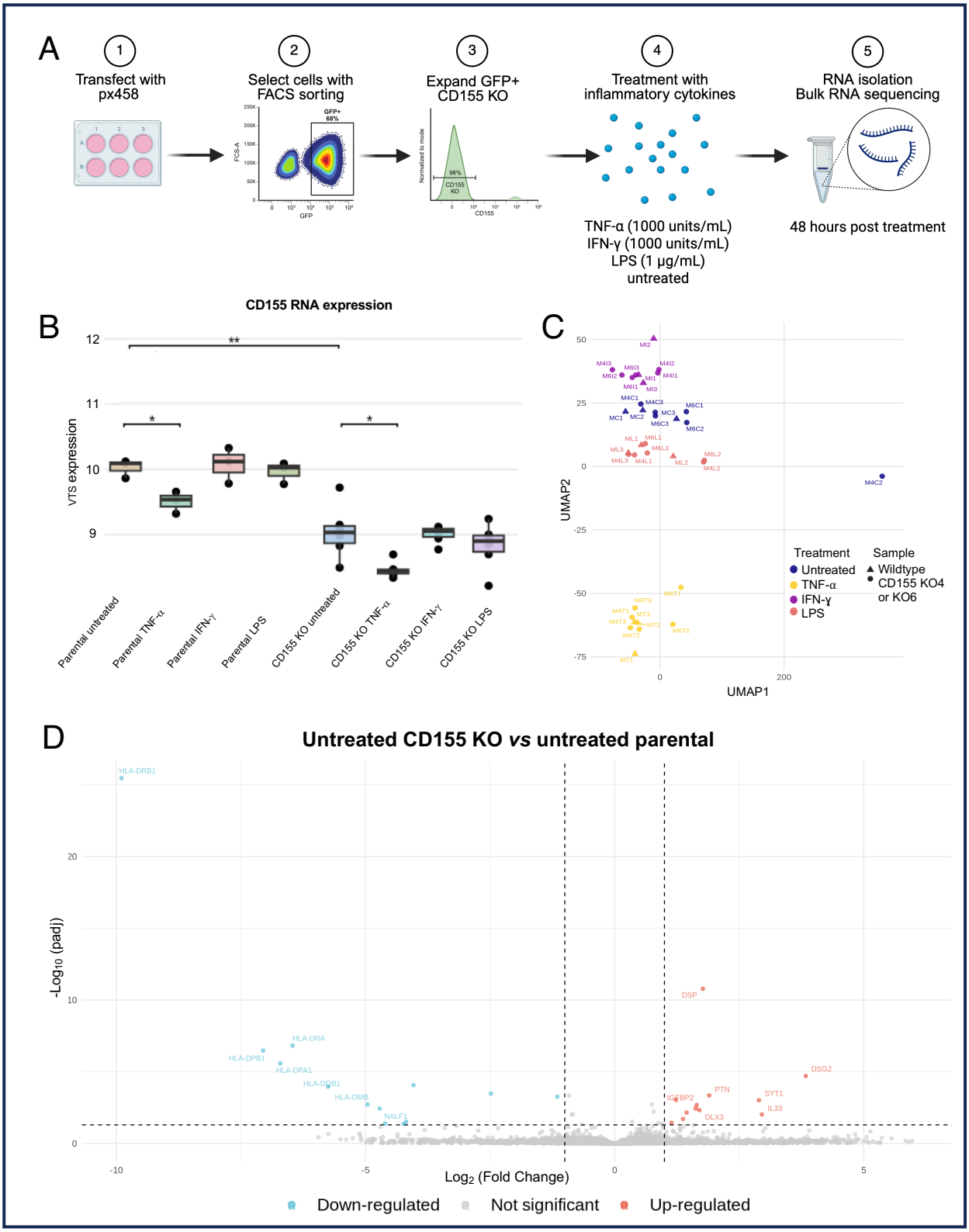
A
1
Transfect with px458
2
Select cells with FACS sorting
3
Expand GFP+ CD155 KO
4
Treatment with inflammatory cytokines
5
RNA isolation Bulk RNA sequencing
TNF-α (1000 units/mL)
IFN-γ (1000 units/mL)
LPS (1 µg/mL)
untreated
48 hours post treatment
B
CD155 RNA expression
VTS expression
Parental untreated
Parental TNF-α
Parental IFN-γ
Parental LPS
CD155 KO untreated
CD155 KO TNF-α
CD155 KO IFN-γ
CD155 KO LPS
C
UMAP1
UMAP2
Treatment
Untreated
TNF-α
IFN-γ
LPS
Sample
Wildtype
CD155 KO4 or KO6
D
Untreated CD155 KO vs untreated parental
-Log10 (padj)
Log2 (Fold Change)
Down-regulated
Not significant
Up-regulated

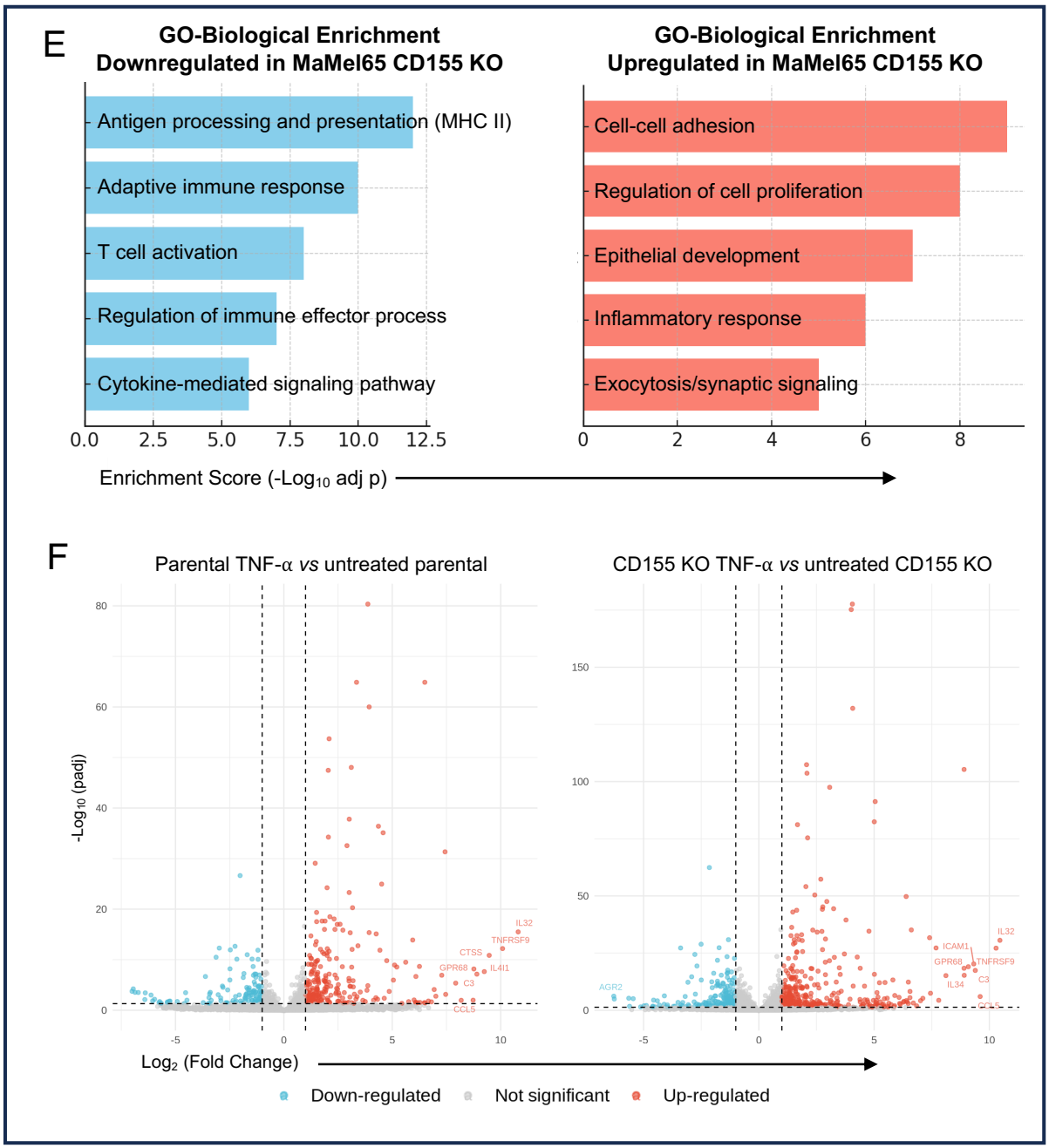

Figure 10: RNA sequencing analysis of CD155 in MaMel65 wildtype and CD155 knock-out cell line. *10A) Schematic overview of the generation and expansion of CD155 knock-out cells via transfection. Figure created with Biorender. B) Bar graph showing normalized CD155 RNA expression levels in MaMel65 wildtype cells and CD155 knock-out cells untreated or treated for 48 hours (TNF-α, IFN-γ, or LPS) (n=3). Mean ± standard deviation. C) Principal Component Analysis (PCA) of all samples (round = MaMel65 wildtype cells and triangle = MaMel65 CD155 knock-out cells) based on treatment: untreated (blue), IFN-γ (purple), LPS (pink), and TNF-α (yellow) showing separate clustering of both TNF-α treated MaMel65 wildtype and CD155 knock-out cells.*

D) Volcano plot representing DEGs comparing untreated MaMel65 wildtype cells and CD155 knock-out cells, P<0.05. E) GO-biological enrichment analysis showing downregulated (left) and upregulated pathways (right) in untreated MaMel65 CD155 knock-out cells. F) Volcano plot representing DEGs comparing TNF-α treated MaMel65 wildtype cells to untreated wildtype cells (left), and TNF-α treated CD155 knock-out to untreated CD155 knock-out cells (right), P<0.05.

4. Chapter 4: Identification of molecular signaling pathways regulating CD155 surface expression in human melanoma

4.1 Introduction

To investigate the intrinsic regulation of CD155, we conducted genome-wide CRISPR knock-out screens in selected human melanoma cell lines. After introducing the sgRNA library, cells were sorted on low CD155 expression and enrichment of sgRNAs was compared to the unsorted population. Based on data presented in Chapter 3, the inducible Cas9 construct was selected as a suitable system for the genome-wide CRISPR knock-out screen. Three different human melanoma cell lines were selected for the genome-wide CRISPR knock-out screen based on their CD155 expression levels (low, intermediate and high) and the oncogenic driver mutations (Fig. 5), to minimize cell line specific effects on the results. The following cell lines were selected: MaMel48a (*HRAS*-mutant), MaMel54a (*BRAF*-mutant) and MaMel60 (*NRAS*-mutant).

4.2 Genome-wide CRISPR knock-out screen in human melanoma cell lines

Inducible Cas9 expressing human melanoma cell lines (MaMel48a, MaMel54a and MaMel60) were lentivirally transduced with the genome-wide CRISPR knock-out screen library (Brunello, Addgene) consisting of 76,441 sgRNAs in two technical replicates (n=2 and for MaMel54a we had two biological replicates n=4). The library contained four sgRNAs per gene and covered 19,12 x 10^3 human protein-coding genes. The transduction was performed at a low multiplicity of infection (MOI) to ensure that each cell was transduced with a single sgRNA (Fig. 11A). Puromycin selection was started two days post-transduction and maintained in the media throughout the entire experiment. Figure 11B shows the viability of transduced cells 48 hours post puromycin selection. As expected, the majority of untransduced iCas9 cells died due to lack of puromycin resistance, while library transduced cells remained viable. This confirmed that transduction with the library construct and antibiotic selection was successful. Puromycin was refreshed every 48 hours. On day 7 post-transduction, 10 x 10^6 library transduced cells per replicate were harvested as an unsorted reference control, and 100 x

10^6 cells per replicate were stained and FACS-sorted for the lowest 3-5 % of CD155 surface expression (Fig. 11C). There were no library transduced cells which expressed higher levels of CD155 and therefore this population was not sorted. To promote pellet formation and prevent cell loss due to adhesion to the tube walls, CD155-low cells were sorted into 100 % FBS in low-binding DNA tubes.

Variable numbers of CD155-low cells were sorted from each library transduced cell line as this number is dependent on the cell line with each different level of CD155 expression and oncogenic driver mutation, as well as different proliferation rates (Table 17). For the first replicate of library transduced inducible Cas9 MaMel48a (*HRAS*-mutant) 4,85 x 10^5 CD155-low cells were sorted, and similar amount was sorted for the second replicate, 6,5 x 10^5 cells. For the first replicate of library transduced inducible Cas9 MaMel54a (*BRAF*-mutant) 4,63 x 10^5 CD155-low cells were sorted, and 5,2 x 10^5 cells for the second replicate. In a repetition of this experiment the same cell line (MaMel54a) 1 x 10^6 CD155-low expressing cells were sorted for both replicates, which was twice as many as in the first experiment. This suggests improved technical execution as well as improved experimental optimization. In the final screen of my PhD using library transduced inducible Cas9 MaMel60 (*NRAS*-mutant) cells, a similar number of CD155-low cells were sorted in both replicates, with 1,2 x 10^6 cells sorted per replicate. These results demonstrate consistent experimental execution.

Table 17: Overview of the number of CD155-low sorted cells

The table shows the number of CD155-low sorted cells, which are the lowest 3-5% CD155 expression of library transduced cells.

Library transduced cell line	Number of CD155-low sorted cells (10^5)
MaMel48a inducible Cas9 replicate 1	4,9 x 10^5
MaMel48a inducible Cas9 replicate 2	6,5 x 10^5
MaMel54a inducible Cas9 replicate 1	4,6 x 10^5
MaMel54a inducible Cas9 replicate 2	5,2 x 10^5
MaMel54a inducible Cas9 replicate 3	10 x 10^5
MaMel54a inducible Cas9 replicate 4	10 x 10^5
MaMel60 inducible Cas9 replicate 1	12 x 10^5
MaMel60 inducible Cas9 replicate 2	12 x 10^5

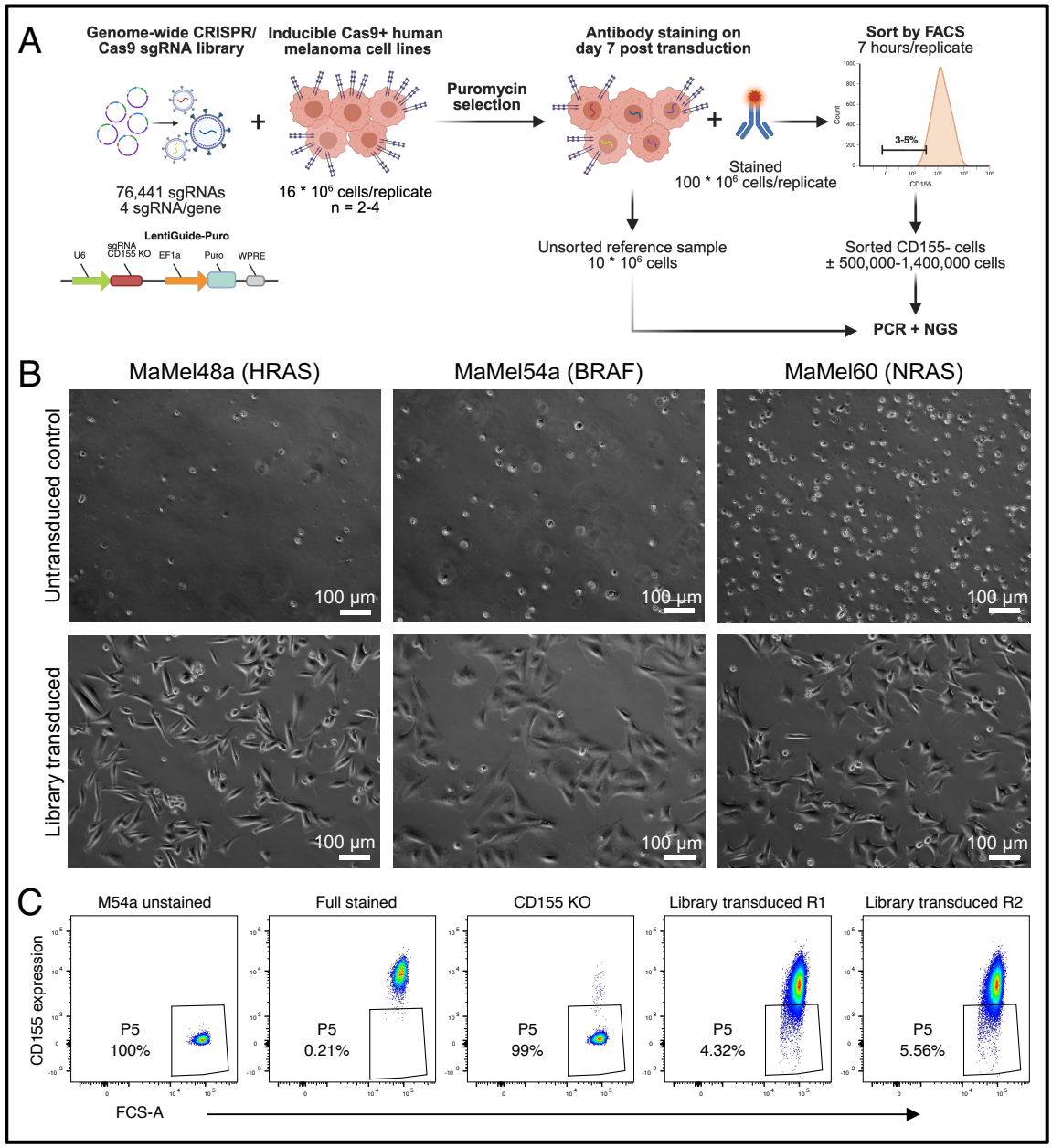

Figure 11: Genome-wide CRISPR knock-out screen in MaMel48a, MaMel54a and MaMel60 expressing inducible Cas9. *A) Schematic overview of the genome-wide CRISPR knock-out screen in inducible Cas9 expressing human melanoma cell lines. Figure created with Biorender. B) Representative microscope images (10x magnification) of library transduced MaMel48a, MaMel54a and MaMel60 48 hours post puromycin selection (2 µg/mL). Untransduced cells were used as a control. Scale bar = 100 µm. C) Representative flow cytometry plots showing sorting strategy for CD155-low (P5)*

library transduced inducible Cas9 MaMel54a cells on day 7 post-transduction (n = 4). Similar sorting strategy was used for the other two library transduced cell lines (MaMel48a and MaMel60, each n = 2. Dead cells and debris were excluded by forward/side scatter and viability dye. Lowest 3-5 % CD155 expressing cells were sorted, which were gated as P5. Sort gate controls included unstained (M54a unstained), positive control LentiGuide-Puro mock transduced cells (Full stained), and negative control CD155 knock-out cells (CD155 KO). Library transduced R1 = replicate 1 and Library transduced R2 = replicate 2. P5 = percentage of single live CD155-low cells. FSC-A = forward scatter area.

The genomic DNA of the library transduced cell lines underwent PCR amplification with the aim of amplifying the sgRNA sequences of the genome-wide CRISPR knock-out library (workflow see Fig. 12). To increase sequence complexity and ensure accurate base calling during the initial cycles of NGS, PCR primers containing staggered (complexity) regions of variable length were incorporated. These stagger sequences introduce artificial base diversity at the beginning of the reads, which facilitates proper signal calibration, reduced low-diversity sequencing artifacts, and improves overall data quality. Subsequently, PCR reactions were performed in replicates. The PCR product was purified before gel electrophoresis. Afterwards, the PCR product was extracted from the gel (amplicon size: 249 base pairs), and purified once more. The desired PCR product of the pooled unsorted fraction as well as the sorted CD155-low fraction was detected in all replicates across the three library transduced cell lines, confirming that PCR amplifications were successful. Each fraction was loaded at 14 % on the cartridge in order to sequence one experiment on a single sequence cartridge, which equals for 42 x 10^6 reads per fraction (four fractions: unsorted replicate 1, unsorted replicate 2, CD155 low-sorted replicate 1 and CD155-low sorted replicate 2). To quantity sgRNA abundance, sequencing reads were compared against the sgRNA library, and the number of reads matching each sgRNA were calculated which were represented as the gene counts for each sgRNA of the library. Quality control was performed by assessing sgRNA representation within the library and comparing the expected loading percentage

with the obtained read distribution. The sgRNA library showed an even distribution, allowing us to proceed with the NGS analysis.

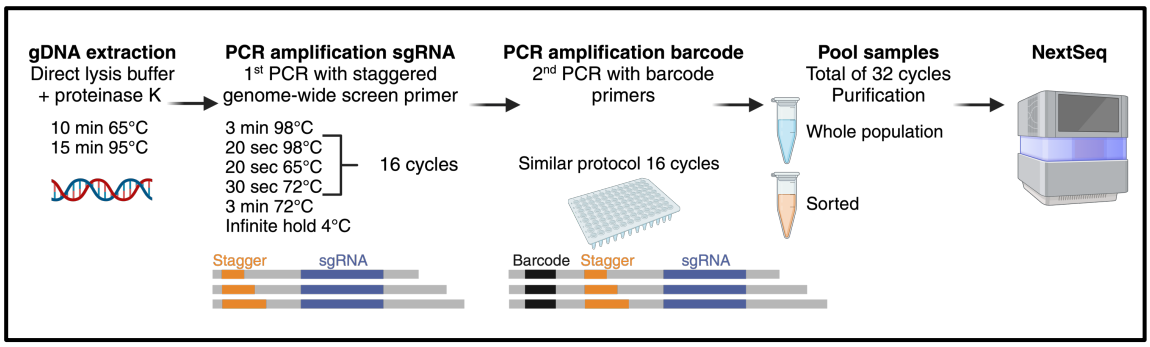

Figure 12: Genome-wide CRISPR knock-out screen sample preparation of unsorted and sorted fraction for Next Generation Sequencing. *Schematic overview of sample preparation for Next Generation Sequencing (NGS). Figure created with Biorender.*

CD155 sgRNAs served as an internal positive control for the genome-wide CRISPR knock-out screen for successful transduction, puromycin selection, FACS sorting, PCR and NGS (Fig. 12). The library consisted of four sgRNAs per gene. Figure 13 shows the read counts per sgRNA per cell line in the unsorted fraction (left) and in the CD155-low sorted fraction (right). The read counts of one sgRNA are connected with a line to compare between both fractions. In MaMel54a library transduced cells, the read counts for each sgRNA CD155 (n = 4) were higher in the CD155-low sorted fraction compared to the unsorted fraction in each replicate (2 replicates with each 4 sgRNAs for CD155, showing 8 lines). In the other library transduced cell lines MaMel48a and MaMel60 similar results were observed (Fig. 13). Taken together, all four sgRNAs targeting CD155 were the most enriched genes in the CD155-low sorted fraction of each replicate across three different library transduced cell lines, confirming successful transduction, puromycin selection, FACS sorting, PCR amplification and NGS. Furthermore, each sgRNA targeting *DYRK1A* (n = 4 sgRNAs) was significantly enriched in the CD155-low sorted MaMel54a library transduced cells in each replicate (n = 4) (Fig. 13).

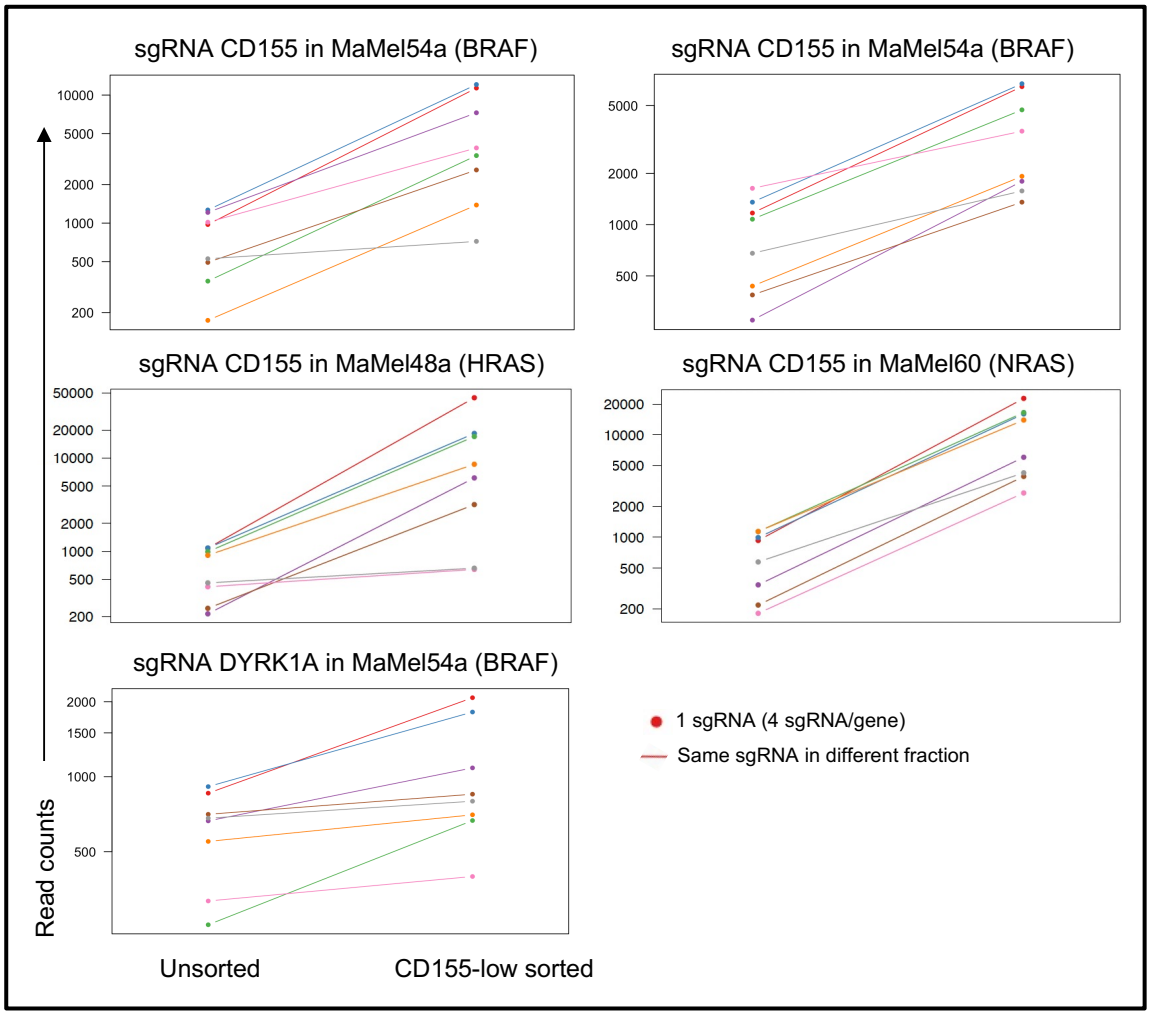

Figure 13: MAGeCK quality control plot comparing sgRNA read counts of CD155 or DYRK1A between the unsorted fraction and the CD155-low sorted fraction per cell line. *Each point represents the normalized read counts for four sgRNA per gene. Lines connect read counts from 1 sgRNA measured in unsorted fraction (left) to the read counts from the similar sgRNA measured in the CD155-low sorted fraction (right). Two biological replicates per cell line and therefore eight dots on each side, connecting eight different lines per plot. The plots show reproducibility and read consistency across all library screened cell lines for CD155 (MaMel48a, MaMel54a, and MaMel60 expressing iCas9), and DYRK1A read counts for only library screened MaMal54a expressing iCas9.*

MAGeCK analysis in R was performed to analyse the genome-wide CRISPR screen NGS data. Robust Ranking Aggregation (RRA) scores are shown in Fig. 14, RRA scores are ranking significantly enriched genes in the CD155-low sorted fraction compared with the unsorted fraction based on their counts and number of sgRNAs per gene. The highest significant enriched genes in CD155-low sorted library transduced MaMel48a cells were *CD155, SOX10*, *NUS1*, *SOX10*, *CWC22*, *VPS28*, *MYC*, *HRAS*, *TUT1,* and *UBL5* (Fig. 14). In MaMel54a the highest significantly enriched genes in the CD155-low sorted fraction were *CD155, SRP54*, *DAD1*, and *CDKN1A*. In the repeat in MaMel54a, the number of sorted CD155-low cells was doubled, which resulted in the identification of a larger set of significantly enriched genes (Fig. 14). Similar genes as in the other replicate, and in addition *DYRK1A*, *NUS1*, *SEC61A1*, *FNDC3B*, *WDR44*, *TLN1*, *ITGB5*, *TP53*, *GMPPB*, and *FERMT1* (Fig. 14). In the *NRAS*-mutant cell line MaMel60 again *CD155* was significantly enriched, and other genes *DNM2*, *SSU72*, *SYMPK*, *CLP1*, *CHMP4B*, *NRF1*, *CPSF3*, and *EEF2* (Fig. 14).

The top significantly enriched genes of each cell line were compared to identify commonly enriched genes across the three library transduced cell lines. Figure 15A shows significant most enriched genes in the CD155-low sorted fraction across three cell lines based on RRA scores. Six genes were commonly significant enriched in the CD155-low sorted fraction across three library transduced cell lines include: *CD155*, *SRP54*, *SEC61A1*, *DHDDS*, *NUS1*, and *ALG11*. Indicating that these genes are enriched in the CD155-low sorted fraction independent of the oncogenic driver mutation, level of CD155 expression and proliferation rate, and could potentially be strong intrinsic regulators of CD155 surface expression. These results showed that individual knock-out of these six genes reduced the surface expression of CD155, a pattern observed consistently across all replicates of the three library transduced cell lines. Furthermore, the CD155-low sorted fraction of MaMel48a and MaMel60 show 25 shared significantly enriched genes, whereas MaMel48a and MaMel54a only show one shared significantly enriched gene. MaMel54a and MaMel60 had no shared enriched genes (Fig. 15A).

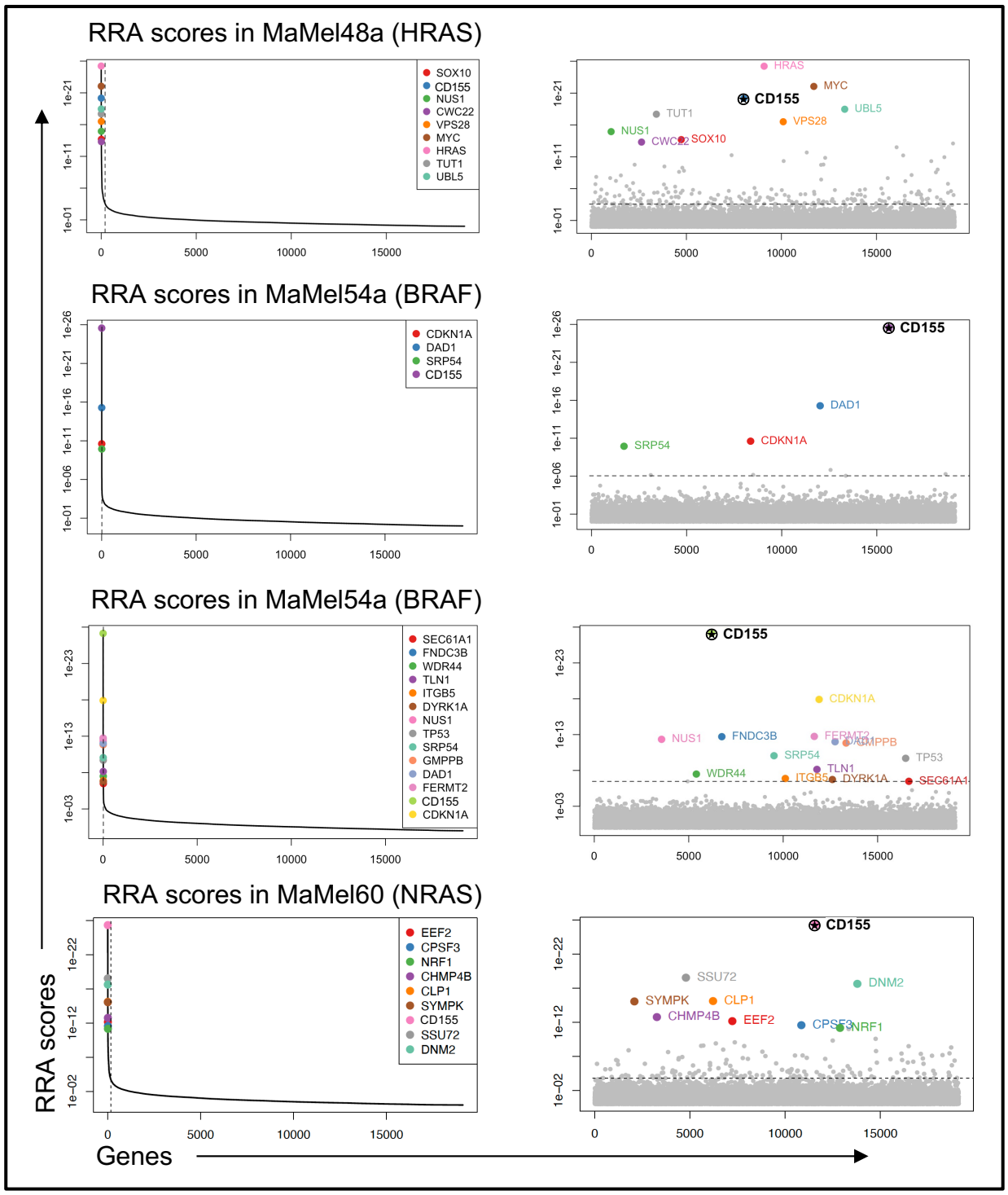

Figure 14: MAGeCK analysis of genome-wide CRISPR knock-out screen in MaMel48a, MaMel54a and MaMel60 expressing inducible Cas9. *Robust Ranking Aggregation (RRA) scores of each gene determined by MAGeCK based on two replicates per cell line. Each dot represents one gene. Genes are significant if RRA score < 0.05, dotted line.*

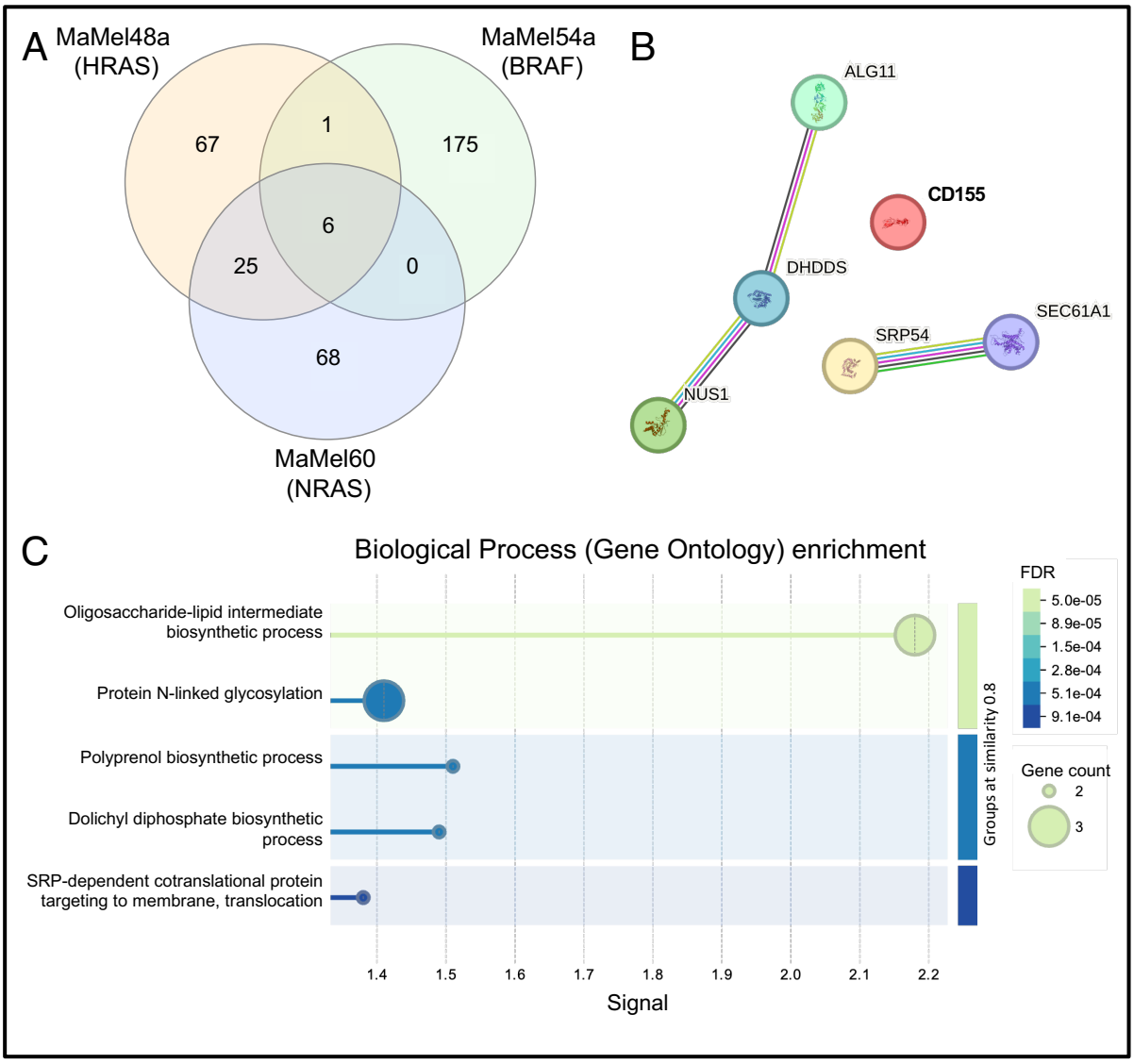

Figure 15: Analysis of six commonly enriched genes identified in genome-wide CRISPR knock-out screen in MaMel48a, MaMel54a and MaMel60 expressing inducible Cas9. *A) Venn diagram showing significantly enriched genes per library transduced cell line, identified by MAGeCK based on RRA scores, and their overlap across all three cell lines MaMel48a, MaMel54a and MaMel60. Shared regions indicate genes that are commonly enriched across two or three cell lines in CD155-low sorted fraction, while unique regions represent cell line specific enriched genes. B) Protein-protein interaction of the six commonly enriched genes across all three cell lines, generated by STRING. C) Gene ontology (GO) enrichment analysis of biological processes associated with the six commonly enriched genes. Significance was assessed using the false discovery rate (FDR<0.05).*

4.3 Glycosylation and protein translocation are important pathways for CD155 surface expression

STRING was used to predict protein-protein interactions between the six shared enriched genes in CD155-low sorted cells across three cell lines. STRING analysis linked *DHDDS*, *NUS1* and *ALG11* (Fig. 15B). This suggests that the connected genes are physically or functionally related to each other. DHDDS and NUS1 form a complex together called Dehydrodolichyl Diphosphate Synthase which is an essential lipid for N-linked glycosylation (Bar-El et al., 2020; Edani et al., 2020). Whereas ALG11 is an important catalyzer for mannosylation in the early stage of N-linked glycosylation (Gao et al., 2004), which is therefore connected to DHDDS and NUS1. These results highlight the importance of glycosylation for CD155, is has previously been shown that CD155 contains five predicted N-glycosylation sites (Zhang et al., 2008). Furthermore, glycosylation has been described to play a role in the stability and confirmation of CD155 and therefore modulating binding to its ligands CD226 or TIGIT (Fuchs et al., 2004; Tahara et al., 2024; Zhang et al., 2008). However, the potential impact of glycosylated CD155 and its interaction with CD96 has not yet been investigated.

On the other hand, STRING analysis connected the gene *SRP54* with *SEC61A1* as they are both important for protein translocation at the membrane of the endoplasmic reticulum (ER) (Lang et al., 2017). CD155 was not predicted to be connected to other enriched genes based on protein-protein interaction analysis in STRING. To understand better the function of these six enriched genes, gene ontology enrichment analysis was performed, and different significant biological processes were identified (Fig. 15C). Two consistent main pathways were identified: protein translocation and N-linked glycosylation, which was expected based on the STRING protein-protein interactions analysis.

5. Chapter 5: Validation using pharmacological and genetic approaches to test their relevance in regulating CD155 surface expression in human melanoma

5.1 Introduction

The five commonly enriched genes (*ALG11*, *DHDDS*, *NUS1*, *SRP54* and *SEC61A1*) in the CD155-low sorted fraction across three cell lines identified in Chapter 4 are essential genes. A single knock-out of one of these identified enriched genes would ultimately lead to cell death, indicating that these genes are no suitable candidates for targeted modulation of CD155. Therefore, we decided to re-analyse the RRA scores of the genes from the genome-wide CRISPR knock-out library to identify additional enriched genes in the CD155-low sorted fraction that may play a role in the intrinsic regulation of CD155.

Figure 14 shows other genes that are significantly enriched in the CD155-low sorted fraction. RRA scores of each sgRNA of dual-specificity tyrosine phosphorylation-regulated kinase 1A (*DYRK1A*) were significantly enriched in CD155-low fraction of MaMel54a (Fig. 13 and 14). In addition, *DYRK1A* related genes such as *CD5L*, *GMFB* and *PTK6* were also significantly enriched in the CD155-low sorted fraction of MaMel54a. DYRK1A is the most studied member of the DYRKs family of proteins, which are known to auto-phosphorylate tyrosine residue during phosphorylation of specific substrates on threonine and serine residues (Lochhead et al., 2005). DYRK1A is important for cell cycle regulation and it induces G0/G1 arrest due to phosphorylation of these different residues. In glioblastoma, DYRK1A is able to regulate cyclin-dependent kinsase-1 (*CDK1*), and inhibitors targeting DYRK1A have shown promising results by reducing glioblastoma progression (Laham et al., 2024; Massey et al., 2021). The role of DYRK1A in cancer remains controversial due to variation across different tumor types, with some studies describing tumor suppressive properties whereas others report a tumor promoting role (Bhansali et al., 2021; Boni et al., 2020; Kaltheuner et al., 2021; Laham et al., 2021; Liu et al., 2014). A single knock-out of *DYRK1A* or the *DYRK1A*-related genes *CD5L*, *GMFB* and *PTK6* in MaMel54a (*BRAF*-

mutant) and MaMel60 (*NRAS*-mutant) was generated to validate their effect on CD155 surface expression. Validation of thirty additional enriched genes was previously performed in Bonn using the suboptimal inducible Cas9 system (data not shown). Many of these genes were essential, and a knock-out was lethal in our melanoma cell lines, making these genes not suited for targeted modulation of CD155. To overcome the limited knock-out efficiency of the inducible Cas9 system, the fluorescent Cas9 variant was used for subsequent validation of the significantly enriched genes identified in the CD155-low sorted fraction (*DYRK1A*, *CD5L*, *GMFB*, and *PTK6*). All presented validation experiments in this thesis were performed in Melbourne during the final months of the PhD.

5.2 Loss of DYRK1A reduces CD155 surface expression in human melanoma

In order to validate enriched genes identified in the CD155-low sorted fraction, single gene knock-outs of the enriched genes were generated and CD155 surface expression was monitored over time. One or two sgRNAs from the screen library (referred to as KO1, KO2, KO3, and KO4), and one or two CRISPick-designed sgRNAs (referred to as KO5 and KO6) were cloned into the same backbone vector used in the genome-wide CRISPR knock-out library described in Chapter 4 (LentiGuide-Puro). MaMel54a (*BRAF*-mutant) and MaMel60 (*HRAS*-mutant) expressing mCherry+ Cas9 were used to generate a single gene knock-out of the following genes: *DYRK1A*, *CD5L*, *GMFB* or *PTK6*. Seven days post-transduction, CD155 surface expression in the knock-out cell lines was measured and normalized to the corresponding mock-transduced cell line, which was transduced with LentiGuide-Puro without a sgRNA insert. Furthermore, a single knock-out of CD155 using LentiGuide-Puro CD155 KO4 plasmid served as a positive experimental control, confirming virus production, transduction efficiency, and puromycin selection.

Figure 16A shows that a knock-out of CD155 in MaMel54a *BRAF*-mutant melanoma cell line expressing mCherry+ Cas9 reduced CD155 surface expression on day 7 post transduction with 98 %. Thus, confirming that virus

production, transduction efficiency and puromycin selection was successful. MaMel54a cells with a knock-out of DYRK1A, transduced with either sgRNA KO1 or KO5, showed a 50 % reduction in CD155 surface expression on day 7 post transduction (Fig. 16A). Whereas a single knock-out of the other three DYRK1A-related genes *CD5L*, *GMFB* or *PTK6* did not show massive reduction in CD155 surface expression in MaMel54a mCherry+ Cas9 (Fig. 16A). Only knock-out of CD5L with sgRNA KO2 and GMFB KO4 resulted in a minimal reduction in CD155 expression levels (5 %).

Figure 16B shows the same experiment in MaMel60 *NRAS*-mutant melanoma cell line expressing mCherry+ Cas9. Knock-out of CD155 in MaMel60 reduced CD155 surface expression on day 7 post transduction (Fig. 16B). Confirming that virus production, transduction efficiency and puromycin selection was successful. Comparable to MaMel54a, knock-out of DYRK1A with sgRNA KO1 in MaMel60 resulted in a 50 % reduction in CD155 surface expression. However, the second sgRNA targeting DYRK1A KO5 induced a smaller reduction (30 %) in CD155 surface expression day 7 post transduction (Fig. 16B). Furthermore, a knock-out of CD5L in MaMel60 reduced CD155 surface expression with 40 %, similar results were observed for CD5L KO1 and KO2. Knock-out with additional self-designed sgRNA targeting CD5L (CD5L KO5) was only able to reduce the CD155 surface expression of MaMel60 with 10 % (Fig. 16B). Similar reductions in CD155 surface expression were observed after knock-out of GMFB in MaMel60, it reduced CD155 surface expression with 40 % with the self-designed sgRNA KO5, whereas the sgRNA GMFB KO4 from the library was only able to reduce CD155 surface expression by 10 % (Fig. 16B).

Since deletion of DYRK1A showed the greatest reduction in CD155 surface levels in both MaMel54a and MaMel60 cell lines, we focused on this gene and repeated the knock-out experiment to ensure the reproducibility. Independent repetition experiments confirmed that a single knock-out of DYRK1A in MaMel54a mCherry+ Cas9 led to a significant 50 % reduction in CD155 surface expression with both sgRNAs (KO1 or KO5) on day 7 post transduction (Fig. 16C and E). Similar significant reduction in CD155 surface expression levels was observed in

MaMel60 mCherry+ Cas9 after knock-out with DYRK1A KO1 (50 %), and knock-out of DYRK1A with DYRK1A KO5 reduced CD155 surface expression by 40 %, however, this was not significant across all our replicates (Fig. 16D and F). CD155 expression in DYRK1A knock-out cells remained consistently low for at least four weeks compared with mock-transduced MaMel54a mCherry+ Cas9 cells or MaMel60 mCherry+ Cas9 cells. Furthermore, the low CD155 surface expression was stable after repeated freeze-thaw cycle (data not shown). These results indicate that DYRK1A is a regulator of CD155 surface expression in both MaMel54a and MaMel60 cell lines, making it an interesting target to modulate CD155 expression.

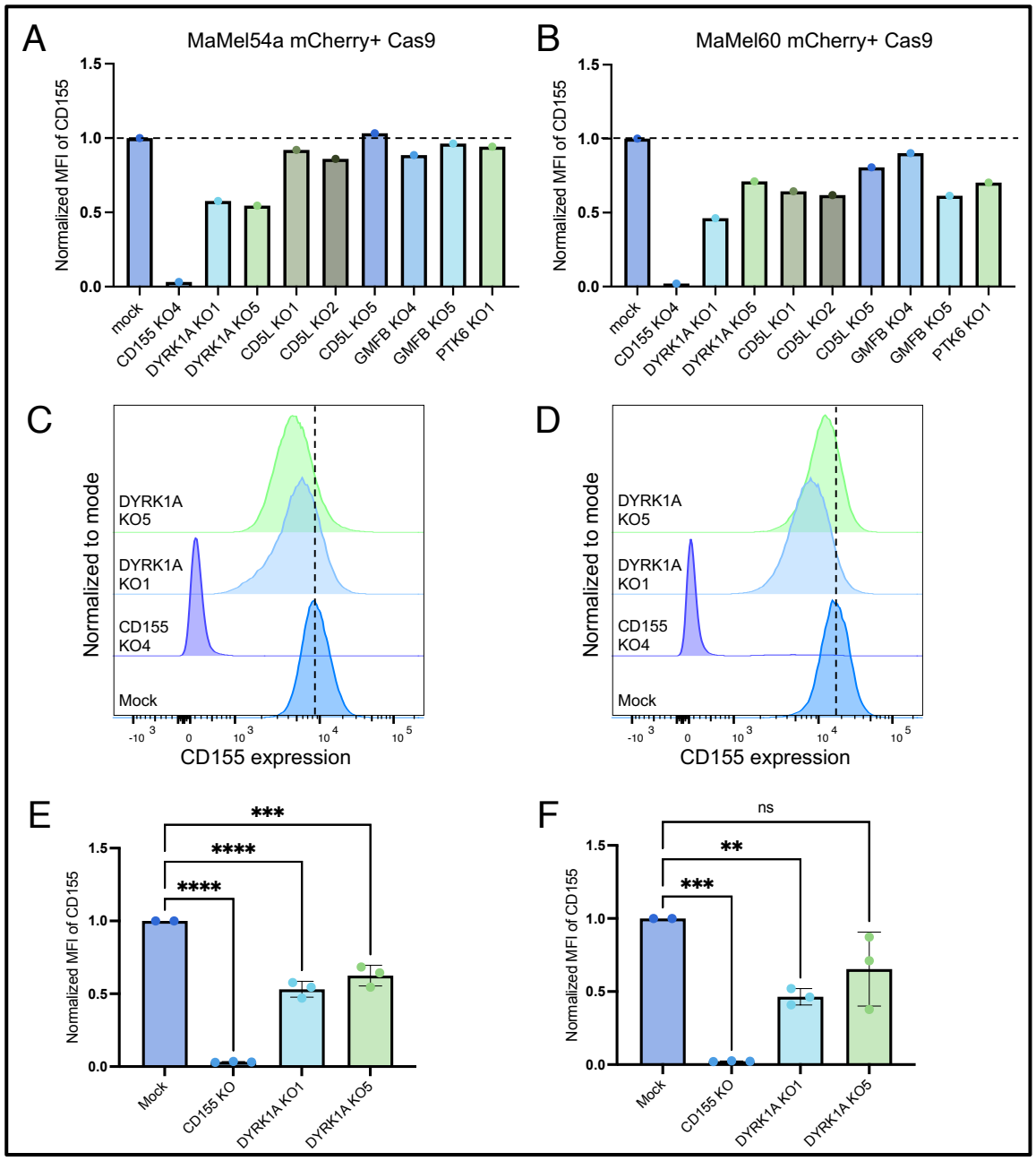

Figure 16: Effect of single gene knock-outs identified in genome-wide CRISPR knock-out screen on CD155 surface expression in human melanoma cell lines. *A-B) Flow cytometric assessment of CD155 surface expression on day 7 upon CRISPR-mediated deletion of CD155, DYRK1A, CD5L, GMFB or PTK6 in MaMel54a and MaMel60 cell lines expressing fluorescent mCherry Cas9. Mock transduced constructed cells (transduced with empty LentiGuide-Puro vector) were used as a control to normalize the MFI of live single mCherry+ cells (n = 1). C-D) Flow cytometric assessment of CD155*

*surface expression normalized to mode on day 7 upon CRISPR-mediated deletion of DYRK1A (with sgRNA KO1 or sgRNA KO5) in MaMel54a and MaMel60 cell lines expressing fluorescent mCherry Cas9 (n = 3). Mock transduced constructed cells were used as a control, and CD155 KO transduced cells were used as a positive control for virus production, transduction efficiency, and puromycin control. Dead cells and debris were excluded based on forward/side scatter and viability dye. E-F) Flow cytometric assessment of normalized MFI of CD155 of live single mCherry+ cells. Mock transduced constructed cells were used as a control to normalize the MFI, and CD155 KO transduced cells were used as a positive control for virus production, transduction efficiency, and puromycin control. Dead cells and debris were excluded based on forward/side scatter and viability dye. P-values were generated using one-way ANOVA: ns = not significant p < 0.05; * = p < 0.05; ** = p < 0.01; *** = p < 0.001; **** = p < 0.0001*

5.3 AKT inhibitor treatment as pharmacological target to reduce CD155 surface expression in human melanoma

DYRK1A has a role in phosphorylation and regulation of mTOR, thereby influencing the AKT signaling pathway (Rammohan et al., 2022; Wang et al., 2024). Deletion of DYRK1A resulted in a significant reduction of CD155 surface expression in human melanoma cell lines MaMel54a (*BRAF*-mutant) and MaMel60 (*NRAS*-mutant). In addition, in MaMel60 a single knock-out of three DYRK1A-related genes (*CD5L*, *GMFB*, or *PTK6*) reduced CD155 surface expression levels. Given the previously described link between DYRK1A and AKT pathway (Rammohan et al., 2022; Wang et al., 2024), we hypothesized that inhibition of AKT could induce similar reduction in CD155 expression as observed after DYRK1A knock-out. Therefore, we investigated whether AKT inhibitors could reduce CD155 surface expression in human melanoma cell lines. We hypothesized that, under healthy conditions, DYRK1A would contribute to AKT phosphorylation, thereby promoting the activation of the AKT pathway and ultimately promoting immune escape and cell survival. In contrast, a single knock-out of DYRK1A would reduce phosphorylation of AKT, thereby inhibiting the

activation of the AKT pathway and limiting immune escape (Fig. 17A). Comparable effects on CD155 downregulation were expected following treatment with AKT inhibitors. There is currently only one FDA approved AKT inhibitor Capivasertib in hormone receptor positive advanced breast cancer, which is a direct pan AKT inhibitor (Turner Nicholas C. et al., 2023). We selected a panel of different direct and indirect AKT inhibitors to treat our melanoma cell lines, which were provided by the Oncogenic Transcription Laboratory in Melbourne. The panel of four different AKT inhibitors consisted of GSK-690693 as a pan-AKT inhibitor and MK-2206 as an allosteric AKT inhibitor. On the other hand, BEZ235 was a dual PI3K and mTOR inhibitor and ZSTK474 was a pan-PI3K inhibitor. As a control we treated the human melanoma cells with QVD, a pan-caspase inhibitor which inhibits apoptosis. This control was used to verify that the observed reduction in CD155 surface expression was caused by the AKT pathway inhibition and not caused by either cell stress or apoptosis.

MaMel54a wildtype cells were treated for 48 hours with either DMSO or QVD or an AKT/PI3K inhibitor, followed by flow cytometric assessment of CD155 surface expression. Figure 17C shows that treatment with allosteric AKT inhibitor MK-2206 significantly reduced CD155 surface expression by 30 %. Similar results were observed after treatments targeting mTOR/PI3K, with BEZ235 or ZSTK474, which significantly reduced CD155 surface expression levels with 40 % (Fig. 17C). On the other hand, GSK-690693, the AKT competitive inhibitor, was the only inhibitor that was not able to reduce CD155 surface expression. This inhibitor, GSK-690693, had been stored at -20 °C which might explain that its efficacy and stability were reduced. Treatment with the pan-caspase inhibitor QVD did not reduce CD155 surface expression (Fig. 17B-C), confirming that the observed reduction in CD155 surface expression after treatment with ATK/PI3K inhibitors was not caused by cell stress or apoptosis, but specifically induced by the inhibition of the AKT/PI3K pathway. These results suggest that inhibition of the AKT/PI3K pathway specifically reduces CD155 surface expression levels in our *BRAF*-mutant MaMel54a cell line. Taken together, these results show that inhibition of the AKT pathway, either via allosteric AKT inhibitor MK-2206 or

inhibitors targeting upstream of AKT pathway at the mTOR or PI3K level (BEZ235 or ZSTK474 respectively), reduces CD155 surface expression in human *BRAF*-mutant MaMel54a cell line.

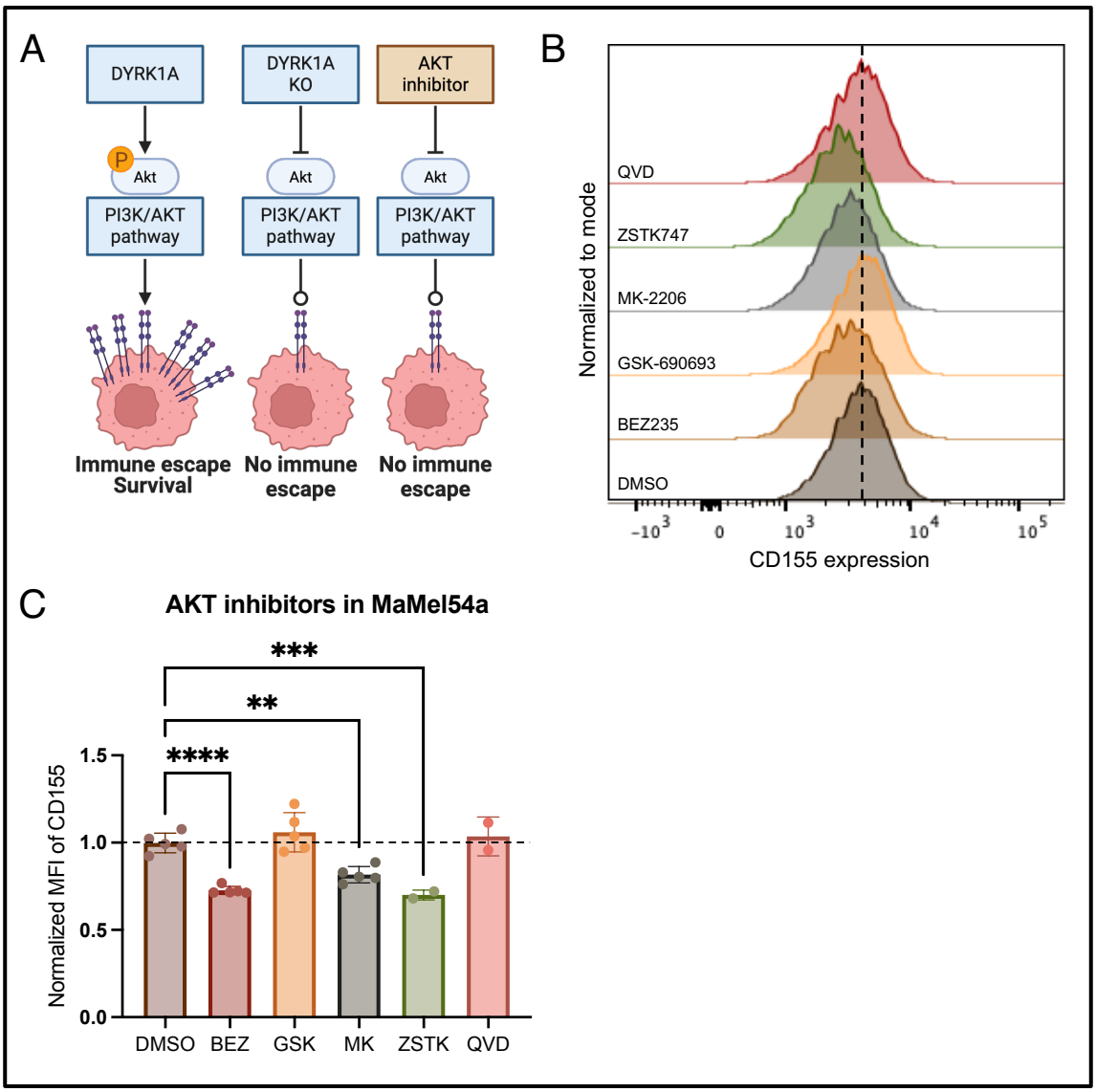

Figure 17: AKT inhibitors reduce the surface expression of CD155 in BRAF-mutant human melanoma cell line. *A) Schematic overview of hypothesis of DYRK1A and AKT/p-AKT and the effect on CD155 expression levels and immune escape. B-C) Flow cytometric assessment of CD155 surface expression 48 hours post treatment in MaMel54a wildtype cell line (n = 2-5). DMSO (0.5 %) treated cells were used as a control, and to normalize the MFI of the live single cells. QVD (Q-VD-OPh, pan-caspase inhibitor, 20 µM) was used as an extra control to*

*ensure that the observed CD155 reduction is caused by AKT pathway inhibition instead of cell stress or apoptosis. AKT inhibitors BEZ235 (Dactolisib, dual Pi3K and mTOR inhibitor, 5 μM), GSK-690693 (pan-AKT inhibitor, 4 μM), MK-2206 (allosteric AKT inhibitor, 2 μM), and ZSTK474 (pan-PI3K inhibitor, 5 μM). P-values were generated using one-way ANOVA: ns = not significant p > 0.05; * = p < 0.05; ** = p < 0.01; *** = p < 0.001; **** = p < 0.0001*

Discussion

Melanoma is a highly aggressive form of skin cancer. While targeted treatments show a strong initial response, resistance remains a problem resulting in a five-year progression free survival rate of only 19 % (Caroline Robert et al., 2019). In contrast, treatment with immunotherapies show lower initial response rates but provide better long-term response (Larkin et al., 2019). Despite the great success of cancer immunotherapies and combinations, a significant group of patients still shows primary resistance or acquired resistance to immunotherapy (Grzywa et al., 2017; Sharma et al., 2017). These limitations highlight the need to identify novel immunotherapy targets that can overcome resistance and improve long-term patient outcome. An interesting target for novel immune therapy is the immune modulatory molecule CD155, which is known to be overexpressed in a broad range of cancers and low expressed on healthy tissue (Abdalla et al., 2025; Bowers et al., 2017; Carlsten et al., 2009; Castriconi et al., 2004; Gromeier et al., 2000; Iguchi-Manaka et al., 2016, 2008; Liu et al., 2025; Masson et al., 2001; Molfetta et al., 2020; Nakai et al., 2010; Ochiai et al., 2004; Pende et al., 2005; Solecki et al., 2002). CD155 overexpression promotes tumor cell adhesion, invasion, migration, proliferation, and more interestingly CD155 induces immune escape. Taken together, CD155 is associated with poor prognosis and increased tumor progression. (Bowers et al., 2017; Braun et al., 2020; Chan et al., 2010; Nakai et al., 2010; Wang et al., 2022; Zhang et al., 2025). Despite the well-studied immunoregulatory function of CD155 and its frequent overexpression across multiple tumor types, little is known about its intrinsic regulation in cancer. Understanding these mechanisms is essential for therapeutic strategies targeting CD155.

Work presented in this thesis aimed to understand the intrinsic regulation of CD155 in human melanoma cell lines. We performed a genome-wide CRISPR knock-out screen in three human melanoma cell lines characterized by different oncogenic driver mutations (*BRAF*, *HRAS*, and *NRAS*) and various differentiation status to identify regulatory mechanisms independent of the genetic and phenotypic background. We were able to identify several candidate genes, which

were subsequently validated with single gene knock-outs. Furthermore, we tested the potential of pharmacological targeting of the identified enriched genes to enable further development of CD155 modulating therapies.

6.1 Key findings of the study and discussion

The aim of Chapter 3 was to characterize the CD155 expression in human cancer cell lines. The main focus was on melanoma and we tested a panel of fifteen different human melanoma cell lines, and several other human cancer cell lines which have been previously described to overexpress CD155 (blood, colon, gastric and lung cancer cell lines).

In our study, CD155 was overexpressed in all tested human melanoma cell lines as well as myeloid blood, gastric, colon and lung cancer cell lines which is in line with the literature (Abdalla et al., 2025; Bowers et al., 2017; Carlsten et al., 2009; Castriconi et al., 2004; Gromeier et al., 2000; Iguchi-Manaka et al., 2016, 2008; Liu et al., 2025; Masson et al., 2001; Nakai et al., 2010; Ochiai et al., 2004; Pende et al., 2005; Tremblay-McLean et al., 2019; Xiong et al., 2025). Lymphoid leukemia cells were slightly positive for CD155 surface expression whereas B-cell leukemias did not show CD155 expression. These findings can be explained as B-cell leukemias arise from B-cells, and two studies based on tissue experiments showed that naïve human B-cells do not express CD155. However, activated B-cells and in the germinal centre do slightly express CD155 (Maier et al., 2007; Zuo et al., 2024), which suggests that further research is needed to analyse CD155 expression in activated B-cell leukemias or in the TME. Zuo and colleagues found similar low CD155 surface expression on B-cell leukemia cell lines NALM-6 and SUP-B15, which was based on flow cytometry experiments (Zuo et al., 2024). We found no evidence in the literature showing CD155 surface expression on SEM, Mino or BEL-1, the absence of supporting data might suggest that these cell lines do not express CD155 on their surface. Further research is needed to validate this. The lack of literature can be considered consistent with our observations and may reflect absence or very low expression of CD155 on B-cell leukemia cell lines. Taken together, our data further supports

the notion that CD155 is broadly overexpressed across a wide range of solid and haematological malignancies emphasizing the importance of understanding its function and regulation.

To better characterize CD155 in human melanoma, the oncogenic driver mutation and the differentiation status of the cell lines were compared to the surface expression levels of CD155. In our panel of fifteen human melanoma cell lines, the majority of the cell lines harboured a *BRAF* mutation (eight cell lines), five cell lines harboured a *NRAS* mutation, and only one cell line harboured a *HRAS* mutation and one cell line was negative for all tested oncogenic driver mutations. Given a broad surface expression of CD155 across all cell lines, with most cell lines expressing intermediate to high surface levels of CD155, our data suggest that there is no correlation between the oncogenic driver mutation and the level of CD155 surface expression. However, given the low number of *HRAS*-mutant and triple negative cell lines in our panel, further research of those two molecular subtypes of human melanoma is needed to confirm our hypothesis.

Although CD155 surface expression did not correlate with specific oncogenic driver mutations, previous studies have suggested that MAPK pathway might be regulating CD155 expression in murine cell lines. In addition, current FDA-approved targeted therapies for melanoma are inhibiting the MAPK pathway, such as BRAF or MEK inhibitors (Bollag et al., 2010; Landras et al., 2022). Hirota et al. (2005) showed that murine CD155 is regulated by V12Ki-Ras and AP-1 binding and activates the MAPK pathway (Hirota et al., 2005). However, human CD155 does not contain an AP-1 binding site but AP-2, and Solecki et al. (2002) showed that human CD155 is regulated by *AP-2*, *NRF*, and sonic hedgehog pathway *in vitro* based on transcriptional promoter assays in two cell lines (Solecki et al., 2002). Since we did not find a correlation between the oncogenic driver mutation and CD155 surface expression levels in our cell lines, our hypothesis supported the idea that MAPK pathway is not involved in the major regulation of human CD155 surface expression. Our study was limited by an unequal representation of oncogenic driver mutations among our panel of fifteen human melanoma cell lines, which might have influenced our findings. Taken

together, this suggests that mouse and human CD155 might be regulated differently and functional experiments, such as a genetic knock-down of these genes, is needed to show that *AP-2*, *NRF* or sonic hedgehog pathway are important for the intrinsic regulation of CD155. Knock-down of these genes, rather than knock-out, represents the most suitable experimental approach, as studies in mouse have shown that knock-out of *AP-2*, *NRF* or genes related to sonic hedgehog pathway is lethal, and an *AP-2* knock-out has also been shown to be lethal in zebrafish (Leung et al., 2003; Mitsunari et al., 2005; Ramesh et al., 2019; Sasai et al., 2019; Stickens et al., 2005; Zhou et al., 2014)

Another factor that could contribute to CD155 surface expression in our panel of human melanoma cell lines is their phenotypic differentiation status. Previous studies have shown that differentiated cells have high MITF expression and immune-cell poor TME, and that MITF expression is important for melanoma progression and response to therapy (Reinhardt et al., 2017; Riesenberg et al., 2015). Since CD155 has an immune regulatory role, we expected an immune-cell poor TME and hypothesized high CD155 expression could be related to high MITF expression. From our data, we can conclude that CD155 surface expression levels are not correlated to the differentiation status of our human melanoma cell lines. A limitation of these findings is that we analysed our panel of fifteen human melanoma cell lines in a two-dimensional culture model, rather than within a TME, where additional factors may affect CD155 expression. Further validation in *in vivo* models or by immunohistochemistry would support our conclusion. Overall, our data indicate that CD155 expression is not determined by oncogenic driver mutation, MAPK pathway or phenotypic differentiation status of the human melanoma cell lines, suggesting that there are other mechanisms involved in the intrinsic regulation of CD155.

To investigate alternative intrinsic regulatory mechanisms, we generated CD155 knock-out cell lines to gain insights into the function of CD155 and its intrinsic regulation. Two independent CD155 knock-out cell lines were established and RNA sequencing analysis was performed comparing wildtype MaMel65 with CD155 knock-out cells. In addition, we treated with different inflammatory

cytokines or stimuli (IFN-γ, TNF-α or LPS). Since studies have shown that inflammatory cytokines, such as IFN-γ, were able to upregulated CD155 expression in healthy human endothelial cells (Escalante et al., 2011), we tested whether inflammatory cytokines had an effect on CD155 expression levels in human melanoma cells. However, we could not detect an effect on CD155 RNA expression after treatment with IFN-γ in our RNA sequencing analysis. The untreated cells clustered together with the cells treated with LPS and IFN-γ for both wildtype and CD155 knock-out cells, suggesting that these treatments do not induce downstream effects important for CD155 RNA expression. Interestingly, melanoma cells treated with TNF-α formed a separate cluster with reduced RNA expression of CD155 in both wildtype and CD155 knock-out cells. Little is known about TNF-α as regulator of CD155 expression. Furthermore, the highest number of DEGs was found after treatment with TNF-α comparing wildtype cells to CD155 knock-out cells. Further validation and testing in more human melanoma cell lines is needed to understand the role of TNF-α in regulating CD155 expression. Studies have shown that TNF-α is often overexpressed in the TME and important for immune modulatory functions (Laha et al., 2021). Given the immune regulatory role of CD155 we expected an effect of TNF-α treatment on CD155 expression. DEGs upregulated in wildtype cells after TNF-α treatment were *IL-32*, *CTSS*, *IL-41*, *C3*, *CCL5*, *GPR68* and *TNFRSF9* which are related to immune response and inflammation. Similar DEGs were found in CD155 knock-out cell lines treated with TNF-α: *IL-32*, *C3*, *CCL5*, *GPR68*, and *TNFRSF9* but in addition also *ICAM1* and *IL-34* which are related to immune response, inflammation, and adhesion. A limitation of this experiment is that RNA sequencing was performed in a single *NRAS*-mutant cell line, MaMel65, and further studies should extend this analysis to additional cell lines to obtain a more comprehensive overview.

To understand the basal function of CD155 and its intrinsic regulation, we focused on the RNA analysis of the untreated cells comparing wildtype MaMel65 with CD155 knock-out cells. Significantly downregulated DEGs in CD155 knock-out cells were related to two biological processes including immune signaling and

antigen processing and presentation (MHC II), which were expected taking into account the immune regulatory role of CD155 inducing immune escape. CD155 can bind to inhibitory ligands TIGIT and CD96 as well as the activating ligand CD226, which indirectly promotes immune escape following internalization upon binding to CD155 (Braun et al., 2020; Paolini and Molfetta, 2023). Another significantly downregulated gene in CD155 knock-out cells was *NALF1*, which is an component of sodium leak channel (Chua et al., 2020), suggesting that sodium leak channel might has a role in CD155. However, no studies are published around NALF1 and CD155. On the other hand, upregulated DEGs (*DSP*, *DSG2*, *PTN*, *SYT1*, *IL-33* and *DLX3*) in CD155 knock-out cells were related to the biological processes cell adhesion, cell growth and stress response. During our experiments when culturing CD155 knock-out cells of different human melanoma cell lines, we have not observed major differences in growth or adhesion compared to wildtype cells. These findings are in contrast to the RNA sequencing analysis, suggest that CD155 alone might not be regulating cell growth and adhesion, but rather acts as a part of a broader regulatory network. From these results we can conclude that a genetic knock-out of CD155 might induce compensatory mechanism such as upregulation of cell-cell adhesion likely due to the reduced signaling from the absence of CD155 surface expression. Taken together, RNA sequencing analysis of CD155 wildtype and knock-out MaMel65 cells did only reveal limited novel insights in CD155. A limitation of this study is that these findings are based on one *NRAS*-mutant cell line and future studies should perform RNA sequencing on a larger panel of human melanoma cell lines, and further compare oncogenic driver mutation, phenotypic differentiation status and CD155 surface expression levels.

Given that RNA sequencing analysis did reveal only limited novel insights in the intrinsic regulation of CD155, we performed a genome-wide CRISPR knock-out screen in different human melanoma cell lines which was presented in Chapter 4. In preparation for this screen, Cas9 expressing cell lines were established (Chapter 3). We started with a stable Cas9 variant and confirmed the presence of Cas9 on both protein and mRNA level. However, functional assays targeting

CD155 showed that stable Cas9 expressing melanoma cell lines had very poor CD155 knock-out efficiency. We started with a heterogenous polyclonal cell population and generated monoclonal cultures in order to achieve homogenous Cas9 expression to explore whether our knock-out efficiency could be improved (data not shown). However, the monoclonal cell lines showed similar low knock-out efficiency of CD155 surface levels across different human melanoma cell lines. These findings were unexpected, as Cas9 was present on both protein and mRNA levels in polyclonal and monoclonal cell lines. The stable Cas9 in these polyclonal and monoclonal cell lines was unable to induce efficient knock-out of our gene of interest. Therefore, we tested an additional variant, the inducible Cas9 variant.

In the inducible Cas9-expressing cell lines we generated, Cas9 was induced by administration of doxycycline, and its expression was confirmed at both protein and mRNA level in our human melanoma cell lines. Functional assays showed a high CD155 knock-out efficiency across different human melanoma cell lines. We concluded that the inducible Cas9 system is more efficient compared to the stable Cas9 system. Therefore, the inducible Cas9 system was used in the genome-wide CRISPR knock-out screens presented in Chapter 4. In addition, a common limitation of inducible Cas9 is basal leakiness, where mock inducible Cas9 cell lines may exhibit some Cas9 expression even in the absence of doxycycline. This was observed in MaMel54a mock in Figure 8B, and should be taken into account when interpreting genetic knock-out to the mock control conditions. All previously described results were performed in Bonn, Germany, in the first years of this project. It is important to note that during the final year of the PhD, which was performed in Melbourne, Australia, an additional fluorescent Cas9 variant was assessed. From these experiments, we can conclude that the fluorescent Cas9 system is the most efficient and suitable Cas9 system for our human melanoma cell lines and genome-wide CRISPR screen purpose. The CD155 knock-out frequency was further improved. Therefore, it is important to note that the findings of the genome-wide CRISPR knock-out screens presented in Chapter 4 were potentially influenced by the lower knock-out efficiency of the used inducible Cas9

variant. The five commonly enriched genes in the CD155-low sorted fraction, of which a knock-out is lethal, were found as the sorted cells might not harbour a full knock-out of these genes, but rather a reduction in gene expression due to the usage of the suboptimal iCas9 construct. For instance, if sorted cells still retain 30 % of the gene expression, this may be sufficient for cell survival. In addition, the lower efficiency of inducible Cas9 compared to the fluorescent Cas9 variant reduced the population of CD155 low-expressing cells, leading to lower number of CD155-low sorted cells, and potentially this was also the cause of the absence of CD155 high-expressing population. Taken together, these limitations had an effect on the NGS analysis of the large-scale screen data across our three human melanoma cell lines and the interpretation of the NGS data should be taken with caution. Validation of the enriched genes found in CD155-low fraction was performed in our improved fluorescent Cas9 system, and we were still able to validate the genes that we found in our screens.

The aim of the genome-wide CRISPR knock-out screens (Chapter 4) was to identify novel pathways and druggable molecules that intrinsically regulate CD155 surface expression in melanoma. The genome-wide CRISPR/Cas9-based knock-out screens were performed in three different melanoma cell lines harbouring different oncogenic driver mutations (*BRAF*, *HRAS* or *NRAS*), with the aim to find cell line independent intrinsic regulators of CD155. During this study the complete workflow of the genome-wide CRISPR/Cas9 screen was established, and optimized for our inducible Cas9 human melanoma cell lines. Puromycin selected library transduced cells were sorted based on the lowest 3 till 5 % of CD155 surface expression on day 7 post transduction, and NGS was performed to compare unsorted and CD155-low sorted fractions of two independent replicates per cell line. From Chapter 4, we can conclude that the highest enriched gene in the sorted fraction across our three screened cell lines was CD155. This data demonstrated the robustness of our approach. A genomic knock-out of CD155 reduces CD155 surface expression levels, and therefore these library transduced cells harbouring sgRNA targeting CD155 were enriched in the CD155-low sorted fraction. To identify candidate genes that intrinsically

regulate CD155, we compared significant enriched genes in the CD155-low sorted fraction across our three human melanoma cell lines (*BRAF*-, *HRAS*- or *NRAS*-mutant). This comparison showed that six genes are commonly enriched across our screened cell lines: *CD155*, *SRP54*, *SEC61A1*, *ALG11*, *DHDDS*, and *NUS1*. These five genes (excluding *CD155*) were related to two main biological pathways protein translocation and N-glycosylation.

Two of the six genes (*SRP54* and SEC61A1) commonly enriched in CD155-low sorted fraction were related to protein translocation. Previous studies have shown that SRP54 is a signal recognition particle, which recognizes and binds specific signal sequences of the ribosome, bringing proteins through the membrane to the endoplasmic reticulum (ER) (Jadhav et al., 2015; Luirink and Sinning, 2004). The second gene SEC61A1 encodes for a protein-conducing channel in the ER membrane. This channel forms a pore in the cell membrane allowing proteins to translocate into the ER or integrate with the ER membrane (Itskanov and Park, 2023). Taken together, SRP54 mediates docking of proteins, while SEC61A1 enables protein passage across the ER membrane, making them both essential for protein translocation. Since CD155 is a transmembrane adhesion molecule with an immune regulatory function, it is expected that protein translocation plays an important role. However, validation of SRP54 and SEC61A1 with a single knock-out of these genes was not possible as protein translocation is essential for cell survival, and knocking out this process will be lethal for the cells. Previous studies have shown that knock-out of SRP54 in zebrafish was lethal (Schürch et al., 2021). Little is known about SEC61A1 knock-out and lethality, one study in human THP-1 cells showed that SEC61A1 knock-out cells were still viable but suffered from growth impairment and ER stress (Itskanov and Park, 2023). Another study showed that knock down of SEC61A1 was not well tolerated in multiple myeloma cell lines (Schubert et al., 2018). In addition, the SEC61 complex is crucial in the ER indicating that full knock-out might be lethal (Lang et al., 2017; Xin et al., 2025). Mutations in *SEC61* are correlated to different diseases and SEC61A1 has been shown to be a biomarker to predict patient outcome of AML (Ji et al., 2024; O'Keefe et al., 2021). From these studies we can

conclude that validation of *SRP54* and *SEC61A1* as intrinsic regulators of CD155 surface expression with a single knock-out experiment will be lethal, making further functional validate these genes challenging. Therefore, future studies are needed to examine the effect of a knock-down of these two genes and their role in regulating CD155 surface expression and their potential as complimentary biomarker to CD155 for human cancers.

The second upregulated pathway across our three screened human melanoma cell lines is N-glycosylation. This pathway was based on three genes *ALG11*, *DHDDS*, and *NUS1* which were commonly enriched in the CD155-low sorted fraction across all three cell lines. Interestingly, studies have shown that DHDDS and NUS1 form a complex together called Dehydrodolichyl Diphosphate Synthase, which is an essential lipid for N-linked glycosylation (Bar-El et al., 2020; Edani et al., 2020). The third commonly enriched gene was *ALG11*. ALG11 has been shown to be an important catalyzer for mannosylation in the early stage of N-linked glycosylation (Gao et al., 2004), which is therefore linked to the previous described enriched genes *DHDDS* and *NUS1*. Posttranslational modifications such as glycosylation are critical for effective ligand recognition and subsequent interaction with immune cells (Pinho and Reis, 2015). Glycosylation plays a central role at the cell surface and glycans are important for cell-cell communication, signaling and receptor activation in healthy conditions. Although glycosylation is not included in the Hallmarks of cancer as described in the Chapter 1, glycosylation does play an important role in cancer. Different studies have shown that glycosylation is important for regulating cancer development and progression (Pinho and Reis, 2015; Rodrigues et al., 2018; Zhang et al., 2021). Cancer cells exhibit increased glycosylation patterns and branches, which are influencing cell signalling, invasion, cell-matrix interactions, angiogenesis and immune modulation. Furthermore, altered glycosylation can affect receptor signaling in the TME and subsequently tumor growth and immune escape (Pinho and Reis, 2015). In addition, studies have shown that glycans are important biomarker and potential therapeutic target. Therapies targeting aberrant glycosylation can improve cancer treatment (Pinho and Reis, 2015; Rodrigues et

al., 2018; Zhang et al., 2021). Focussing on CD155 and glycosylation, studies have shown that glycosylation of CD155 is important for its immune regulatory role by binding to ligands CD266 and TIGIT (Fuchs et al., 2004; Tahara et al., 2024; Zhang et al., 2008). Little is known about the effect of glycosylation of CD155 and binding to its third ligand CD96. From these studies, we can conclude that glycosylation is important for the function of CD155, but glycosylation is not intrinsically regulating CD155 surface expression. In addition, enrichment of glycosylation genes in genome-wide CRISPR knock-out screens targeting surface receptors in cancer is not surprising as different studies also found glycosylation genes enriched (Jutzi et al., 2022; Oliveira et al., 2021). It is important to note that knock-out of genes related to glycosylation, alterations in glycosylation can effect on receptor ligand binding as well as antibody binding (Huang et al., 2021). Using FACS sorting as a screen read-out which dependents on flow antibody binding, the enrichment of the identified glycosylation genes in our screen might be caused by failure of antibody binding. Therefore, it could be explained that the enriched glycosylation genes in the CD155-low sorted fraction are not necessarily intrinsically regulating CD155 surface expression but rather important for impairing CD155 antibody binding. Similar to commonly enriched genes *SRP54* and *SEC61A1*, glycosylation genes are essential for cell communication and a knock-out of *SRP54* or *SEC61A1* is lethal to the cells. For instance, in experimental murine models, a single knock-out of either *DHDDS*, *NUS1*, or *ALG11* has been shown to be lethal, indicating that these genes are essential and making further validation using a single knock-out approach difficult (Brooker et al., 2025; DeRamus et al., 2020; Lang et al., 2017; Regal et al., 2015). These findings indicate that a knock-out of glycosylation-related genes can have significant consequences for surface receptor binding, surface receptor function, and antibody binding. The glycosylation-related genes enriched in our study represent a more general effect on surface receptors, rather than functioning as intrinsic regulators of CD155 surface expression on human melanoma cell lines.

As the main objective of our project was to identify intrinsic regulators of CD155 surface expression in human melanoma, we analysed the NGS data from the

genome-wide CRISPR knock-out screens presented in Chapter 4. Another interesting significantly enriched gene was *DYRK1A*, which was enriched in MaMel54a (*BRAF*-mutant) sorted CD155-low cells. This finding is consistent with a recent study showing that *DYRK1A* regulates CD155 expression, based on a CRISPR knock-out screen conducted in murine cancer cell lines. This study aimed to identify genes related to resistance to PD-1 blockade in head and neck squamous cell carcinoma, and found *DYRK1A* as a regulator of CD155 expression. They validated this finding with a single knock-out of *DYRK1A* and DYRK1A inhibitors, which both were able to reduce CD155 surface expression in their head and neck squamous cell carcinoma cell lines (Kawase et al., 2025). In addition, they showed that downregulation of CD155 was important to overcome resistance to PD-L1 in the head and neck squamous cell carcinoma cell lines via the PI3K/AKT signaling pathway. They highlighted the clinical relevance of their findings in 96 head and neck squamous cell carcinoma patients showing a significant correlation between CD155 expression and AKT phosphorylation, impacting resistance to PD-1 blockade (Kawase et al., 2025). These findings suggest that PI3K/AKT signaling might be important for the intrinsic regulation of CD155 expression. Comparison of our NGS data with their findings revealed additional genes related to the PI3K/AKT pathway and AKT phosphorylation, which were significantly enriched in the CD155-low sorted fraction of our *BRAF*-mutant MaMel54a iCas9 cell line: *CD5L*, *GMFB* and *PTK6*. Previous studies have shown that deletion of these genes is not lethal in murine models (Dwyer et al., 2021; Oliveira et al., 2024; Wozniak et al., 2017; Yin et al., 2022), making validation with a single knock-out feasible and highlighting these enriched genes as promising candidates for further investigation.

We proceeded to further investigate these genes to validate their potential in regulating CD155 expression in human melanoma as well as their role of PI3K/AKT pathway. To validate these candidate genes, individual knock-outs were generated and CD155 surface expression was monitored over time. The individual knock-outs were generated in two of the three melanoma cells lines screened in Chapter 4, MaMel54a (*BRAF*-mutant) and MaMel60 (*NRAS*-mutant)

expressing fluorescent Cas9. These validation experiments showed a significant two-fold reduction in CD155 surface expression in *DYRK1A* knock-out cells in both human melanoma cell lines MaMel54a and MaMel60. We can conclude that *DYRK1A* is validated as a regulator of CD155 surface expression based on only flow cytometry analysis. To further validate these findings, Sanger sequencing is required to confirm the knock-out efficiency of *DYRK1A* at the DNA level in our cell lines, which could not be performed due to time constraints. This genomic data could help explain the observed differences in CD155 reduction between both cell lines or both sgRNAs (KO1 and KO5). In addition, analysis of mRNA and protein levels of both CD155 and DYRK1A is necessary to further verify functional reduction or loss, and to gain mechanistic insights into how DYRK1A intrinsically regulates CD155 surface expression in our human melanoma cell lines. The other three enriched genes related to *DYRK1A*, the PI3K/AKT pathway and phosphorylation of AKT (*CD5L*, *GMFB* and *PTK6*) were also validated with a single knock-out in both MaMel54a and MaMel60 expressing fluorescent Cas9. In MaMel60, knock-out of *CD5L* or *GMFB* reduced CD155 surface expression levels by 40 %. In MaMel54a, only a knock-out of *CD5L* was able to reduce CD155 surface expression levels by 10 % and no effect was observed after *GMFB* knock-out. The knock-out of *PTK6* did not change CD155 surface expression in both cell lines. This experiment was limited by the low number of replicates, and further validation is required, including generation of knock-outs in a larger panel of human melanoma cell lines, assessment of the knock-out frequency on genomic level, and analysis of both mRNA and protein expression of these genes.

Given the preliminary results, time constraints and the recently published paper (Kawase et al., 2025), we focused on *DYRK1A* as this gene might regulate CD155 surface expression via PI3K/AKT signaling. Another study described the role of DYRK1A in activating ERK and AKT based on a murine model (Abekhoukh et al., 2013). Furthermore, a study on CD155 expressing in colorectal cancer tissues and human colorectal cell lines showed that PI3K/AKT/NF-κß pathway promotes cancer progression (Liang et al., 2025). Taken together, these findings

suggest that DYRK1A can play an interesting role in regulating CD155 expression through modulation of the PI3K/AKT pathway, highlighting DYRK1A as a potential pharmacological target for novel therapies. This hypothesis links kinase activity to surface expression and immune modulation. We hypothesized that high surface expression of CD155 could be associated with increased AKT phosphorylation and activation of the PI3K/AKT pathway, thereby promoting tumor progression and immune evasion. Conversely, we hypothesized that *DYRK1A* deletion reduces CD155 surface expression levels as well as AKT phosphorylation in our human melanoma cell lines, subsequently reducing the activation of the PI3K/AKT pathway and preventing immune escape.

Therefore, we wanted to test the effect of PI3K/AKT inhibitors on CD155 surface expression in our melanoma cell lines. Our results showed that AKT activity regulates the surface expression of CD155 in human melanoma cell line MaMel54a (*BRAF*-mutant). Inhibition of the AKT pathway with MK-2206, BEZ235, or ZSTK474 significantly reduced CD155 surface expression levels in MaMel54a wildtype cells. These results suggest that AKT phosphorylation and AKT signaling promote upregulation of CD155 surface expression, potentially through downstream effectors such as mTOR or PI3K. In contrast, the ATP-competitive inhibitor GSK-690693, which has previously been shown to enhance AKT phosphorylation (Romorini et al., 2016), failed to reduce CD155 expression as expected. These findings support our hypothesis that elevated AKT phosphorylation levels is associated with increased CD155 surface expression levels. The use of the pan-caspase inhibitor QVD as a control confirmed that the observed reduction in CD155 surface expression in our cell line was not induced by cell stress or apoptosis, but specifically by inhibition of the AKT pathway. Taken together, these findings support our hypothesis that DYRK1A and phosphorylated AKT are important regulators of CD155 surface expression in human melanoma cell lines. However, future studies should assess AKT phosphorylation levels in wild type cells, *DYRK1A* knock-out cells and AKT inhibitor treated cells to further validate the role of DYRK1A and phosphorylated AKT in intrinsically regulating CD155 surface expression.

To date, there are no FDA-approved AKT or DYRK1A inhibitors. There are currently different clinical trials studying the effect of AKT inhibitors in cancer, and there is only one FDA-approved in combination of AKT inhibitor (Capivasertib) with HER2 antagonist in breast cancer (Turner Nicholas C. et al., 2023). Currently, there are no approved DYRK1A inhibitors in the clinic. However, Kaltheuner et al. (2021) showed that FDA-approved CDK4/6 inhibitor Abemaciclib can also inhibit DYRK1A in breast cancer (Kaltheuner et al., 2021), making Abemaciclib an indirect FDA-approved DYRK1A inhibitor. Another orphan drug granted for breast cancer, in other words almost FDA-approved, is ERFR/HER2 inhibitor Varlitinib. It has been shown to reduce DYRK1A expression in mice (Kim et al., 2022). These publications highlight the pharmacological potential and clinical relevance of DYRK1A in intrinsically regulating CD155 surface expression in cancer. Future studies are needed to assess the expression levels of DYRK1A and CD155 in breast cancer patient samples treated with Abemaciclib or breast cancer patients treated with Varlitinib. Furthermore, additional experiments are needed in melanoma and other cancers that overexpress CD155 to broaden its therapeutical potential. For additional functional validation *in vitro* experiments, such as IncuCyte, would allow real-time monitoring of cell growth, proliferation, and cell death in the cell lines treated with DYRK1A inhibitors. Besides reducing DYRK1A, another study showed that Abemaciclib in combination with radiotherapy and PD-1 blockade has a synergistic effect in inhibiting tumor growth as well as modifying the TME to enhance anti-tumor immunity in breast cancer (Yang et al., 2025). In addition, a Phase 1 clinical trial is currently investigating monoclonal antibody targeting CD155, alone or in combination with PD-L1 blockade as treatment for solid malignancies (NCT05378425). Together, these findings highlight the therapeutic potential of targeting DYRK1A in combination with inhibition of immune receptors such as CD155 or PD-L1 to enhance anti-tumor immunity.

Overall, we can conclude that DYRK1A plays a key role in regulating CD155 surface expression in human melanoma, with the PI3K/AKT pathway contributing to this regulation. Inhibition of DYRK1A may reduce AKT phosphorylation,

leading to decreased CD155 surface expression levels and decreased tumor immune escape. Similarly, direct targeting of AKT with specific inhibitors could reduce CD155 surface levels and suppress CD155 mediated immune escape and improve patient outcome. Furthermore, combining AKT or DYRK1A inhibitors with CD155 immune blockade may induce a synergistic effect and induce an immune reaction against the tumor cells. These observations highlight the therapeutic potential of targeting the DYRK1A, AKT, and CD155 axis to enhance anti-tumor immunity in melanoma, and potentially across different cancer types.

6.2 Relevance

Further improvement of cancer immunotherapies targeting immune escape is dependent on the characterisation and understanding of the biology of immune receptors. The immune modulating receptor CD155 is known to be overexpressed across different types of cancer and its known to induce immune escape, and therefore overexpression of CD155 in cancer is related to poor patient outcome. Furthermore, CD155 is low expressed on healthy cells, making it an interesting target for novel therapies. Current therapies for melanoma are either targeted showing a high initial response but lacking long term response and resistance remains a problem, whereas the other available option with immunotherapies showed less initial response, however, a long-term response and potential cure (Larkin et al., 2019; Caroline Robert et al., 2019). Therefore, there is a need for new immune-based therapies to improve the initial response and patient outcome.

Besides targeting CD155 with novel therapies, CD155 can be used as biomarker for cancer disease progression, which has been shown in several studies using sCD155 as a biomarker for cancer progression in breast, gastric, lung and gynaecological cancers (Iguchi-Manaka et al., 2016; Okumura et al., 2020). Considering the role of DYRK1A in intrinsically regulating CD155 surface expression, and its relation to the PI3K/AKT pathway, and subsequentially influencing immune escape, DYRK1A, AKT and p-AKT could be considered as additional biomarkers next to CD155. In order to highlight the clinical relevance

of targeting PI3K/AKT pathway and DYRK1A, more studies are needed to assess CD155, DYRK1A, AKT and p-AKT expression levels in human melanoma cell lines and patient samples. To further study how DYRK1A is intrinsically regulating CD155 surface expression levels in cancer, functional assays such as co-culture assay of T cells with cancer cells can be performed, comparing the killing efficiency of wildtype cells with DYRK1A knock-out cells or CD155 knock-out cells. This will give more mechanistic insights in the intrinsic regulation of CD155 in cancer. In addition, intracellular staining of CD155 is required to study if CD155 gets internalized after analysing a reduction in CD155 surface expression levels. To examine whether CD155 and DYRK1A are pharmacological therapeutic targets, more human melanoma cell lines need to be treated with Abemaciclib or AKT or DYRK1A inhibitors, and the surface expression of CD155 has to be assessed. Finally, it is important to take into consideration that intrinsic regulation of human CD155 can be different than mouse as in human CD155 AP-1 is important, and in mice this regulated by AP-2 (Hirota et al., 2005; Solecki et al., 2002). It might be useful to generate a DYRK1A knock-out murine model to test all the above-described experiments *in vivo*. In addition, mice can be treated with Abemaciclib, other DRYK1A inhibitors or AKT inhibitors, both alone and in combination with immune checkpoint blockade or monoclonal antibody targeting CD155 to analyse potential synergistic effects. Taken together, DYRK1A was validated as intrinsic regulator of CD155 expression, and more research is needed to validate this in different human melanoma cell lines. Finally, DYRK1A can be used as target for CD155 overexpressing cancers.

References

Abdalla, A.Z., Khallaf, S.M., Zahran, A.M., Rayan, N.A., Elzaher, A.R.A., 2025. CD155 as a prognostic and predictive biomarker in acute myeloid leukemia. Discov Oncol 16, 902. https://doi.org/10.1007/s12672-025-02665-2

Abe, A., Fukui, H., Fujii, S., Kono, T., Mukawa, K., Yoshitake, N., Sekikawa, A., Ichikawa, K., Tomita, S., Yamagishi, H., Imai, Y., Shinoda, M., Ishizaki, H., Tanaka-Okamoto, M., Kubota, K., Miyoshi, J., Takai, Y., Fujimori, T., 2009. Role of Necl-5 in the pathophysiology of colorectal lesions induced by dimethylhydrazine and/or dextran sodium sulphate. J Pathol 217, 42–53. https://doi.org/10.1002/path.2431

Abekhoukh, S., Planque, C., Ripoll, C., Urbaniak, P., Paul, J.-L., Delabar, J.-M., Janel, N., 2013. Dyrk1A, a Serine/Threonine Kinase, is Involved in ERK and Akt Activation in the Brain of Hyperhomocysteinemic Mice. Molecular Neurobiology 47, 105–116. https://doi.org/10.1007/s12035-012-8326-1

Adhikari, E., Liu, Q., Johnson, J., Stewart, P., Marusyk, V., Fang, B., Izumi, V., Bowers, K., Guzman, K.M., Koomen, J.M., Marusyk, A., Lau, E.K., 2023. Brain metastasis-associated fibroblasts secrete fucosylated PVR/CD155 that induces breast cancer invasion. Cell Rep 42, 113463. https://doi.org/10.1016/j.celrep.2023.113463

Agaimy, A., Stoehr, R., Hornung, A., Popp, J., Erdmann, M., Heinzerling, L., Hartmann, A., 2021. Dedifferentiated and Undifferentiated Melanomas: Report of 35 New Cases With Literature Review and Proposal of Diagnostic Criteria. Am J Surg Pathol 45, 240–254. https://doi.org/10.1097/PAS.0000000000001645

Aliazis, K., Christofides, A., Shah, R., Yeo, Y.Y., Jiang, S., Charest, A., Boussiotis, V.A., 2025. The tumor microenvironment's role in the response to immune checkpoint blockade. Nature Cancer 6, 924–937. https://doi.org/10.1038/s43018-025-00986-3

Anna, B., Blazej, Z., Jacqueline, G., Andrew, C.J., Jeffrey, R., Andrzej, S., 2007. Mechanism of UV-related carcinogenesis and its contribution to nevi/melanoma. Expert Rev Dermatol 2, 451–469. https://doi.org/10.1586/17469872.2.4.451

Ardolino, M., Zingoni, A., Cerboni, C., Cecere, F., Soriani, A., Iannitto, M.L., Santoni, A., 2011. DNAM-1 ligand expression on Ag-stimulated T lymphocytes is mediated by ROS-dependent activation of DNA-damage response: relevance for NK-T cell interaction. Blood 117, 4778–4786. https://doi.org/10.1182/blood-2010-08-300954

Atkins, M.B., Lotze, M.T., Dutcher, J.P., Fisher, R.I., Weiss, G., Margolin, K., Abrams, J., Sznol, M., Parkinson, D., Hawkins, M., Paradise, C., Kunkel, L., Rosenberg, S.A., 1999. High-dose recombinant interleukin 2 therapy for patients with metastatic melanoma: analysis of 270 patients treated between 1985 and 1993. J Clin Oncol 17, 2105–2116. https://doi.org/10.1200/JCO.1999.17.7.2105

Bandi, P., Minihan, A.K., Siegel, R.L., Islami, F., Nargis, N., Jemal, A., Fedewa, S.A., 2021. Updated Review of Major Cancer Risk Factors and Screening Test Use in the United States in 2018 and 2019, with a Focus on Smoking Cessation. Cancer Epidemiology, Biomarkers & Prevention 30, 1287–1299. https://doi.org/10.1158/1055-9965.EPI-20-1754

Barbato, M.I., Nashed, J., Bradford, D., Ren, Y., Khasar, S., Miller, C.P., Zolnik, B.S., Zhao, H., Li, Y., Bi, Y., Shord, S.S., Amatya, A.K., Mishra-Kalyani, P.S., Scepura, B., Al-Matari, R.A., Pazdur, R., Kluetz, P.G., Donoghue, M., Singh, H., Drezner, N., 2024. FDA Approval Summary: Dabrafenib in Combination with Trametinib for BRAFV600E Mutation-Positive Low-Grade Glioma. Clin Cancer Res 30, 263–268. https://doi.org/10.1158/1078-0432.CCR-23-1503

Bar-El, M.L., Vaňková, P., Yeheskel, A., Simhaev, L., Engel, H., Man, P., Haitin, Y., Giladi, M., 2020. Structural basis of heterotetrameric assembly and disease mutations in the human cis-prenyltransferase complex. Nature Communications 11, 5273. https://doi.org/10.1038/s41467-020-18970-z

Begg, C.B., Orlow, I., Hummer, A.J., Armstrong, B.K., Kricker, A., Marrett, L.D., Millikan, R.C., Gruber, S.B., Anton-Culver, H., Zanetti, R., Gallagher, R.P., Dwyer, T., Rebbeck, T.R., Mitra, N., Busam, K., From, L., Berwick, M., for the Genes Environment and Melanoma (GEM) Study Group, 2005. Lifetime Risk of Melanoma in CDKN2A Mutation Carriers in a Population-Based Sample. JNCI: Journal of the National Cancer Institute 97, 1507–1515. https://doi.org/10.1093/jnci/dji312

Bhansali, R.S., Rammohan, M., Lee, P., Laurent, A.P., Wen, Q., Suraneni, P., Yip, B.H., Tsai, Y.-C., Jenni, S., Bornhauser, B., Siret, A., Fruit, C., Pacheco-Benichou, A., Harris, E., Besson, T., Thompson, B.J., Goo, Y.A., Hijiya, N., Vilenchik, M., Izraeli, S., Bourquin, J.-P., Malinge, S., Crispino, J.D., 2021. DYRK1A regulates B cell acute lymphoblastic leukemia through phosphorylation of FOXO1 and STAT3. J Clin Invest 131, 135937. https://doi.org/10.1172/JCI135937

Bollag, G., Hirth, P., Tsai, J., Zhang, J., Ibrahim, P.N., Cho, H., Spevak, W., Zhang, C., Zhang, Y., Habets, G., Burton, E.A., Wong, B., Tsang, G., West, B.L., Powell, B., Shellooe, R., Marimuthu, A., Nguyen, H., Zhang, K.Y.J., Artis, D.R., Schlessinger, J., Su, F., Higgins, B., Iyer, R., D'Andrea, K., Koehler, A., Stumm, M., Lin, P.S., Lee, R.J., Grippo, J., Puzanov, I., Kim, K.B., Ribas, A., McArthur, G.A., Sosman, J.A., Chapman, P.B., Flaherty, K.T., Xu, X., Nathanson, K.L., Nolop, K., 2010. Clinical efficacy

of a RAF inhibitor needs broad target blockade in BRAF-mutant melanoma. Nature 467, 596–599. https://doi.org/10.1038/nature09454

Boni, J., Rubio-Perez, C., López-Bigas, N., Fillat, C., de la Luna, S., 2020. The DYRK Family of Kinases in Cancer: Molecular Functions and Therapeutic Opportunities. Cancers (Basel) 12. https://doi.org/10.3390/cancers12082106

Bottino, C., Castriconi, R., Pende, D., Rivera, P., Nanni, M., Carnemolla, B., Cantoni, C., Grassi, J., Marcenaro, S., Reymond, N., Vitale, M., Moretta, L., Lopez, M., Moretta, A., 2003. Identification of PVR (CD155) and Nectin-2 (CD112) as Cell Surface Ligands for the Human DNAM-1 (CD226) Activating Molecule. Journal of Experimental Medicine 198, 557–567. https://doi.org/10.1084/jem.20030788

Bowers, J.R., Readler, J.M., Sharma, P., Excoffon, K.J.D.A., 2017. Poliovirus Receptor: More than a simple viral receptor. Virus Research 242, 1–6. https://doi.org/10.1016/j.virusres.2017.09.001

Brash, D.E., 2015. UV signature mutations. Photochem Photobiol 91, 15–26. https://doi.org/10.1111/php.12377

Braun, M., Aguilera, A.R., Sundarrajan, A., Corvino, D., Stannard, K., Krumeich, S., Das, I., Lima, L.G., Meza Guzman, L.G., Li, K., Li, R., Salim, N., Jorge, M.V., Ham, S., Kelly, G., Vari, F., Lepletier, A., Raghavendra, A., Pearson, S., Madore, J., Jacquelin, S., Effern, M., Quine, B., Koufariotis, L.T., Casey, M., Nakamura, K., Seo, E.Y., Hölzel, M., Geyer, M., Kristiansen, G., Taheri, T., Ahern, E., Hughes, B.G.M., Wilmott, J.S., Long, G.V., Scolyer, R.A., Batstone, M.D., Landsberg, J., Dietrich, D., Pop, O.T., Flatz, L., Dougall, W.C., Veillette, A., Nicholson, S.E., Möller, A., Johnston, R.J., Martinet, L., Smyth, M.J., Bald, T., 2020. CD155 on Tumor Cells Drives Resistance to Immunotherapy by Inducing the Degradation of the Activating Receptor CD226 in CD8(+) T Cells. Immunity 53, 805-823.e15. https://doi.org/10.1016/j.immuni.2020.09.010

Briukhovetska, D., Suarez-Gosalvez, J., Voigt, C., Markota, A., Giannou, A.D., Schübel, M., Jobst, J., Zhang, T., Dörr, J., Märkl, F., Majed, L., Müller, P.J., May, P., Gottschlich, A., Tokarew, N., Lücke, J., Oner, A., Schwerdtfeger, M., Andreu-Sanz, D., Grünmeier, R., Seifert, M., Michaelides, S., Hristov, M., König, L.M., Cadilha, B.L., Mikhaylov, O., Anders, H.-J., Rothenfusser, S., Flavell, R.A., Cerezo-Wallis, D., Tejedo, C., Soengas, M.S., Bald, T., Huber, S., Endres, S., Kobold, S., 2023. T cell-derived interleukin-22 drives the expression of CD155 by cancer cells to suppress NK cell function and promote metastasis. Immunity 56, 143-161.e11. https://doi.org/10.1016/j.immuni.2022.12.010

Brooker, S.M., Novelli, M., Coukos, R., Prakash, N., Kamel, W.A., Amengual-Gual, M., Anheim, M., Barcia, G., Bardakjian, T., Baur, F., Berweck, S., Bölsterli, B.K., Brugger, M., Cassini, T., Chatron, N., Corner, B., Dafsari,

H.S., De Sainte Agathe, J., Ellis, C.A., Ezell, K.M., Foucard, C., Frucht, S.J., Garcia, M.C., Gill, D., Guimier, A., Hamid, R., Heine-Suñer, D., Herkenrath, P., Hully, M., Isaias, I.U., Januel, L., Laurencin, C., Laut, T., Lavillaureix, A., Lesca, G., Lesieur-Sebellin, M., Magistrelli, L., Marelli, C., Mefford, H.C., Mendelsohn, B.A., Mercimek-Andrews, S., Miller, C., Mohammad, S.S., Morgante, F., Nandipati, S., Opladen, T., Padmanaban, M., Pauni, M., Pezzoli, G., Piton, A., Ramond, F., Riboldi, G.M., Rougeot-Jung, C., Santos-Simarro, F., Scheffer, I.E., Serari, N., Stahl, C.M., Kung, A.S., Tarongí Sanchez, S., Thauvin-Robinet, C., Till, M., Tranchant, C., Troedson, C., Tropea, T.F., Vanakker, O., Vega, P., Wiese, M.L., Wieshmann, U., Williams, L.J., Wirth, T., Zech, M., Zempel, H., Roze, E., Leuzzi, V., Galosi, S., Fung, V.S.C., Carvill, G., Krainc, D., Gerard, E., Mencacci, N.E., 2025. The Spectrum of Neurologic Phenotypes Associated With *NUS1* Pathogenic Variants: A Comprehensive Case Series. Annals of Neurology 98, 561–572. https://doi.org/10.1002/ana.27272

Burnet, M., 1957. Cancer: a biological approach. III. Viruses associated with neoplastic conditions. IV. Practical applications. Br Med J 1, 841–847. https://doi.org/10.1136/bmj.1.5023.841

Cameron, F., Whiteside, G., Perry, C., 2011. Ipilimumab: first global approval. Drugs 71, 1093–1104. https://doi.org/10.2165/11594010-000000000-00000

Cancer Genome Atlas Network, 2015. Genomic Classification of Cutaneous Melanoma. Cell 161, 1681–1696. https://doi.org/10.1016/j.cell.2015.05.044

Carlsten, M., Norell, H., Bryceson, Y.T., Poschke, I., Schedvins, K., Ljunggren, H.-G., Kiessling, R., Malmberg, K.-J., 2009. Primary human tumor cells expressing CD155 impair tumor targeting by down-regulating DNAM-1 on NK cells. J Immunol 183, 4921–4930. https://doi.org/10.4049/jimmunol.0901226

Castriconi, R., Dondero, A., Corrias, M.V., Lanino, E., Pende, D., Moretta, L., Bottino, C., Moretta, A., 2004. Natural killer cell-mediated killing of freshly isolated neuroblastoma cells: critical role of DNAX accessory molecule-1-poliovirus receptor interaction. Cancer Res 64, 9180–9184. https://doi.org/10.1158/0008-5472.CAN-04-2682

Chadéneau, C., LeCabellec, M., LeMoullac, B., Meflah, K., Denis, M.G., 1996. Over-expression of a novel member of the immunoglobulin superfamily in Min mouse intestinal adenomas. International Journal of Cancer 68, 817–821. https://doi.org/10.1002/(SICI)1097-0215(19961211)68:6%3C817::AID-IJC21%3E3.0.CO;2-W

Chadéneau, C., LeMoullac, B., Denis, M.G., 1994. A novel member of the immunoglobulin gene superfamily expressed in rat carcinoma cell lines.

Journal of Biological Chemistry 269, 15601–15605. https://doi.org/10.1016/S0021-9258(17)40723-X

Chan, C.J., Andrews, D.M., McLaughlin, N.M., Yagita, H., Gilfillan, S., Colonna, M., Smyth, M.J., 2010. DNAM-1/CD155 interactions promote cytokine and NK cell-mediated suppression of poorly immunogenic melanoma metastases. J Immunol 184, 902–911. https://doi.org/10.4049/jimmunol.0903225

Chan, C.J., Martinet, L., Gilfillan, S., Souza-Fonseca-Guimaraes, F., Chow, M.T., Town, L., Ritchie, D.S., Colonna, M., Andrews, D.M., Smyth, M.J., 2014. The receptors CD96 and CD226 oppose each other in the regulation of natural killer cell functions. Nat Immunol 15, 431–438. https://doi.org/10.1038/ni.2850

Chapman, P.B., Hauschild, A., Robert, C., Haanen, J.B., Ascierto, P., Larkin, J., Dummer, R., Garbe, C., Testori, A., Maio, M., Hogg, D., Lorigan, P., Lebbe, C., Jouary, T., Schadendorf, D., Ribas, A., O'Day, S.J., Sosman, J.A., Kirkwood, J.M., Eggermont, A.M.M., Dreno, B., Nolop, K., Li, J., Nelson, B., Hou, J., Lee, R.J., Flaherty, K.T., McArthur, G.A., 2011. Improved survival with vemurafenib in melanoma with BRAF V600E mutation. N Engl J Med 364, 2507–2516. https://doi.org/10.1056/NEJMoa1103782

Chen, D.S., Mellman, I., 2013. Oncology meets immunology: the cancer-immunity cycle. Immunity 39, 1–10. https://doi.org/10.1016/j.immuni.2013.07.012

Cho, M.M., Song, L., Quamine, A.E., Szewc, F., Shi, L., Ebben, J.D., Turicek, D.P., Kline, J.M., Burpee, D.M., Lafeber, E.O., Phillips, M.F., Ceas, A.S., Bates, P.D., Forsberg, M.H., Kink, J.A., Erbe, A.K., Capitini, C.M., 2025. CD155 blockade enhances allogeneic natural killer cell-mediated antitumor response against osteosarcoma. Journal for ImmunoTherapy of Cancer 13, e008755. https://doi.org/10.1136/jitc-2023-008755

Chocarro, L., Bocanegra, A., Blanco, E., Fernández-Rubio, L., Arasanz, H., Echaide, M., Garnica, M., Ramos, P., Piñeiro-Hermida, S., Vera, R., Escors, D., Kochan, G., 2022. Cutting-Edge: Preclinical and Clinical Development of the First Approved Lag-3 Inhibitor. Cells 11. https://doi.org/10.3390/cells11152351

Chua, H.C., Wulf, M., Weidling, C., Rasmussen, L.P., Pless, S.A., 2020. The NALCN channel complex is voltage sensitive and directly modulated by extracellular calcium. Sci Adv 6, eaaz3154. https://doi.org/10.1126/sciadv.aaz3154

Coutant, K., Magne, B., Ferland, K., Fuentes-Rodriguez, A., Chancy, O., Mitchell, A., Germain, L., Landreville, S., 2024. Melanocytes in regenerative

medicine applications and disease modeling. J Transl Med 22, 336. https://doi.org/10.1186/s12967-024-05113-x

Debniak, T., 2004. Familial malignant melanoma - overview. Hered Cancer Clin Pract 2, 123–129. https://doi.org/10.1186/1897-4287-2-3-123

DeRamus, M.L., Davis, S.J., Rao, S.R., Nyankerh, C., Stacks, D., Kraft, T.W., Fliesler, S.J., Pittler, S.J., 2020. Selective Ablation of Dehydrodolichyl Diphosphate Synthase in Murine Retinal Pigment Epithelium (RPE) Causes RPE Atrophy and Retinal Degeneration. Cells 9. https://doi.org/10.3390/cells9030771

Doench, J.G., Fusi, N., Sullender, M., Hegde, M., Vaimberg, E.W., Donovan, K.F., Smith, I., Tothova, Z., Wilen, C., Orchard, R., Virgin, H.W., Listgarten, J., Root, D.E., 2016. Optimized sgRNA design to maximize activity and minimize off-target effects of CRISPR-Cas9. Nature Biotechnology 34, 184–191. https://doi.org/10.1038/nbt.3437

Dougall, W.C., Kurtulus, S., Smyth, M.J., Anderson, A.C., 2017. TIGIT and CD96: new checkpoint receptor targets for cancer immunotherapy. Immunological Reviews 276, 112–120. https://doi.org/10.1111/imr.12518

Dunn, G.P., Bruce, A.T., Ikeda, H., Old, L.J., Schreiber, R.D., 2002. Cancer immunoediting: from immunosurveillance to tumor escape. Nature Immunology 3, 991–998. https://doi.org/10.1038/ni1102-991

Dwyer, A.R., Kerkvliet, C.P., Krutilina, R.I., Playa, H.C., Parke, D.N., Thomas, W.A., Smeester, B.A., Moriarity, B.S., Seagroves, T.N., Lange, C.A., 2021. Breast Tumor Kinase (Brk/PTK6) Mediates Advanced Cancer Phenotypes via SH2-Domain Dependent Activation of RhoA and Aryl Hydrocarbon Receptor (AhR) Signaling. Mol Cancer Res 19, 329–345. https://doi.org/10.1158/1541-7786.MCR-20-0295

Edani, B.H., Grabińska, K.A., Zhang, R., Park, E.J., Siciliano, B., Surmacz, L., Ha, Y., Sessa, W.C., 2020. Structural elucidation of the cis-prenyltransferase NgBR/DHDDS complex reveals insights in regulation of protein glycosylation. Proceedings of the National Academy of Sciences 117, 20794–20802. https://doi.org/10.1073/pnas.2008381117

Eggermont, A.M.M., Kirkwood, J.M., 2004. Re-evaluating the role of dacarbazine in metastatic melanoma: what have we learned in 30 years? Eur J Cancer 40, 1825–1836. https://doi.org/10.1016/j.ejca.2004.04.030

Ellerhorst, J.A., Greene, V.R., Ekmekcioglu, S., Warneke, C.L., Johnson, M.M., Cooke, C.P., Wang, L.-E., Prieto, V.G., Gershenwald, J.E., Wei, Q., Grimm, E.A., 2011. Clinical correlates of NRAS and BRAF mutations in primary human melanoma. Clin Cancer Res 17, 229–235. https://doi.org/10.1158/1078-0432.CCR-10-2276

Erdei, E., Torres, S.M., 2010. A new understanding in the epidemiology of melanoma. Expert Rev Anticancer Ther 10, 1811–1823. https://doi.org/10.1586/era.10.170

Escalante, N.K., von Rossum, A., Lee, M., Choy, J.C., 2011. CD155 on human vascular endothelial cells attenuates the acquisition of effector functions in CD8 T cells. Arterioscler Thromb Vasc Biol 31, 1177–1184. https://doi.org/10.1161/ATVBAHA.111.224162

Feichtenschlager, V., Zheng, Y.J., Qu, T., Hohlova, D., Callanan, C., Chen, L., Chen, C., Ho, W., Lee, A., Hwang, Y., Courtright, A., Nguyen, T., Marsicovetere, O., Muñoz, D.P., Rappersberger, K., Coppe, J.-P., Ortiz-Urda, S., 2025. Suppression of NRAS-mutant melanoma growth with NRAS-targeting Antisense Oligonucleotide treatment reveals therapeutically relevant kinase co-dependencies. Communications Medicine 5, 216. https://doi.org/10.1038/s43856-025-00932-5

Ferlay, J., Colombet, M., Soerjomataram, I., Parkin, D.M., Piñeros, M., Znaor, A., Bray, F., 2021. Cancer statistics for the year 2020: An overview. International Journal of Cancer 149, 778–789. https://doi.org/10.1002/ijc.33588

Freeman, G.J., Long, A.J., Iwai, Y., Bourque, K., Chernova, T., Nishimura, H., Fitz, L.J., Malenkovich, N., Okazaki, T., Byrne, M.C., Horton, H.F., Fouser, L., Carter, L., Ling, V., Bowman, M.R., Carreno, B.M., Collins, M., Wood, C.R., Honjo, T., 2000. Engagement of the PD-1 immunoinhibitory receptor by a novel B7 family member leads to negative regulation of lymphocyte activation. J Exp Med 192, 1027–1034. https://doi.org/10.1084/jem.192.7.1027

Fridman, W.H., Meylan, M., Pupier, G., Calvez, A., Hernandez, I., Sautès-Fridman, C., 2023. Tertiary lymphoid structures and B cells: An intratumoral immunity cycle. Immunity 56, 2254–2269. https://doi.org/10.1016/j.immuni.2023.08.009

Fuchs, A., Cella, M., Giurisato, E., Shaw, A.S., Colonna, M., 2004. Cutting edge: CD96 (tactile) promotes NK cell-target cell adhesion by interacting with the poliovirus receptor (CD155). J Immunol 172, 3994–3998. https://doi.org/10.4049/jimmunol.172.7.3994

Fuchs, A., Colonna, M., 2006. The role of NK cell recognition of nectin and nectin-like proteins in tumor immunosurveillance. Semin Cancer Biol 16, 359–366. https://doi.org/10.1016/j.semcancer.2006.07.002

Gao, X.-D., Nishikawa, A., Dean, N., 2004. Physical interactions between the Alg1, Alg2, and Alg11 mannosyltransferases of the endoplasmic reticulum. Glycobiology 14, 559–570. https://doi.org/10.1093/glycob/cwh072

Giuliano, S., Cheli, Y., Ohanna, M., Bonet, C., Beuret, L., Bille, K., Loubat, A., Hofman, V., Hofman, P., Ponzio, G., Bahadoran, P., Ballotti, R., Bertolotto, C., 2010. Microphthalmia-associated transcription factor controls the DNA damage response and a lineage-specific senescence program in melanomas. Cancer Res 70, 3813–3822. https://doi.org/10.1158/0008-5472.CAN-09-2913

Gong, J.-N., Djajawi, T.M., Moujalled, D.M., Pomilio, G., Khong, T., Zhang, L.-P., Fedele, P.L., Low, M.S., Anderson, M.A., Riffkin, C.D., White, C.A., Lan, P., Lessene, G., Herold, M.J., Strasser, A., Spencer, A., Grigoriadis, G., Wei, A.H., van Delft, M.F., Roberts, A.W., Huang, D.C.S., 2025. Re-appraising assays on permeabilized blood cancer cells testing venetoclax or other BH3 mimetic agents selectively targeting pro-survival BCL2 proteins. Cell Death & Differentiation 32, 1382–1396. https://doi.org/10.1038/s41418-025-01487-7

Gromeier, M., Solecki, D., Patel, D.D., Wimmer, E., 2000. Expression of the Human Poliovirus Receptor/CD155 Gene during Development of the Central Nervous System: Implications for the Pathogenesis of Poliomyelitis. Virology 273, 248–257. https://doi.org/10.1006/viro.2000.0418

Grzywa, T.M., Paskal, W., Włodarski, P.K., 2017. Intratumor and Intertumor Heterogeneity in Melanoma. Translational Oncology 10, 956–975. https://doi.org/10.1016/j.tranon.2017.09.007

Hanahan, D., 2022. Hallmarks of Cancer: New Dimensions. Cancer Discov 12, 31–46. https://doi.org/10.1158/2159-8290.CD-21-1059

Hanahan, D., Weinberg, R.A., 2011. Hallmarks of cancer: the next generation. Cell 144, 646–674. https://doi.org/10.1016/j.cell.2011.02.013

Harbour, J.W., Onken, M.D., Roberson, E.D.O., Duan, S., Cao, L., Worley, L.A., Council, M.L., Matatall, K.A., Helms, C., Bowcock, A.M., 2010. Frequent mutation of BAP1 in metastasizing uveal melanomas. Science 330, 1410–1413. https://doi.org/10.1126/science.1194472

Hargadon, K.M., Johnson, C.E., Williams, C.J., 2018. Immune checkpoint blockade therapy for cancer: An overview of FDA-approved immune checkpoint inhibitors. International Immunopharmacology 62, 29–39. https://doi.org/10.1016/j.intimp.2018.06.001

Hieken, T.J., Zahrieh, D., Flotte, T.J., Dronca, R.S., Domingo-Musibay, E., Nelson, G.D., Strand, C.A., Kottschade, L.A., Montane, H.N., Piltin, M.A., Chen, R., McWilliams, R.R., Jakub, J.W., Khariwala, S.S., Dudek, A.Z., Johnson, J.E., Markovic, S.N., Dimou, A., Tasche, K.K., Block, M.S., 2025. NeoACTIVATE Arm C: Phase II trial of neoadjuvant atezolizumab and tiragolumab for high-risk operable Stage III melanoma. Eur J Cancer 227, 115688. https://doi.org/10.1016/j.ejca.2025.115688

Hirota, T., Irie, K., Okamoto, R., Ikeda, W., Takai, Y., 2005. Transcriptional activation of the mouse Necl-5/Tage4/PVR/CD155 gene by fibroblast growth factor or oncogenic Ras through the Raf-MEK-ERK-AP-1 pathway. Oncogene 24, 2229–2235. https://doi.org/10.1038/sj.onc.1208409

Hodi, F.S., O'Day, S.J., McDermott, D.F., Weber, R.W., Sosman, J.A., Haanen, J.B., Gonzalez, R., Robert, C., Schadendorf, D., Hassel, J.C., Akerley, W., van den Eertwegh, A.J.M., Lutzky, J., Lorigan, P., Vaubel, J.M., Linette, G.P., Hogg, D., Ottensmeier, C.H., Lebbé, C., Peschel, C., Quirt, I., Clark, J.I., Wolchok, J.D., Weber, J.S., Tian, J., Yellin, M.J., Nichol, G.M., Hoos, A., Urba, W.J., 2010. Improved survival with ipilimumab in patients with metastatic melanoma. N Engl J Med 363, 711–723. https://doi.org/10.1056/NEJMoa1003466

Hodis, E., Watson, I.R., Kryukov, G.V., Arold, S.T., Imielinski, M., Theurillat, J.-P., Nickerson, E., Auclair, D., Li, L., Place, C., Dicara, D., Ramos, A.H., Lawrence, M.S., Cibulskis, K., Sivachenko, A., Voet, D., Saksena, G., Stransky, N., Onofrio, R.C., Winckler, W., Ardlie, K., Wagle, N., Wargo, J., Chong, K., Morton, D.L., Stemke-Hale, K., Chen, G., Noble, M., Meyerson, M., Ladbury, J.E., Davies, M.A., Gershenwald, J.E., Wagner, S.N., Hoon, D.S.B., Schadendorf, D., Lander, E.S., Gabriel, S.B., Getz, G., Garraway, L.A., Chin, L., 2012. A landscape of driver mutations in melanoma. Cell 150, 251–263. https://doi.org/10.1016/j.cell.2012.06.024

Holland, J.J., McLaren, L.C., 1961. The location and nature of enterovirus receptors in susceptible cells. J Exp Med 114, 161–171. https://doi.org/10.1084/jem.114.2.161

Hölzel, M., Tüting, T., 2016. Inflammation-Induced Plasticity in Melanoma Therapy and Metastasis. Trends in Immunology 37, 364–374. https://doi.org/10.1016/j.it.2016.03.009

Huang, A.C., Zappasodi, R., 2022. A decade of checkpoint blockade immunotherapy in melanoma: understanding the molecular basis for immune sensitivity and resistance. Nature Immunology 23, 660–670. https://doi.org/10.1038/s41590-022-01141-1

Huang, H.-C., Lai, Y.-J., Liao, C.-C., Wang, F.-Y., Huang, K.-B., Lee, I.-J., Chou, W.-C., Wang, S.-H., Wang, L.-H., Hsu, J.-M., Sun, C.-P., Kuo, C.-T., Wang, J., Hsiao, T.-C., Yang, P.-J., Lee, T.-A., Huang, W., Li, F.-A., Shen, C.-Y., Lin, Y.-L., Tao, M.-H., Li, C.-W., 2021. Targeting conserved N-glycosylation blocks SARS-CoV-2 variant infection in vitro. eBioMedicine 74. https://doi.org/10.1016/j.ebiom.2021.103712

Huo, Z., Li, C., Xu, X., Ge, F., Wang, R., Wen, Y., Peng, H., Wu, X., Liang, H., Peng, G., Li, R., Huang, D., Chen, Y., Zhong, R., Cheng, B., Xiong, S., Lin, W., He, J., Liang, W., 2020. Cancer Risks in Solid Organ Transplant Recipients: Results from a Comprehensive Analysis of 72 Cohort Studies.

Oncoimmunology 9, 1848068. https://doi.org/10.1080/2162402X.2020.1848068

Hussussian, C.J., Struewing, J.P., Goldstein, A.M., Higgins, P.A., Ally, D.S., Sheahan, M.D., Clark, W.H.J., Tucker, M.A., Dracopoli, N.C., 1994. Germline p16 mutations in familial melanoma. Nat Genet 8, 15–21. https://doi.org/10.1038/ng0994-15

Iguchi-Manaka, A., Kai, H., Yamashita, Y., Shibata, K., Tahara-Hanaoka, S., Honda, S., Yasui, T., Kikutani, H., Shibuya, K., Shibuya, A., 2008. Accelerated tumor growth in mice deficient in DNAM-1 receptor. J Exp Med 205, 2959–2964. https://doi.org/10.1084/jem.20081611

Iguchi-Manaka, A., Okumura, G., Kojima, H., Cho, Y., Hirochika, R., Bando, H., Sato, T., Yoshikawa, H., Hara, H., Shibuya, A., Shibuya, K., 2016. Increased Soluble CD155 in the Serum of Cancer Patients. PLoS One 11, e0152982. https://doi.org/10.1371/journal.pone.0152982

Itskanov, S., Park, E., 2023. Mechanism of Protein Translocation by the Sec61 Translocon Complex. Cold Spring Harb Perspect Biol 15. https://doi.org/10.1101/cshperspect.a041250

Jadhav, B., McKenna, M., Johnson, N., High, S., Sinning, I., Pool, M.R., 2015. Mammalian SRP receptor switches the Sec61 translocase from Sec62 to SRP-dependent translocation. Nature Communications 6, 10133. https://doi.org/10.1038/ncomms10133

Ji, G., Yang, X., Li, J., 2024. High SEC61A1 expression predicts poor outcome of acute myeloid leukemia. Open Med (Wars) 19, 20240944. https://doi.org/10.1515/med-2024-0944

Johnston, R.J., Lee, P.S., Strop, P., Smyth, M.J., 2021. Cancer Immunotherapy and the Nectin Family. Annu. Rev. Cancer Biol. 5, 203–219. https://doi.org/10.1146/annurev-cancerbio-060920-084910

Jutzi, J.S., Marneth, A.E., Ciboddo, M., Guerra-Moreno, A., Jiménez-Santos, M.J., Kosmidou, A., Dressman, J.W., Liang, H., Hamel, R., Lozano, P., Rumi, E., Doench, J.G., Gotlib, J., Krishnan, A., Elf, S., Al-Shahrour, F., Mullally, A., 2022. Whole-genome CRISPR screening identifies N-glycosylation as a genetic and therapeutic vulnerability in CALR-mutant MPNs. Blood 140, 1291–1304. https://doi.org/10.1182/blood.2022015629

Kakunaga, S., Ikeda, W., Shingai, T., Fujito, T., Yamada, A., Minami, Y., Imai, T., Takai, Y., 2004. Enhancement of serum- and platelet-derived growth factor-induced cell proliferation by Necl-5/Tage4/poliovirus receptor/CD155 through the Ras-Raf-MEK-ERK signaling. J Biol Chem 279, 36419–36425. https://doi.org/10.1074/jbc.M406340200

Kalal, B.S., Upadhya, D., Pai, V.R., 2017. Chemotherapy Resistance Mechanisms in Advanced Skin Cancer. Oncol Rev 11, 326. https://doi.org/10.4081/oncol.2017.326

Kaltheuner, I.H., Anand, K., Moecking, J., Düster, R., Wang, J., Gray, N.S., Geyer, M., 2021. Abemaciclib is a potent inhibitor of DYRK1A and HIP kinases involved in transcriptional regulation. Nat Commun 12, 6607. https://doi.org/10.1038/s41467-021-26935-z

Kamb, A., Shattuck-Eidens, D., Eeles, R., Liu, Q., Gruis, N.A., Ding, W., Hussey, C., Tran, T., Miki, Y., Weaver-Feldhaus, J., 1994. Analysis of the p16 gene (CDKN2) as a candidate for the chromosome 9p melanoma susceptibility locus. Nat Genet 8, 23–26. https://doi.org/10.1038/ng0994-22

Kamran, N., Takai, Y., Miyoshi, J., Biswas, S.K., Wong, J.S.B., Gasser, S., 2013. Toll-like receptor ligands induce expression of the costimulatory molecule CD155 on antigen-presenting cells. PLoS One 8, e54406. https://doi.org/10.1371/journal.pone.0054406

Kawase, K., Kawashima, S., Nishi, T., Inozume, T., Morinaga, T., Kawazu, M., Hanazawa, T., Togashi, Y., 2025. PI3K/Akt signaling pathway regulates CD155 expression involved in resistance to cancer immunotherapy. Cancer Immunol Res. https://doi.org/10.1158/2326-6066.CIR-24-0853

Kawashima, S., Inozume, T., Kawazu, M., Ueno, T., Nagasaki, J., Tanji, E., Honobe, A., Ohnuma, T., Kawamura, T., Umeda, Y., Nakamura, Y., Kawasaki, T., Kiniwa, Y., Yamasaki, O., Fukushima, S., Ikehara, Y., Mano, H., Suzuki, Y., Nishikawa, H., Matsue, H., Togashi, Y., 2021. TIGIT/CD155 axis mediates resistance to immunotherapy in patients with melanoma with the inflamed tumor microenvironment. J Immunother Cancer 9, e003134. https://doi.org/10.1136/jitc-2021-003134

Kim, H.C., Jang, H.W., Lee, H.J., 2012. Imaging finding of malignant melanoma of Eustachian tube with extension to middle ear cavity: case report. Korean J Radiol 13, 812–815. https://doi.org/10.3348/kjr.2012.13.6.812

Kim, J., Kim, S.-J., Jeong, H.-R., Park, J.-H., Moon, M., Hoe, H.-S., 2022. Inhibiting EGFR/HER-2 ameliorates neuroinflammatory responses and the early stage of tau pathology through DYRK1A. Front Immunol 13, 903309. https://doi.org/10.3389/fimmu.2022.903309

Koike, S., Horie, H., Ise, I., Okitsu, A., Yoshida, M., Iizuka, N., Takeuchi, K., Takegami, T., Nomoto, A., 1990. The poliovirus receptor protein is produced both as membrane-bound and secreted forms. EMBO J 9, 3217–3224. https://doi.org/10.1002/j.1460-2075.1990.tb07520.x

Koike, S., Yamasaki, K., 2020. Melanogenesis Connection with Innate Immunity and Toll-Like Receptors. Int J Mol Sci 21. https://doi.org/10.3390/ijms21249769

Kono, T., Imai, Y., Yasuda, S., Ohmori, K., Fukui, H., Ichikawa, K., Tomita, S., Imura, J., Kuroda, Y., Ueda, Y., Fujimori, T., 2008. The CD155/poliovirus receptor enhances the proliferation of ras-mutated cells. Int J Cancer 122, 317–324. https://doi.org/10.1002/ijc.23080

Krummel, M.F., Allison, J.P., 1995. CD28 and CTLA-4 have opposing effects on the response of T cells to stimulation. J Exp Med 182, 459–465. https://doi.org/10.1084/jem.182.2.459

Kučan Brlić, P., Lenac Roviš, T., Cinamon, G., Tsukerman, P., Mandelboim, O., Jonjić, S., 2019. Targeting PVR (CD155) and its receptors in anti-tumor therapy. Cellular & Molecular Immunology 16, 40–52. https://doi.org/10.1038/s41423-018-0168-y

Laha, D., Grant, R., Mishra, P., Nilubol, N., 2021. The Role of Tumor Necrosis Factor in Manipulating the Immunological Response of Tumor Microenvironment. Front Immunol 12, 656908. https://doi.org/10.3389/fimmu.2021.656908

Laham, A.J., El-Awady, R., Saber-Ayad, M., Wang, N., Yan, G., Boudreault, J., Ali, S., Lebrun, J.-J., 2024. Targeting the DYRK1A kinase prevents cancer progression and metastasis and promotes cancer cells response to G1/S targeting chemotherapy drugs. npj Precis. Onc. 8, 128. https://doi.org/10.1038/s41698-024-00614-w

Laham, A.J., Saber-Ayad, M., El-Awady, R., 2021. DYRK1A: a down syndrome-related dual protein kinase with a versatile role in tumorigenesis. Cell Mol Life Sci 78, 603–619. https://doi.org/10.1007/s00018-020-03626-4

Landras, A., Reger de Moura, C., Villoutreix, B.O., Battistella, M., Sadoux, A., Dumaz, N., Menashi, S., Fernández-Recio, J., Lebbé, C., Mourah, S., 2022. Novel treatment strategy for NRAS-mutated melanoma through a selective inhibitor of CD147/VEGFR-2 interaction. Oncogene 41, 2254–2264. https://doi.org/10.1038/s41388-022-02244-7

Lang, S., Pfeffer, S., Lee, P.-H., Cavalié, A., Helms, V., Förster, F., Zimmermann, R., 2017. An Update on Sec61 Channel Functions, Mechanisms, and Related Diseases. Front Physiol 8, 887. https://doi.org/10.3389/fphys.2017.00887

Lange, R., Peng, X., Wimmer, E., Lipp, M., Bernhardt, G., 2001. The Poliovirus Receptor CD155 Mediates Cell-to-Matrix Contacts by Specifically Binding to Vitronectin. Virology 285, 218–227. https://doi.org/10.1006/viro.2001.0943

Larkin, J., Chiarion-Sileni, V., Gonzalez, R., Grob, J.-J., Rutkowski, P., Lao, C.D., Cowey, C.L., Schadendorf, D., Wagstaff, J., Dummer, R., Ferrucci, P.F., Smylie, M., Hogg, D., Hill, A., Márquez-Rodas, I., Haanen, J., Guidoboni, M., Maio, M., Schöffski, P., Carlino, M.S., Lebbé, C., McArthur, G.,

Ascierto, P.A., Daniels, G.A., Long, G.V., Bastholt, L., Rizzo, J.I., Balogh, A., Moshyk, A., Hodi, F.S., Wolchok, J.D., 2019. Five-Year Survival with Combined Nivolumab and Ipilimumab in Advanced Melanoma. N Engl J Med 381, 1535–1546. https://doi.org/10.1056/NEJMoa1910836

Lawrence, M.S., Stojanov, P., Polak, P., Kryukov, G.V., Cibulskis, K., Sivachenko, A., Carter, S.L., Stewart, C., Mermel, C.H., Roberts, S.A., Kiezun, A., Hammerman, P.S., McKenna, A., Drier, Y., Zou, L., Ramos, A.H., Pugh, T.J., Stransky, N., Helman, E., Kim, J., Sougnez, C., Ambrogio, L., Nickerson, E., Shefler, E., Cortés, M.L., Auclair, D., Saksena, G., Voet, D., Noble, M., DiCara, D., Lin, P., Lichtenstein, L., Heiman, D.I., Fennell, T., Imielinski, M., Hernandez, B., Hodis, E., Baca, S., Dulak, A.M., Lohr, J., Landau, D.-A., Wu, C.J., Melendez-Zajgla, J., Hidalgo-Miranda, A., Koren, A., McCarroll, S.A., Mora, J., Crompton, B., Onofrio, R., Parkin, M., Winckler, W., Ardlie, K., Gabriel, S.B., Roberts, C.W.M., Biegel, J.A., Stegmaier, K., Bass, A.J., Garraway, L.A., Meyerson, M., Golub, T.R., Gordenin, D.A., Sunyaev, S., Lander, E.S., Getz, G., 2013. Mutational heterogeneity in cancer and the search for new cancer-associated genes. Nature 499, 214–218. https://doi.org/10.1038/nature12213

Leung, L., Kwong, M., Hou, S., Lee, C., Chan, J.Y., 2003. Deficiency of the Nrf1 and Nrf2 transcription factors results in early embryonic lethality and severe oxidative stress. J Biol Chem 278, 48021–48029. https://doi.org/10.1074/jbc.M308439200

Liang, R., Liu, L., Ding, D., Li, Y., Ren, J., Wei, B., 2025. CD155 promotes the progression of colorectal cancer by restraining CD8+ T cells via the PI3K/AKT/NF-κB pathway. Cancer Immunology, Immunotherapy 74, 94. https://doi.org/10.1007/s00262-025-03947-y

Lin, J.Y., Fisher, D.E., 2007. Melanocyte biology and skin pigmentation. Nature 445, 843–850. https://doi.org/10.1038/nature05660

Liu, F., Huang, J., Xiong, Y., Li, S., Liu, Z., 2019. Large-scale analysis reveals the specific clinical and immune features of CD155 in glioma. Aging (Albany NY) 11, 5463–5482. https://doi.org/10.18632/aging.102131

Liu, Q., Liu, N., Zang, S., Liu, H., Wang, P., Ji, C., Sun, X., 2014. Tumor suppressor DYRK1A effects on proliferation and chemoresistance of AML cells by downregulating c-Myc. PLoS One 9, e98853. https://doi.org/10.1371/journal.pone.0098853

Liu, S., Zhang, H., Li, M., Hu, D., Li, C., Ge, B., Jin, B., Fan, Z., 2013. Recruitment of Grb2 and SHIP1 by the ITT-like motif of TIGIT suppresses granule polarization and cytotoxicity of NK cells. Cell Death & Differentiation 20, 456–464. https://doi.org/10.1038/cdd.2012.141

Liu, X., Sun, Y., Lin, B., Xiong, H., Lu, X., Tan, B., Zhang, C., Liu, M., Qin, J., Zhang, N., Du, B., 2025. Pan-cancer analysis identifies CD155 as a promising target for CAR-T cell therapy. Genome Med 17, 64. https://doi.org/10.1186/s13073-025-01490-0

Liu, X., Xu, C., Guo, T., Zhan, S., Quan, Q., Li, M., Wang, Z., Zhang, X., Guo, L., Cao, L., 2023. Clinical significance of CD155 expression and correlation with cellular components of tumor microenvironment in gastric adenocarcinoma. Front Immunol 14, 1173524. https://doi.org/10.3389/fimmu.2023.1173524

Lochhead, P.A., Sibbet, G., Morrice, N., Cleghon, V., 2005. Activation-loop autophosphorylation is mediated by a novel transitional intermediate form of DYRKs. Cell 121, 925–936. https://doi.org/10.1016/j.cell.2005.03.034

Luirink, J., Sinning, I., 2004. SRP-mediated protein targeting: structure and function revisited. Biochimica et Biophysica Acta (BBA) - Molecular Cell Research 1694, 17–35. https://doi.org/10.1016/j.bbamcr.2004.03.013

Maier, M.K., Seth, S., Czeloth, N., Qiu, Q., Ravens, I., Kremmer, E., Ebel, M., Müller, W., Pabst, O., Förster, R., Bernhardt, G., 2007. The adhesion receptor CD155 determines the magnitude of humoral immune responses against orally ingested antigens. Eur J Immunol 37, 2214–2225. https://doi.org/10.1002/eji.200737072

Marco Rastrelli, SAVERIA TROPEA, CARLO RICCARDO ROSSI, MAURO ALAIBAC, 2014. Melanoma: Epidemiology, Risk Factors, Pathogenesis, Diagnosis and Classification. In Vivo 28, 1005.

Martínez-Jiménez, F., Chowell, D., 2025. Genetic immune escape in cancer: timing and implications for treatment. Trends in Cancer 11, 286–294. https://doi.org/10.1016/j.trecan.2024.11.002

Massey, A.J., Benwell, K., Burbridge, M., Kotschy, A., Walmsley, D.L., 2021. Targeting DYRK1A/B kinases to modulate p21-cyclin D1-p27 signalling and induce anti-tumour activity in a model of human glioblastoma. J Cell Mol Med 25, 10650–10662. https://doi.org/10.1111/jcmm.17002

Masson, D., Jarry, A., Baury, B., Blanchardie, P., Laboisse, C., Lustenberger, P., Denis, M.G., 2001. Overexpression of the CD155 gene in human colorectal carcinoma. Gut 49, 236–240. https://doi.org/10.1136/gut.49.2.236

McCarthy, E.F., 2006. The toxins of William B. Coley and the treatment of bone and soft-tissue sarcomas. Iowa Orthop J 26, 154–158.

Mekhloufi, A., Kosta, A., Stabile, H., Molfetta, R., Zingoni, A., Soriani, A., Cippitelli, M., Paolini, R., Gismondi, A., Ricciardi, M.R., Petrucci, M.T., Masuelli, L., Caracciolo, G., Palchetti, S., Santoni, A., Fionda, C., 2020.

Bone Marrow Stromal Cell-Derived IL-8 Upregulates PVR Expression on Multiple Myeloma Cells via NF-kB Transcription Factor. Cancers (Basel) 12. https://doi.org/10.3390/cancers12020440

Mellman, I., Chen, D.S., Powles, T., Turley, S.J., 2023. The cancer-immunity cycle: Indication, genotype, and immunotype. Immunity 56, 2188–2205. https://doi.org/10.1016/j.immuni.2023.09.011

Mendelsohn, C.L., Wimmer, E., Racaniello, V.R., 1989. Cellular receptor for poliovirus: molecular cloning, nucleotide sequence, and expression of a new member of the immunoglobulin superfamily. Cell 56, 855–865. https://doi.org/10.1016/0092-8674(89)90690-9

Mensurado, S., Condeço, C., Sánchez-Martínez, D., Shirley, S., Coelho, R.M.L., Tirado, N., Vinyoles, M., Blanco-Domínguez, R., Barros, L., Galvão, B., Custódio, N., Gomes da Silva, M., Menéndez, P., Silva-Santos, B., 2024. CD155/PVR determines acute myeloid leukemia targeting by Delta One T cells. Blood 143, 1488–1495. https://doi.org/10.1182/blood.2023022992

Mitsunari, T., Nakatsu, F., Shioda, N., Love, P.E., Grinberg, A., Bonifacino, J.S., Ohno, H., 2005. Clathrin adaptor AP-2 is essential for early embryonal development. Mol Cell Biol 25, 9318–9323. https://doi.org/10.1128/MCB.25.21.9318-9323.2005

Molfetta, R., Zitti, B., Lecce, M., Milito, N.D., Stabile, H., Fionda, C., Cippitelli, M., Gismondi, A., Santoni, A., Paolini, R., 2020. CD155: A Multi-Functional Molecule in Tumor Progression. Int J Mol Sci 21. https://doi.org/10.3390/ijms21030922

Muller, W.A., 2009. Mechanisms of transendothelial migration of leukocytes. Circ Res 105, 223–230. https://doi.org/10.1161/CIRCRESAHA.109.200717

Nakai, R., Maniwa, Y., Tanaka, Y., Nishio, W., Yoshimura, M., Okita, Y., Ohbayashi, C., Satoh, N., Ogita, H., Takai, Y., Hayashi, Y., 2010. Overexpression of Necl-5 correlates with unfavorable prognosis in patients with lung adenocarcinoma. Cancer Sci 101, 1326–1330. https://doi.org/10.1111/j.1349-7006.2010.01530.x

Nasti, T.H., Timares, L., 2015. MC1R, Eumelanin and Pheomelanin: Their Role in Determining the Susceptibility to Skin Cancer. Photochemistry and Photobiology 91, 188–200. https://doi.org/10.1111/php.12335

Ochiai, H., Moore, S.A., Archer, G.E., Okamura, T., Chewning, T.A., Marks, J.R., Sampson, J.H., Gromeier, M., 2004. Treatment of intracerebral neoplasia and neoplastic meningitis with regional delivery of oncolytic recombinant poliovirus. Clin Cancer Res 10, 4831–4838. https://doi.org/10.1158/1078-0432.CCR-03-0694

Oda, T., Ohka, S., Nomoto, A., 2004. Ligand stimulation of CD155alpha inhibits cell adhesion and enhances cell migration in fibroblasts. Biochem Biophys Res Commun 319, 1253–1264. https://doi.org/10.1016/j.bbrc.2004.05.111

O'Donnell, Jake.S., Madore, J., Li, X.-Y., Smyth, M.J., 2020. Tumor intrinsic and extrinsic immune functions of CD155. Seminars in Cancer Biology 65, 189–196. https://doi.org/10.1016/j.semcancer.2019.11.013

O'Donnell, J.S., Teng, M.W.L., Smyth, M.J., 2019. Cancer immunoediting and resistance to T cell-based immunotherapy. Nat Rev Clin Oncol 16, 151–167. https://doi.org/10.1038/s41571-018-0142-8

Ohka, S., Ohno, H., Tohyama, K., Nomoto, A., 2001. Basolateral sorting of human poliovirus receptor alpha involves an interaction with the mu1B subunit of the clathrin adaptor complex in polarized epithelial cells. Biochem Biophys Res Commun 287, 941–948. https://doi.org/10.1006/bbrc.2001.5660

O'Keefe, S., Zong, G., Duah, K.B., Andrews, L.E., Shi, W.Q., High, S., 2021. An alternative pathway for membrane protein biogenesis at the endoplasmic reticulum. Communications Biology 4, 828. https://doi.org/10.1038/s42003-021-02363-z

Okumura, G., Iguchi-Manaka, A., Murata, R., Yamashita-Kanemaru, Y., Shibuya, A., Shibuya, K., 2020. Tumor-derived soluble CD155 inhibits DNAM-1-mediated antitumor activity of natural killer cells. J Exp Med 217, 1. https://doi.org/10.1084/jem.20191290

Oliveira, L., Silva, M.C., Gomes, A.P., Santos, R.F., Cardoso, M.S., Nóvoa, A., Luche, H., Cavadas, B., Amorim, I., Gärtner, F., Malissen, B., Mallo, M., Carmo, A.M., 2024. CD5L as a promising biological therapeutic for treating sepsis. Nature Communications 15, 4119. https://doi.org/10.1038/s41467-024-48360-8

Oliveira, T., Zhang, M., Joo, E.J., Abdel-Azim, H., Chen, C.-W., Yang, L., Chou, C.-H., Qin, X., Chen, J., Alagesan, K., Almeida, A., Jacob, F., Packer, N.H., von Itzstein, M., Heisterkamp, N., Kolarich, D., 2021. Glycoproteome remodeling in MLL-rearranged B-cell precursor acute lymphoblastic leukemia. Theranostics 11, 9519–9537. https://doi.org/10.7150/thno.65398

Olszańska, J., Pietraszek-Gremplewicz, K., Nowak, D., 2021. Melanoma Progression under Obesity: Focus on Adipokines. Cancers (Basel) 13. https://doi.org/10.3390/cancers13092281

Ozmadenci, D., Shankara Narayanan, J.S., Andrew, J., Ojalill, M., Barrie, A.M., Jiang, S., Iyer, S., Chen, X.L., Rose, M., Estrada, V., Molinolo, A., Bertotto, T., Mikulski, Z., McHale, M.C., White, R.R., Connolly, D.C., Pachter, J.A., Kuchroo, V.K., Stupack, D.G., Schlaepfer, D.D., 2022. Tumor FAK

orchestrates immunosuppression in ovarian cancer via the CD155/TIGIT axis. Proc Natl Acad Sci U S A 119, e2117065119. https://doi.org/10.1073/pnas.2117065119

Ozyuncu, N., Sahin, M., Altin, T., Karaoguz, R., Guldal, M., Akyurek, O., 2006. Cardiac metastasis of malignant melanoma: a rare cause of complete atrioventricular block. EP Europace 8, 545–548. https://doi.org/10.1093/europace/eul058

Paillerets, B.B., Lesueur, F., Bertolotto, C., 2014. A germline oncogenic MITF mutation and tumor susceptibility. European Journal of Cell Biology 93, 71–75. https://doi.org/10.1016/j.ejcb.2013.10.002

Paolini, R., Molfetta, R., 2023. CD155 and Its Receptors as Targets for Cancer Therapy. Int J Mol Sci 24. https://doi.org/10.3390/ijms241612958

Park, B., Ahn, K.H., Choi, Y., Kim, J.H., Seong, H., Kim, Y.J., Choi, J.Y., Song, J.Y., Lee, E., Jun, Y.H., Yoon, Y.K., Choi, W.S., Lee, M., Seong, J., Kim, S.-W., 2022. Cancer Incidence Among Adults With HIV in a Population-Based Cohort in Korea. JAMA Netw Open 5, e2224897. https://doi.org/10.1001/jamanetworkopen.2022.24897

Pende, D., Spaggiari, G.M., Marcenaro, S., Martini, S., Rivera, P., Capobianco, A., Falco, M., Lanino, E., Pierri, I., Zambello, R., Bacigalupo, A., Mingari, M.C., Moretta, A., Moretta, L., 2005. Analysis of the receptor-ligand interactions in the natural killer-mediated lysis of freshly isolated myeloid or lymphoblastic leukemias: evidence for the involvement of the Poliovirus receptor (CD155) and Nectin-2 (CD112). Blood 105, 2066–2073. https://doi.org/10.1182/blood-2004-09-3548

Pinho, S.S., Reis, C.A., 2015. Glycosylation in cancer: mechanisms and clinical implications. Nature Reviews Cancer 15, 540–555. https://doi.org/10.1038/nrc3982

Qin, S., Xu, L., Yi, M., Yu, S., Wu, K., Luo, S., 2019. Novel immune checkpoint targets: moving beyond PD-1 and CTLA-4. Molecular Cancer 18, 155. https://doi.org/10.1186/s12943-019-1091-2

Raimondi, S., Sera, F., Gandini, S., Iodice, S., Caini, S., Maisonneuve, P., Fargnoli, M.C., 2008. MC1R variants, melanoma and red hair color phenotype: a meta-analysis. Int J Cancer 122, 2753–2760. https://doi.org/10.1002/ijc.23396

Ramesh, S.T., Navyasree, K.V., Ashok, A.B., Qathoon, N., Mohanty, S., Swain, R.K., Umasankar, P.K., 2019. Allosteric feed-forward activation of AP-2 via FCHO-BMP2K axis promotes clathrin-mediated endocytosis. bioRxiv. https://doi.org/10.1101/870899

Rammohan, M., Harris, E., Bhansali, R.S., Zhao, E., Li, L.S., Crispino, J.D., 2022. The chromosome 21 kinase DYRK1A: emerging roles in cancer biology and potential as a therapeutic target. Oncogene 41, 2003–2011. https://doi.org/10.1038/s41388-022-02245-6

Regal, L., van Hasselt, P.M., Foulquier, F., Cuppen, I., Prinsen, H., Jansen, K., Keldermans, L., De Meirleir, L., Matthijs, G., Jaeken, J., 2015. ALG11-CDG: Three novel mutations and further characterization of the phenotype. Molecular Genetics and Metabolism Reports 2, 16–19. https://doi.org/10.1016/j.ymgmr.2014.11.006

Reinhardt, J., Landsberg, J., Schmid-Burgk, J.L., Ramis, B.B., Bald, T., Glodde, N., Lopez-Ramos, D., Young, A., Ngiow, S.F., Nettersheim, D., Schorle, H., Quast, T., Kolanus, W., Schadendorf, D., Long, G.V., Madore, J., Scolyer, R.A., Ribas, A., Smyth, M.J., Tumeh, P.C., Tüting, T., Hölzel, M., 2017a. MAPK Signaling and Inflammation Link Melanoma Phenotype Switching to Induction of CD73 during Immunotherapy. Cancer Res 77, 4697–4709. https://doi.org/10.1158/0008-5472.CAN-17-0395

Reinhardt, J., Landsberg, J., Schmid-Burgk, J.L., Ramis, B.B., Bald, T., Glodde, N., Lopez-Ramos, D., Young, A., Ngiow, S.F., Nettersheim, D., Schorle, H., Quast, T., Kolanus, W., Schadendorf, D., Long, G.V., Madore, J., Scolyer, R.A., Ribas, A., Smyth, M.J., Tumeh, P.C., Tüting, T., Hölzel, M., 2017b. MAPK Signaling and Inflammation Link Melanoma Phenotype Switching to Induction of CD73 during Immunotherapy. Cancer Research 77, 4697–4709. https://doi.org/10.1158/0008-5472.CAN-17-0395

Ren, Y., Liang, H., Huang, Y., Miao, Y., Li, R., Qiang, J., Wu, L., Qi, J., Li, Y., Xia, Y., Huang, L., Wang, S., Kong, X., Zhou, Y., Zhang, Q., Zhu, G., 2024. Key candidate genes and pathways in T lymphoblastic leukemia/lymphoma identified by bioinformatics and serological analyses. Frontiers in Immunology Volume 15-2024. https://doi.org/10.3389/fimmu.2024.1341255

Reymond, N., Imbert, A.-M., Devilard, E., Fabre, S., Chabannon, C., Xerri, L., Farnarier, C., Cantoni, C., Bottino, C., Moretta, A., Dubreuil, P., Lopez, M., 2004. DNAM-1 and PVR regulate monocyte migration through endothelial junctions. J Exp Med 199, 1331–1341. https://doi.org/10.1084/jem.20032206

Riesenberg, S., Groetchen, A., Siddaway, R., Bald, T., Reinhardt, J., Smorra, D., Kohlmeyer, J., Renn, M., Phung, B., Aymans, P., Schmidt, T., Hornung, V., Davidson, I., Goding, C.R., Jönsson, G., Landsberg, J., Tüting, T., Hölzel, M., 2015. MITF and c-Jun antagonism interconnects melanoma dedifferentiation with pro-inflammatory cytokine responsiveness and myeloid cell recruitment. Nat Commun 6, 8755. https://doi.org/10.1038/ncomms9755

Robert Caroline, Grob Jean J., Stroyakovskiy Daniil, Karaszewska Boguslawa, Hauschild Axel, Levchenko Evgeny, Chiarion Sileni Vanna, Schachter Jacob, Garbe Claus, Bondarenko Igor, Gogas Helen, Mandalá Mario, Haanen John B.A.G., Lebbé Celeste, Mackiewicz Andrzej, Rutkowski Piotr, Nathan Paul D., Ribas Antoni, Davies Michael A., Flaherty Keith T., Burgess Paul, Tan Monique, Gasal Eduard, Voi Maurizio, Schadendorf Dirk, Long Georgina V., 2019. Five-Year Outcomes with Dabrafenib plus Trametinib in Metastatic Melanoma. New England Journal of Medicine 381, 626–636. https://doi.org/10.1056/NEJMoa1904059

Rodrigues, J.G., Balmaña, M., Macedo, J.A., Poças, J., Fernandes, Â., de-Freitas-Junior, J.C.M., Pinho, S.S., Gomes, J., Magalhães, A., Gomes, C., Mereiter, S., Reis, C.A., 2018. Glycosylation in cancer: Selected roles in tumour progression, immune modulation and metastasis. Cellular Immunology 333, 46–57. https://doi.org/10.1016/j.cellimm.2018.03.007

Romorini, L., Garate, X., Neiman, G., Luzzani, C., Furmento, V.A., Guberman, A.S., Sevlever, G.E., Scassa, M.E., Miriuka, S.G., 2016. AKT/GSK3β signaling pathway is critically involved in human pluripotent stem cell survival. Scientific Reports 6, 35660. https://doi.org/10.1038/srep35660

Rosenberg, S.A., 2014. IL-2: the first effective immunotherapy for human cancer. J Immunol 192, 5451–5458. https://doi.org/10.4049/jimmunol.1490019

Saginala, K., Barsouk, Adam, Aluru, J.S., Rawla, P., Barsouk, Alexander, 2021. Epidemiology of Melanoma. Med Sci (Basel) 9. https://doi.org/10.3390/medsci9040063

Sanson, K.R., Hanna, R.E., Hegde, M., Donovan, K.F., Strand, C., Sullender, M.E., Vaimberg, E.W., Goodale, A., Root, D.E., Piccioni, F., Doench, J.G., 2018. Optimized libraries for CRISPR-Cas9 genetic screens with multiple modalities. Nature Communications 9, 5416. https://doi.org/10.1038/s41467-018-07901-8

Santeufemia, D.A., Palmieri, G., Miolo, G., Colombino, M., Doro, M.G., Frogheri, L., Paliogiannis, P., Capobianco, G., Madonia, M., Cossu, A., Lo Re, G., Corona, G., 2023. Current Trends in Mucosal Melanomas: An Overview. Cancers (Basel) 15. https://doi.org/10.3390/cancers15051356

Sasai, N., Toriyama, M., Kondo, T., 2019. Hedgehog Signal and Genetic Disorders. Front Genet 10, 1103. https://doi.org/10.3389/fgene.2019.01103

Schadendorf, D., Dummer, R., Flaherty, K.T., Robert, C., Arance, A., de Groot, J.W.B., Garbe, C., Gogas, H.J., Gutzmer, R., Krajsová, I., Liszkay, G., Loquai, C., Mandalà, M., Yamazaki, N., Queirolo, P., Guenzel, C., Polli, A., Thakur, M., di Pietro, A., Ascierto, P.A., 2024. COLUMBUS 7-year update: A randomized, open-label, phase III trial of encorafenib plus binimetinib versus vemurafenib or encorafenib in patients with BRAF

V600E/K-mutant melanoma. Eur J Cancer 204, 114073. https://doi.org/10.1016/j.ejca.2024.114073

Schmid-Burgk, J.L., Schmidt, T., Gaidt, M.M., Pelka, K., Latz, E., Ebert, T.S., Hornung, V., 2014. OutKnocker: a web tool for rapid and simple genotyping of designer nuclease edited cell lines. Genome Res 24, 1719–1723. https://doi.org/10.1101/gr.176701.114

Schubert, D., Klein, M.-C., Hassdenteufel, S., Caballero-Oteyza, A., Yang, L., Proietti, M., Bulashevska, A., Kemming, J., Kühn, J., Winzer, S., Rusch, S., Fliegauf, M., Schäffer, A.A., Pfeffer, S., Geiger, R., Cavalié, A., Cao, H., Yang, F., Li, Y., Rizzi, M., Eibel, H., Kobbe, R., Marks, A.L., Peppers, B.P., Hostoffer, R.W., Puck, J.M., Zimmermann, R., Grimbacher, B., 2018. Plasma cell deficiency in human subjects with heterozygous mutations in Sec61 translocon alpha 1 subunit (SEC61A1). J Allergy Clin Immunol 141, 1427–1438. https://doi.org/10.1016/j.jaci.2017.06.042

Schürch, C., Schaefer, T., Müller, J.S., Hanns, P., Arnone, M., Dumlin, A., Schärer, J., Sinning, I., Wild, K., Skokowa, J., Welte, K., Carapito, R., Bahram, S., Konantz, M., Lengerke, C., 2021. SRP54 mutations induce congenital neutropenia via dominant-negative effects on XBP1 splicing. Blood 137, 1340–1352. https://doi.org/10.1182/blood.2020008115

Setlow, R.B., Carrier, W.L., 1966. Pyrimidine dimers in ultraviolet-irradiated DNA's. J Mol Biol 17, 237–254. https://doi.org/10.1016/s0022-2836(66)80105-5

Shain, A.H., Bastian, B.C., 2016. From melanocytes to melanomas. Nature Reviews Cancer 16, 345–358. https://doi.org/10.1038/nrc.2016.37

Sharma, P., Hu-Lieskovan, S., Wargo, J.A., Ribas, A., 2017. Primary, Adaptive, and Acquired Resistance to Cancer Immunotherapy. Cell 168, 707–723. https://doi.org/10.1016/j.cell.2017.01.017

Shibuya, A., Campbell, D., Hannum, C., Yssel, H., Franz-Bacon, K., McClanahan, T., Kitamura, T., Nicholl, J., Sutherland, G.R., Lanier, L.L., Phillips, J.H., 1996. DNAM-1, A Novel Adhesion Molecule Involved in the Cytolytic Function of T Lymphocytes. Immunity 4, 573–581. https://doi.org/10.1016/S1074-7613(00)70060-4

Shrestha, M., Wang, D.-Y., Ben-David, Y., Zacksenhaus, E., 2023. CDK4/6 inhibitors and the pRB-E2F1 axis suppress PVR and PD-L1 expression in triple-negative breast cancer. Oncogenesis 12, 29. https://doi.org/10.1038/s41389-023-00475-1

Sloan, K.E., Eustace, B.K., Stewart, J.K., Zehetmeier, C., Torella, C., Simeone, M., Roy, J.E., Unger, C., Louis, D.N., Ilag, L.L., Jay, D.G., 2004. CD155/PVR plays a key role in cell motility during tumor cell invasion and migration. BMC Cancer 4, 73. https://doi.org/10.1186/1471-2407-4-73

Smyth, M.J., Dunn, G.P., Schreiber, R.D., 2006. Cancer Immunosurveillance and Immunoediting: The Roles of Immunity in Suppressing Tumor Development and Shaping Tumor Immunogenicity, in: Advances in Immunology. Academic Press, pp. 1–50. https://doi.org/10.1016/S0065-2776(06)90001-7

Solecki, D.J., Gromeier, M., Mueller, S., Bernhardt, G., Wimmer, E., 2002. Expression of the human poliovirus receptor/CD155 gene is activated by sonic hedgehog. J Biol Chem 277, 25697–25702. https://doi.org/10.1074/jbc.M201378200

Song, J., Durrin, L.K., Wilkinson, T.A., Krontiris, T.G., Chen, Y., 2004. Identification of a SUMO-binding motif that recognizes SUMO-modified proteins. Proc Natl Acad Sci U S A 101, 14373–14378. https://doi.org/10.1073/pnas.0403498101

Soriani, A., Iannitto, M.L., Ricci, B., Fionda, C., Malgarini, G., Morrone, S., Peruzzi, G., Ricciardi, M.R., Petrucci, M.T., Cippitelli, M., Santoni, A., 2014. Reactive oxygen species- and DNA damage response-dependent NK cell activating ligand upregulation occurs at transcriptional levels and requires the transcriptional factor E2F1. J Immunol 193, 950–960. https://doi.org/10.4049/jimmunol.1400271

Soriani, A., Zingoni, A., Cerboni, C., Iannitto, M.L., Ricciardi, M.R., Di Gialleonardo, V., Cippitelli, M., Fionda, C., Petrucci, M.T., Guarini, A., Foà, R., Santoni, A., 2009. ATM-ATR-dependent up-regulation of DNAM-1 and NKG2D ligands on multiple myeloma cells by therapeutic agents results in enhanced NK-cell susceptibility and is associated with a senescent phenotype. Blood 113, 3503–3511. https://doi.org/10.1182/blood-2008-08-173914

Stickens, D., Zak, B.M., Rougier, N., Esko, J.D., Werb, Z., 2005. Mice deficient in Ext2 lack heparan sulfate and develop exostoses. Development 132, 5055–5068. https://doi.org/10.1242/dev.02088

Strub, T., Giuliano, S., Ye, T., Bonet, C., Keime, C., Kobi, D., Le Gras, S., Cormont, M., Ballotti, R., Bertolotto, C., Davidson, I., 2011. Essential role of microphthalmia transcription factor for DNA replication, mitosis and genomic stability in melanoma. Oncogene 30, 2319–2332. https://doi.org/10.1038/onc.2010.612

Sullivan, D.P., Seidman, M.A., Muller, W.A., 2013. Poliovirus receptor (CD155) regulates a step in transendothelial migration between PECAM and CD99. Am J Pathol 182, 1031–1042. https://doi.org/10.1016/j.ajpath.2012.11.037

Sun, Y., Shen, Y., Liu, Q., Zhang, H., Jia, L., Chai, Y., Jiang, H., Wu, M., Li, Y., 2025. Global trends in melanoma burden: A comprehensive analysis from the Global Burden of Disease Study, 1990-2021. Journal of the American

Academy of Dermatology 92, 100–107. https://doi.org/10.1016/j.jaad.2024.09.035

Tahara, S., Okumura, G., Matsuo, T., Shibuya, A., Shibuya, K., 2024. Essential role of CD155 glycosylation in functional binding to DNAM-1 on natural killer cells. International Immunology 36, 317–325. https://doi.org/10.1093/intimm/dxae005

Tahara-Hanaoka, S., Shibuya, K., Onoda, Y., Zhang, H., Yamazaki, S., Miyamoto, A., Honda, S.-I., Lanier, L.L., Shibuya, A., 2004. Functional characterization of DNAM-1 (CD226) interaction with its ligands PVR (CD155) and nectin-2 (PRR-2/CD112). Int Immunol 16, 533–538. https://doi.org/10.1093/intimm/dxh059

Takai, Y., Irie, K., Shimizu, K., Sakisaka, T., Ikeda, W., 2003. Nectins and nectin-like molecules: roles in cell adhesion, migration, and polarization. Cancer Sci 94, 655–667. https://doi.org/10.1111/j.1349-7006.2003.tb01499.x

Takai, Y., Miyoshi, J., Ikeda, W., Ogita, H., 2008. Nectins and nectin-like molecules: roles in contact inhibition of cell movement and proliferation. Nature Reviews Molecular Cell Biology 9, 603–615. https://doi.org/10.1038/nrm2457

Tane, S., Maniwa, Y., Hokka, D., Tauchi, S., Nishio, W., Okita, Y., Yoshimura, M., 2013. The role of Necl-5 in the invasive activity of lung adenocarcinoma. Experimental and Molecular Pathology 94, 330–335. https://doi.org/10.1016/j.yexmp.2012.12.003

Tawbi, H.A., Schadendorf, D., Lipson, E.J., Ascierto, P.A., Matamala, L., Castillo Gutiérrez, E., Rutkowski, P., Gogas, H.J., Lao, C.D., De Menezes, J.J., Dalle, S., Arance, A., Grob, J.-J., Srivastava, S., Abaskharoun, M., Hamilton, M., Keidel, S., Simonsen, K.L., Sobiesk, A.M., Li, B., Hodi, F.S., Long, G.V., 2022. Relatlimab and Nivolumab versus Nivolumab in Untreated Advanced Melanoma. N Engl J Med 386, 24–34. https://doi.org/10.1056/NEJMoa2109970

Tremblay-McLean, A., Coenraads, S., Kiani, Z., Dupuy, F.P., Bernard, N.F., 2019. Expression of ligands for activating natural killer cell receptors on cell lines commonly used to assess natural killer cell function. BMC Immunology 20, 8. https://doi.org/10.1186/s12865-018-0272-x

Triki, H., Declerck, K., Charfi, S., Ben Kridis, W., Chaabane, K., Ben Halima, S., Sellami, T., Rebai, A., Berghe, W.V., Cherif, B., 2021. Immune checkpoint CD155 promoter methylation profiling reveals cancer-associated behaviors within breast neoplasia. Cancer Immunol Immunother. https://doi.org/10.1007/s00262-021-03064-6

Turner Nicholas C., Oliveira Mafalda, Howell Sacha J., Dalenc Florence, Cortes Javier, Gomez Moreno Henry L., Hu Xichun, Jhaveri Komal, Krivorotko

Petr, Loibl Sibylle, Morales Murillo Serafin, Okera Meena, Park Yeon Hee, Sohn Joohyuk, Toi Masakazu, Tokunaga Eriko, Yousef Samih, Zhukova Lyudmila, de Bruin Elza C., Grinsted Lynda, Schiavon Gaia, Foxley Andrew, Rugo Hope S., 2023. Capivasertib in Hormone Receptor–Positive Advanced Breast Cancer. New England Journal of Medicine 388, 2058–2070. https://doi.org/10.1056/NEJMoa2214131

Ugurel, S., Thirumaran, R.K., Bloethner, S., Gast, A., Sucker, A., Mueller-Berghaus, J., Rittgen, W., Hemminki, K., Becker, J.C., Kumar, R., Schadendorf, D., 2007. B-RAF and N-RAS mutations are preserved during short time in vitro propagation and differentially impact prognosis. PLoS One 2, e236. https://doi.org/10.1371/journal.pone.0000236

van Elsas, A., Hurwitz, A.A., Allison, J.P., 1999. Combination immunotherapy of B16 melanoma using anti-cytotoxic T lymphocyte-associated antigen 4 (CTLA-4) and granulocyte/macrophage colony-stimulating factor (GM-CSF)-producing vaccines induces rejection of subcutaneous and metastatic tumors accompanied by autoimmune depigmentation. J Exp Med 190, 355–366. https://doi.org/10.1084/jem.190.3.355

Wang, D., Gu, Y., Yan, X., Huo, C., Wang, G., Zhao, Y., Teng, M., Li, Y., 2022. Role of CD155/TIGIT in Digestive Cancers: Promising Cancer Target for Immunotherapy. Front. Oncol. 12, 844260. https://doi.org/10.3389/fonc.2022.844260

Wang, P., Sarkar, S., Zhang, M., Xiao, T., Kong, F., Zhang, Z., Balasubramanian, D., Jayaram, N., Datta, S., He, R., Wu, P., Chao, P., Zhang, Y., Washburn, M.P., Florens, L., Nagarkar-Jaiswal, S., Jaiswal, M., Mohan, M., 2024. DYRK1A Interacts with the Tuberous Sclerosis Complex and Promotes mTORC1 Activity. https://doi.org/10.7554/elife.88318.2

Wang, Y., Li, Jiajia, Li, Jingjing, Li, P., Wang, L., Di, L., 2020. An Enhancer-Based Analysis Revealed a New Function of Androgen Receptor in Tumor Cell Immune Evasion. Frontiers in Genetics Volume 11-2020. https://doi.org/10.3389/fgene.2020.595550

Wolchok, J.D., Chiarion-Sileni, V., Gonzalez, R., Rutkowski, P., Grob, J.-J., Cowey, C.L., Lao, C.D., Wagstaff, J., Schadendorf, D., Ferrucci, P.F., Smylie, M., Dummer, R., Hill, A., Hogg, D., Haanen, J., Carlino, M.S., Bechter, O., Maio, M., Marquez-Rodas, I., Guidoboni, M., McArthur, G., Lebbé, C., Ascierto, P.A., Long, G.V., Cebon, J., Sosman, J., Postow, M.A., Callahan, M.K., Walker, D., Rollin, L., Bhore, R., Hodi, F.S., Larkin, J., 2017. Overall Survival with Combined Nivolumab and Ipilimumab in Advanced Melanoma. N Engl J Med 377, 1345–1356. https://doi.org/10.1056/NEJMoa1709684

Wozniak, D.J., Kajdacsy-Balla, A., Macias, V., Ball-Kell, S., Zenner, M.L., Bie, W., Tyner, A.L., 2017. PTEN is a protein phosphatase that targets active

PTK6 and inhibits PTK6 oncogenic signaling in prostate cancer. Nat Commun 8, 1508. https://doi.org/10.1038/s41467-017-01574-5

Wu, S., Zhu, W., Thompson, P., Hannun, Y.A., 2018. Evaluating intrinsic and non-intrinsic cancer risk factors. Nature Communications 9, 3490. https://doi.org/10.1038/s41467-018-05467-z

Xin, J., Yin, K., Li, S., Gu, P., Shao, S., 2025. Exploring the ER channel protein Sec61: recent advances in pathophysiological significance and novel pharmacological inhibitors. Front Pharmacol 16, 1580086. https://doi.org/10.3389/fphar.2025.1580086

Xiong, T., Wang, G., Yu, P., Li, Zhenlong, Li, D., Zhang, J., Lu, S., Yang, R., Lian, X., Mi, J., Ma, R., Li, Zhiyao, Marcucci, G., Zhao, T., Caligiuri, M.A., Yu, J., 2025. CAR-T cells targeting CD155 reduce tumor burden in preclinical models of leukemia and solid tumors. Journal of Clinical Investigation 135, e189920. https://doi.org/10.1172/JCI189920

Yan, Z., 2015. Increased expression of CD155 and CD112 on monocytes in septic patients (INC6P.327). The Journal of Immunology.

Yang, W.-C., Wei, M.-F., Shen, Y.-C., Huang, C.-S., Kuo, S.-H., 2025. CDK4/6 inhibitors synergize with radiotherapy to prime the tumor microenvironment and enhance the antitumor effect of anti-PD-L1 immunotherapy in triple-negative breast cancer. J Biomed Sci 32, 79. https://doi.org/10.1186/s12929-025-01173-3

Yin, G., Zeng, W., Li, R., Zeng, M., Chen, R., Liu, Y., Jiang, R., Wang, Y., 2022. Glia Maturation Factor-β Supports Liver Regeneration by Remodeling Actin Network to Enhance STAT3 Proliferative Signals. Cell Mol Gastroenterol Hepatol 14, 1123–1145. https://doi.org/10.1016/j.jcmgh.2022.07.016

Yu, X., Harden, K., C Gonzalez, L., Francesco, M., Chiang, E., Irving, B., Tom, I., Ivelja, S., Refino, C.J., Clark, H., Eaton, D., Grogan, J.L., 2009. The surface protein TIGIT suppresses T cell activation by promoting the generation of mature immunoregulatory dendritic cells. Nature Immunology 10, 48–57. https://doi.org/10.1038/ni.1674

Zhang, B., Zhao, W., Li, H., Chen, Y., Tian, H., Li, L., Zhang, L., Gao, C., Zheng, J., 2016. Immunoreceptor TIGIT inhibits the cytotoxicity of human cytokine-induced killer cells by interacting with CD155. Cancer Immunol Immunother 65, 305–314. https://doi.org/10.1007/s00262-016-1799-4

Zhang, D., Liu, J., Zheng, M., Meng, C., Liao, J., 2022. Prognostic and clinicopathological significance of CD155 expression in cancer patients: a meta-analysis. World Journal of Surgical Oncology 20, 351. https://doi.org/10.1186/s12957-022-02813-w

Zhang, J., ten Dijke, P., Wuhrer, M., Zhang, T., 2021. Role of glycosylation in TGF-β signaling and epithelial-to-mesenchymal transition in cancer. Protein & Cell 12, 89–106. https://doi.org/10.1007/s13238-020-00741-7

Zhang, K., Mi, Y., Zhang, B., Xue, X., Ding, Y., Ma, J., Yuan, E., Zhao, X., Zheng, P., 2025. Preclinical application of a CD155 targeting chimeric antigen receptor T cell therapy for digestive system cancers. Oncogene 44, 1463–1474. https://doi.org/10.1038/s41388-025-03322-2

Zhang, P., Mueller, S., Morais, M.C., Bator, C.M., Bowman, V.D., Hafenstein, S., Wimmer, E., Rossmann, M.G., 2008. Crystal structure of CD155 and electron microscopic studies of its complexes with polioviruses. Proc Natl Acad Sci U S A 105, 18284–18289. https://doi.org/10.1073/pnas.0807848105

Zheng, Q., Wang, B., Gao, J., Xin, N., Wang, W., Song, X., Shao, Y., Zhao, C., 2018. CD155 knockdown promotes apoptosis via AKT/Bcl-2/Bax in colon cancer cells. J Cell Mol Med 22, 131–140. https://doi.org/10.1111/jcmm.13301

Zhong, X., Xie, H., Wang, S., Ren, T., Chen, J., Huang, Y., Yang, N., 2024. TIGIT regulates CD4+ T cell immunity against polymicrobial sepsis. Frontiers in Immunology Volume 15-2024. https://doi.org/10.3389/fimmu.2024.1290564

Zhou, J., Chen, Q., Lanske, B., Fleming, B.C., Terek, R., Wei, X., Zhang, G., Wang, S., Li, K., Wei, L., 2014. Disrupting the Indian hedgehog signaling pathway in vivo attenuates surgically induced osteoarthritis progression in Col2a1-CreERT2; Ihhfl/fl mice. Arthritis Res Ther 16, R11. https://doi.org/10.1186/ar4437

Zitti, B., Molfetta, R., Fionda, C., Quatrini, L., Stabile, H., Lecce, M., de Turris, V., Ricciardi, M.R., Petrucci, M.T., Cippitelli, M., Gismondi, A., Santoni, A., Paolini, R., 2017. Innate immune activating ligand SUMOylation affects tumor cell recognition by NK cells. Scientific Reports 7, 10445. https://doi.org/10.1038/s41598-017-10403-0

Zuo, L., Weger, J., Yang, Q., Goldstein, A.M., Tucker, M.A., Walker, G.J., Hayward, N., Dracopoli, N.C., 1996. Germline mutations in the p16INK4a binding domain of CDK4 in familial melanoma. Nat Genet 12, 97–99. https://doi.org/10.1038/ng0196-97

Zuo, S., Li, C., Sun, X., Deng, B., Zhang, Y., Han, Y., Ling, Z., Xu, J., Duan, J., Wang, Z., Yu, X., Zheng, Q., Xu, X., Zong, J., Tian, Z., Shan, L., Tang, K., Huang, H., Song, Y., Niu, Q., Zhou, D., Feng, S., Han, Z., Wang, G., Wu, T., Pan, J., Feng, X., 2024. C-JUN overexpressing CAR-T cells in acute myeloid leukemia: preclinical characterization and phase I trial. Nat Commun 15, 6155. https://doi.org/10.1038/s41467-024-50485-9